NORTHWESTERN UNIVERSITY

Engineering Substrate-Mediated Gene Delivery with Self-Assembled Monolayers and Soft Lithography

A DISSERTATION

SUBMITTED TO THE GRADUATE SCHOOL
IN PARTIAL FULFILLMENT OF THE REQUIREMENTS

for the degree

DOCTOR OF PHILOSOPHY

Field of Interdepartmental Biological Sciences

By

Angela Kaye Pannier

EVANSTON, ILLINOIS

June 2007

© Copyright by Angela Kaye Pannier, 2007
All Rights Reserved

Abstract

Engineering Substrate-Mediated Gene Delivery with Self-Assembled Monolayers and Soft Lithography

Angela Kaye Pannier

Substrate-mediated delivery involves the immobilization of DNA, complexed with nonviral vectors, to a biomaterial or surface that supports cell adhesion. Cells cultured on the substrate are exposed to elevated DNA concentrations within the local microenvironment, which enhances transfection. As surface properties are critical to this delivery approach, self-assembled monolayers (SAMs) of alkanethiols on gold were used to investigate the effect of surface chemistries on substrate-mediated delivery. Surface hydrophilicity and ionization affected nonspecific complex immobilization and transfection, with SAMs presenting carboxylic acid groups resulting in the greatest immobilization and transfection. Subsequent studies used SAMs to investigate the effect of surfaces presenting oligo(ethylene glycol) (EG) groups on substrate-mediated delivery. Nonspecific complex immobilization to SAMs containing combinations of EG- and carboxylic acid- terminated alkanethiols resulted in substantially greater transfection than surfaces containing no EG groups or EG groups combined with other functional groups. Transfection enhancement could not be attributed to binding or release profiles. Atomic force microscopy imaging of immobilized complexes revealed that EG groups within SAMs affected complex size and appearance, indicating the ability of these surfaces to preserve complex morphology upon binding. To control binding and release profiles, complexes were covalently linked to SAMs presenting appropriate functional groups. Covalent tethering by multiple

crosslinkers resulted in lower complex binding than corresponding conditions without the crosslinker, and no transfection. The principles guiding complex immobilization and tethering could be extended to biomaterial surfaces for tissue engineering applications.

Finally, soft lithography techniques were used to pattern complex deposition and transfection, on SAMs and cell culture surfaces, for the formation of a transfected cell array, a high-throughput technique to correlate gene expression with functional cell responses. We developed an array that combines a two-plasmid system and dual bioluminescence imaging to quantitatively normalize for variability in transfection and increase sensitivity. The array was applied to quantify estrogen receptor α (ERα) activity in breast cancer cells. ER induction mimicked results obtained through traditional assay methods. Furthermore, the array captured a dose response to estrogen, demonstrating the sensitivity of bioluminescence quantification. Our system should serve as a standard for fabrication of transfected cell arrays to report on signaling pathways.

Acknowledgements

Lonnie, I cannot thank you enough for all of the support and guidance you have given me. You taught me guiding principles so that I could develop into an independent scientist. Erik, Heike, Guillermo, and Prof. Kelso, thank you for serving on my committee and for the helpful discussions. Eric Ariazi, thank you for seeing the potential of the array project, and collaborating with us. Kevin, Pam, and Jae, thank you being the original leaders of the lab and for setting up the Shea L.A.B. standards and culture. Brian, thank you for helping to shape the SAM projects. David, Chris, Julie, Michael, Elizabeth, Marina, Anne, and Rob, thank you for assistance with my projects, fun in the lab, and for sharing your time with me. Abbie, thank you for your help with the array studies; I am confident you will take this project to new heights. Yang, Courtney, Laura D., Jen, Laura S., and Nisha, thank you for your help both in and out of lab, and for being wonderful friends. Erin, thank you for your friendship, our "discussions", and for helping me whenever I needed something small pipeted. Tiffany, thank you for being one of my best friends, for taking time each morning to talk about science and life, and for your inspirational work ethic. Zain, thank you for your leadership, advice, and all of those "scientific" discussions; you inspire me in the way you live your life both in and out of lab. Tatiana, thank you for being my mentor, role model, and friend, and for your guidance and vision. To my family, thank you for your love and support and visits. Mom and Dad, I cannot thank you enough for your unending love and support. You have always believed in me and without you, my success would not have been possible. To the love of my life, Tyler, thank you for loving me, helping me, supporting me, splitting cells with me, taking care of things when I was too busy in lab, and never letting me quit. Finally, Baby Pannier, thank you for inspiring me, motivating me, and for not making me sick so I could finish my experiments and thesis.

Dedication

To
Baby Pannier and Tyler,
Mom and Dad.

List of Abbreviations

SAMs	Self-assembled monolayers
EG	Oligo(ethylene glycol)
ER	Estrogen Receptor
PLL	Poly(L-lysine)
PEI	Polyethylenimine
N/P	Nitrogen to phosphate ratio
NLS	Nuclear localization sequence
PLGA	Poly(lactide-co-glycolide)
PAMAM	Polyamidoamine dendrimers
DT10	1-Decanethiol; methyl terminated
MUOH	Mercapto-1-undecanol; hydroxyl-terminated
MUA	11-Mercaptoundecanoic acid; carboxylic acid-terminated
$COOH/COO^-$	Carboxylic acid
CH_3	Methyl group
OH	Hydroxyl group
μCP	Microcontact printing
PDMS	Polydimethylsiloxane
CFs	Condensation figures
ANOVA	Analysis of variance
RNAi	RNA interference
siRNA	Small interfering RNA
E_2	17β-estradiol
ERE	Estrogen response element
XPS	X-ray photoelectron spectroscopy
LUC	Luciferase
EGFP	Enhanced green fluorescent protein
βGAL	β-galactosidase
CMV	Cytomegalovirus
SIMS	Secondary ion mass spectrometry
PBS	Phosphate-buffered saline
O8SH	1,8-Octanedithiol; thiol-terminated
HPMS	2-Hydroxypentamethylene sulfide; aldehyde-terminated
FBS	Fetal bovine serum
EDC	1-Ethyl-3-(3-Dimethylaminopropyl) carbodiimde Hydrochloride; carboxylic acid and amine reactive
NHSS	N-hydroxysulfosuccinimide; carboxylic acid and amine reactive
$NaCNBH_3$	Sodium cyanborohydride
AAD	Adipic acid dihydrazide
Sulfo-SMCC	Sulfosuccinimidyl 4-(N-maleimidomethyl)cyclohexane-1-carboxylate; amine and thiol-reactive

AEDP	3-[(2-Aminoethyl)dithio]propionic acid – HCL; amine and carboxylic acid-reactive
Sulfo-LC-SMPT	Sulfosuccinimidyl 6-[α–methyl-α-(2-pyridulditho)toluamido]hexanoate; amine and thiol-reactive
DTT	Dithiothreitol
dATP	2'-Deoxyadenosine 5'-triphosphate
RLU	Relative light units
PEG	Polyethylene glycol
EDTA	Ethylenediaminetetraacetic acid
AFM	Atomic force microscopy
RMS	Root-mean-square
ffLUC	Firefly luciferase
rLUC	Renilla luciferase
FUL	Anti-estrogen fulvestrant
TK	Minimal herpes simplex thymidine kinase promoter
CCD	Charge-coupled device
FITC	Fluorescein isothiocyanate
ROI	Region of interest
FTIR	Fourier transform infrared spectroscopy
VEGF	Vascular endothelial growth factor
MMP	Matrix metalloproteinases

Table of Contents

List of Figures

List of Tables

Chapter 1

Introduction: Thesis Overview

1.1 Motivation and objective

Gene expression within a cell population can be directly altered through gene delivery approaches, which have tremendous potential for therapeutic uses, such as gene therapy or tissue engineering, or in research applications, such as functional genomics. However, inefficient gene delivery is a critical factor limiting the development of these applications. DNA delivery to cells can be limited by mass transport limitations or deactivation processes, such as degradation and aggregation (1). Substrate-mediated delivery, also termed solid phase delivery, describes the immobilization of DNA, complexed with nonviral vectors, to a biomaterial or substrate through specific or nonspecific interactions. Cells cultured on the substrate are exposed to elevated DNA concentrations within the local microenvironment, which enhances transfection (2-6).

For substrate-mediated gene delivery, the properties of the surface are critical to both immobilization strategies and transfection efficiencies. However, the properties of the substrate that mediate gene transfer remain poorly understood. Surfaces with controlled chemistries were explored in this thesis as a means to study the effect of the surface properties on substrate-mediated gene delivery and to use those findings to enhance and pattern delivery. Self-assembled monolayers (SAMs) of alkanethiols on gold were used to provide a controlled surface to investigate the mechanisms of transfection resulting from DNA complexes immobilized to a substrate through non-specific and specific interactions, to elucidate surface design parameters that maximize the delivery efficiency for applications including tissue engineering and

transfected cell arrays. By examining surface properties necessary to maximize transfection, as well as utilizing that knowledge to chemically pattern the surface, an array of DNA complexes can result in an array of transfection. Patterning different genes into an array format, followed by cell seeding, was used to create a transfected cell array that can report on the activity of signal transduction pathways in cancer cells and correlate that output to cellular conditions.

1.2 Thesis outline

After this brief introductory chapter, Chapters 2 and 3 provide background material relevant to the experimental work. Chapter 2 describes substrate-mediated gene delivery in detail, beginning with descriptions of nonviral gene delivery, barriers to gene delivery, and then exploring the evolution of substrate-mediated gene delivery. Chapter 2 concludes with a section detailing the properties of self-assembled monolayers, used extensively throughout this thesis. Chapter 3 details all applications of substrate-mediated gene delivery, including tissue engineering and transfected cell arrays, and concludes with a section on using such arrays for breast cancer profiling, in particular of the estrogen receptor, which will be of interest in Chapter 7. Chapters 4 through 7 describe the experimental work, and Chapter 8 describes the conclusions of the research presented, as well as future directions of the work.

An overview of the experimental work presented in this thesis is provided in Figure 1-1. Focus 1 describes the use of SAMs to study the effect of surface properties (ionization, hydrophilicity, and presence of hydrophilic polymer, oligo(ethylene) glycol) on substrate-mediated gene delivery by nonspecifically immobilized complexes (Chapters 4 and 6). Within these studies, the composition of the surface was related to various properties of the complex,

including binding densities, transfection efficiencies, release profiles, and complex morphology on the surface. The results presented within these chapters could be applied to tissue engineering scaffold design, as well as design of surfaces for in vitro gene delivery. Within focus 1, the ability to use soft lithographic techniques to pattern SAMs and subsequently DNA immobilization and transfection was also established (Chapter 4). Specifically, a strategy to pattern deposition of DNA complexes in droplets formed on hydrophilic regions on SAM substrates in a background of hydrophobic regions was developed, resulting in patterned transfection. Patterned transfection has the potential to be used in multiple applications, from tissue engineering to functional genomic screens in cell-based assays.

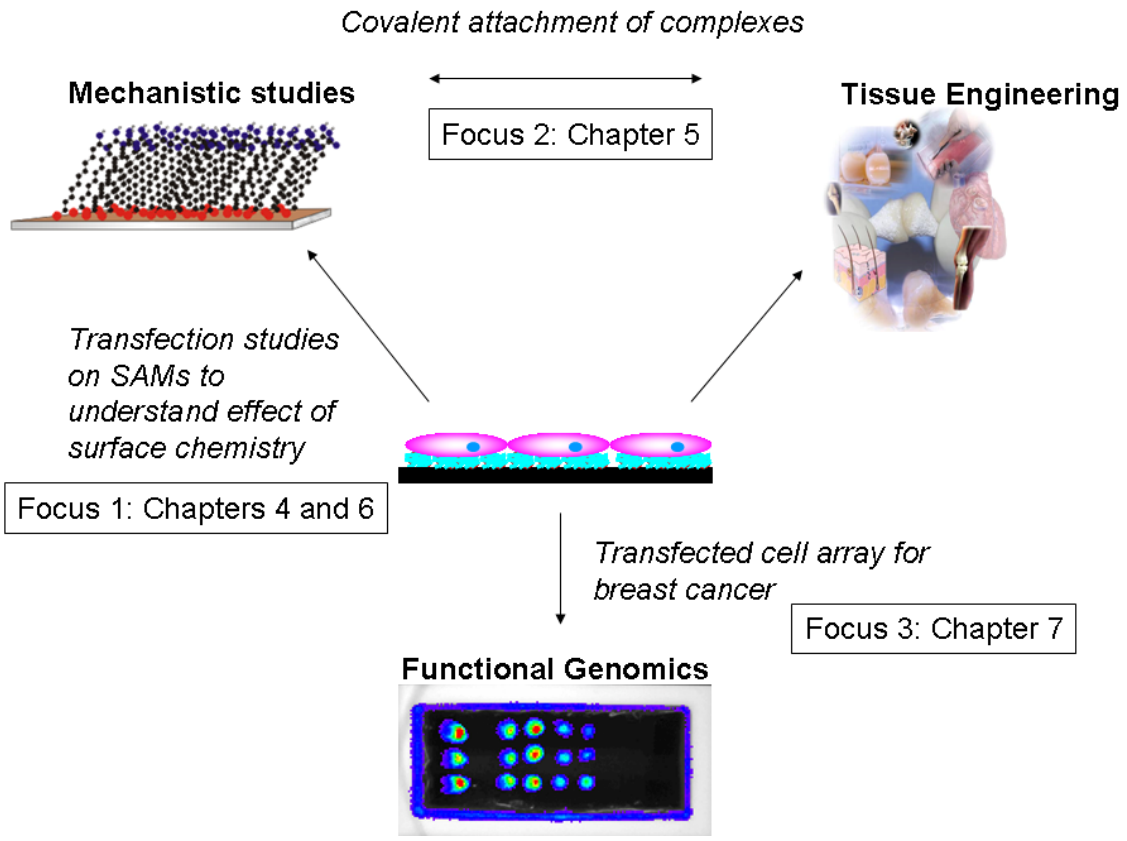

Figure 1-1 Overview of substrate-mediated gene delivery foci addressed in this thesis.

After the mechanisms of substrate-mediated transfection by nonspecifically bound complexes on SAMs were established, the ability to specifically tether complexes to further modulate release profiles was examined in Focus 2 (Chapter 5). DNA, complexed with a cationic polymer, was covalently linked to SAMs presenting appropriate functional groups through a fraction of the functional groups available on the polymer present in the complex. Six coupling strategies were explored for the ability to tether active complexes, and subsequently release complexes for substrate-mediated transfection. The results from this focus can be applied to rationale design of tissue engineering scaffolds used for gene delivery.

The third and final focus of the thesis concerns the development of a transfected cell array using soft lithography techniques, which can be assessed through bioluminescence imaging for normalization of estrogen receptor activity in breast cancer cells (Chapter 7). The array presented in this thesis represents significant improvements for transfected cell array technology, including the use of two plasmids within each spot of the array, one of which provides a signal for normalization, as well as luciferase imaging to sensitively measure both plasmids without post-transfectional processing, in a biologically relevant system.

Collectively, the three foci of this thesis explore the mechanisms of substrate-mediated gene delivery, from both nonspecifically and specifically immobilized complexes, using surfaces with defined chemistries. Furthermore, the ability to pattern transfection, using microcontact printing of SAMs or alternative soft lithographic techniques on polystyrene, was established and translated to a functional array reporting on a transcription factor in a breast cancer model.

Chapter 2

Substrate-Mediated Gene Delivery

2.1 Introduction

Gene transfer, the introduction of exogenous genes into cells, has many potential applications in basic science (e.g., to study function and regulation of gene expression and proteins), therapeutics (e.g., gene therapy to treat genetic diseases), tissue engineering (e.g., to present factors in tissue regeneration matrices), and functional genomics (e.g., transfected cell arrays). Both extracellular and intracellular barriers exist that prevent efficient gene transfer. Methods such as complexing DNA with nonviral vectors, as well as delivery mechanisms such as substrate-mediated gene delivery, have been developed to overcome both extracellular and intracellular barriers. Substrate-mediated delivery, also termed solid phase delivery, describes the immobilization of DNA to a biomaterial or substrate, which functions to support cell adhesion. As the properties of both the vector and surface are critical to this delivery approach, self-assembled monolayers were explored in this thesis as a means to investigate the effect of surface properties and patterning on substrate-mediated gene delivery.

2.2 Nonviral gene delivery

While naked DNA provides transfection in vivo, complexing DNA with nonviral vectors can facilitate uptake and transfection in vitro and in vivo (7-9). Typical nonviral gene delivery systems involve the ionic complexation of negatively charged DNA with cationic polymers to form complexes (Figure 2-1) termed polyplexes (10,11) or cationic lipids to form lipoplexes

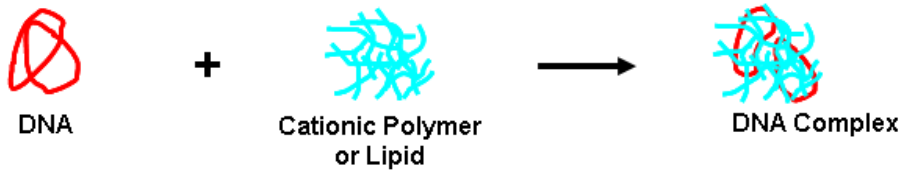

Figure 2-1 DNA complex formation. Negatively charged plasmid DNA electrostatically associates with cationic polymers or lipids to form a condensed DNA complex.

(12). Cationic polymers and lipids protect DNA against degradation by nucleases and serum components (13). Complexation of DNA enhances cellular uptake by reducing the effective size of DNA, enhancing interactions between positively charged DNA complexes and the negatively charged cellular membrane and altering cell permeability (9,13). Cationic polymers and lipids can further promote internalization by designing them to target delivery to specific cell types through receptor-ligand interactions (9). These complexation agents can also facilitate intracellular trafficking, which includes endosomal escape, cytoplasmic transport, and nuclear entry, while also dissociating from the DNA to allow expression (7,14). Nonviral vectors are safer and easier to prepare than viral vectors and do not stimulate immune responses typical of viral vectors, but have lower efficiency and shorter duration of gene expression.

Lipids were the first cationic species to be examined for gene delivery (15). Several types of cationic lipids have since been used, including quaternary ammonium detergents, cationic derivatives of cholesterol and diacylgylcerol, and lipid derivatives of polyamines (16). Cationic lipids are composed of a cationic head group, linker, and hydrophobic moiety (12), typically two alkyl chains (17). The cationic head group serves to condense the DNA and bind

the complex to the cell surface. The linker can be used to introduce specific functional groups to the lipid. The hydrophobic moiety provides self-association to form liposomes in the presence of a helper lipid. The lipid chain length, degree of unsaturation, and asymmetry of dual hydrocarbon chains, as well as the chemistry of the linker and cationic head group, affect transfection properties, as can mixing conditions and cell lines (12). Most cationic lipid reagents in use today are formulated as liposomes containing two lipid species, a cationic amphiphile and a neutral phospholipid or helper lipid (18), to facilitate the release of plasmid DNA from the endosome after endocytic uptake of the complex (16). Cationic lipids are available as a variety of commercially available products, including Lipofectamine 2000, Lipofectamine LTX, and Effectene, which is composed of both polymers and lipids, but all of which have formulations which are propriety.

There are several cationic polymers which have been studied for gene delivery. Poly(L-lysine) (PLL), polyethylenimine (PEI), polysaccharide-based polymers (cyclodextrins, chitosan), dendrimers, poly-L-ornithine, poly(β-aminoesters), and polyphosphoesters have been used for nonviral gene delivery, as well as derivatives of each, created by attaching specific moieties to the polymer to mediate protein binding, cell targeting, biodegradability, and endosomal escape (19,20). Cationic polymers are more effective at condensing DNA than lipids, and can be synthesized in different lengths, with different geometries (17). The most widely used cationic polymer, and the one employed in the studies presented in this thesis, is polyethylenimine (PEI). PEI can be synthesized as either a linear or branched polymer, but generally branched is more successful at mediating cellular transfection (10,11). Branched PEI contains primary, secondary and tertiary amines, each with the potential to be protonated, making it an effective buffer over a

wide pH range, especially in the endosomal compartment (10). PEI is hypothesized to act as a proton sponge, which causes a large influx of water into the endosome, followed by rupture and escape of the PEI/DNA complexes into the cytosol (10,11,21).

Other than the choice of cationic polymer or lipid, the properties of the resulting complex formed between the polymer or lipid and DNA are dictated by several factors. The ratio at which complexes are formed between polymers or lipids and DNA (N/P, referring to a ratio of nitrogen groups found in the amine groups typically found on the cationic polymer or lipid to the phosphate groups in the DNA backbone) determines the charge of the complex and its size, and therefore typically its efficacy (17), as complex size is a critical parameter influencing transfection. Large complexes typically result in greater transgene expression than small complexes. However, the number of cells expressing the transgene is increased with small complexes relative to large complexes (22). The complexing ratio will also determine its ability to protect the DNA, but may also influence cytotoxicity. Complexes formed at high N/P ratios are typically smaller and more positively charged, but may be more toxic, due to the presence of excess free cationic polymer or lipid. The composition of solvents used to prepare the complexes, as well as concentration of the DNA and polymer/lipid and the temperature can also contribute to final complex properties (16) and must be carefully considered during complex formation procedures.

2.3 Barriers to nonviral gene delivery

Even with complexation strategies as described above, both extracellular and intracellular barriers exist that prevent efficient nonviral gene transfer. Extracellular barriers to gene delivery

include mass transport limitations, cytotoxicity, degradation, and aggregation (1), as well as cell targeting and uptake. The physical and chemical stability of DNA and its delivery vehicle in the extracellular compartment is affected by the presence of nucleases that can lead to degradation, and proteins, which upon binding to the DNA complexes can facilitate aggregation (20,23), which can occur rapidly in solution and reduces the activity of DNA complexes (1). In vivo, extracellular factors that limit delivery also include plasmid clearance or degradation, which can be further mediated by sequence specific recognition from the immune system. Immune responses to the plasmid are affected by the methylation pattern of CpG sequences, which in turn can affect the duration of transgene expression (8).

Once a complex reaches a target cell, intracellular barriers to gene transfer include cell binding, cell entry, release from the endosomal/lysosomal compartments (endosomolysis), cytosolic transit, nuclear entry (23,24), and subsequently expression of the transgene (16) (Figure 2-2). Complex binding to the cell can occur through receptor binding (if the cationic polymer or lipid contains a targeting ligand) or nonspecific binding, presumably mediated by the cationic nature of the complexes and the anionic cell surface proteoglycans (16,17,23). Upon binding to a cell, nearly all nonviral vectors enter the cell through an endocytic pathway, even vectors that bind nonspecifically (17,23). Once internalized within an endosome, endosomal escape is believed to be a major barrier to efficient gene transfer (23). Escape has been postulated to be attributed to pore formation within the membrane, membrane fusion of the cationic lipids and the endosomal membrane, a proton sponge process causing an influx of water and thus rupture, or membrane disruption (17,23). Once outside of the endosome, the complexes must traffic through the cytosol towards the nucleus, and this transit may be accomplished in vesicles along

the cytoskeleton, or via DNA diffusion through the cytosol, which is affected by the size of the DNA (23). Nuclear entry is mediated by specific factors that actively transport molecules into the nucleus, and in absence of these moieties, is thought to be accomplished through nuclear

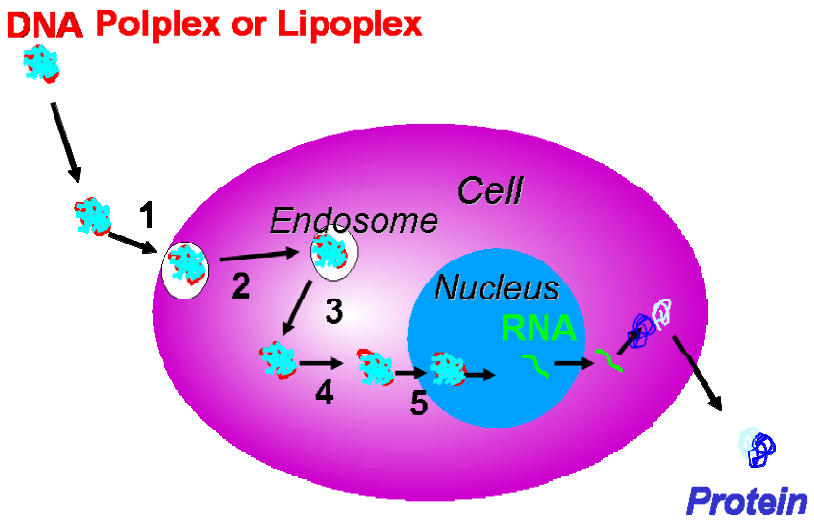

Figure 2-2 Barriers to gene delivery. DNA complex trafficking must overcome barriers once reaching the target cell: 1) cell binding, 2) cell entry/endocytosis, 3) endosomolysis, 4) cytosolic transit and 5) nuclear entry.

breakdown in mitosis or through the nuclear pores (23). As the nuclear pores have a narrow diameter (25 nm) they would not be expected to allow passage of plasmid DNA (17). However, active transport may contribute to nuclear entry of DNA, as some promoters are thought to bind to nuclear localization sequence (NLS)-containing cyotplasmic proteins such as transcription factors (17,25), which could then shuttle the DNA into the nucleus.

While the above descriptions of barriers to gene delivery highlight the overall process of gene transfer, the exact mechanisms involved in gene delivery are still poorly understood because of the complexity of the process. The choice of cationic polymer or lipid and complex

properties, including the size of the complex, may be a contributing factor in determining which entry and intracellular pathway the complex travels (24). Modification to the DNA and the cationic lipids or polymers, as well as the development of alternative delivery mechanisms like substrate-mediated gene delivery described below, have been developed to overcome both the extracellular and intracellular barriers to successful gene delivery (7,14), as well as to understand the underlying gene transfer process. For example, many strategies to enhance cationic polymer delivery and to reduce cytotoxicity involve the modification of the cationic polymer with ligands that target endocytosis (26), polymers that prevent protein interactions (27), and peptides or surfactants that can facilitate escape from the endosome (28,29).

2.4 Substrate-mediated gene delivery

The adaptation of controlled release technologies to the delivery of nonviral vectors has the potential to overcome extracellular barriers that limit gene therapy, including aggregation of complexes, degradation of complexes, and in particular mass transport limitations that result in low concentration of DNA at the cell surface. Increasing DNA concentrations in the cellular microenvironment has been shown to improve gene delivery (30,31). In substrate-mediated delivery, plasmid DNA or DNA complexes are immobilized to a surface or biomaterial that supports cell adhesion, placing the DNA directly in the cellular microenvironment and increasing its local concentration (Figure 2-3). Furthermore, immobilization of DNA complexes to a substrate has the ability to preserve size observed in solution and inhibits complex aggregation, which can reduce activity (1).

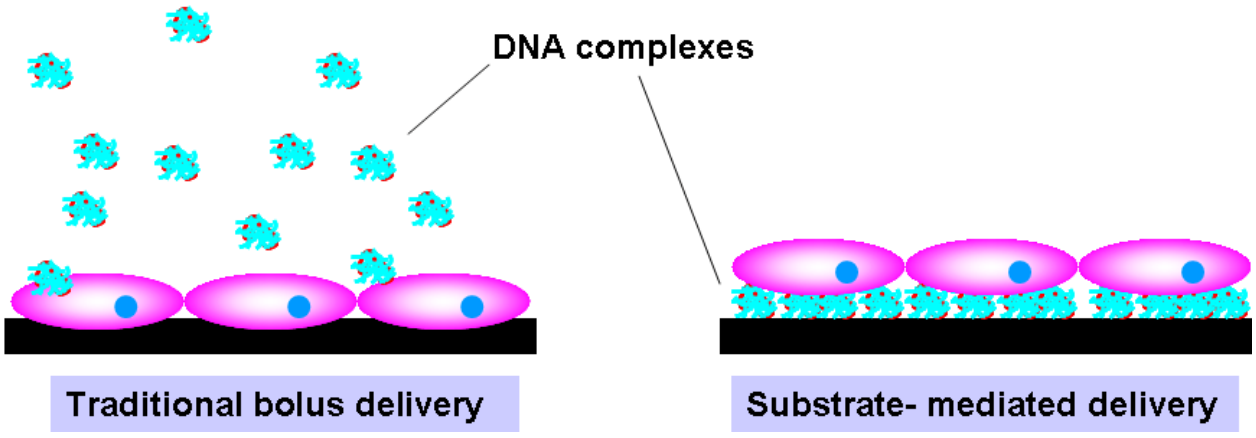

Figure 2-3 Bolus versus substrate-mediated gene delivery. For traditional bolus delivery, cells are plated prior to delivery and complexes must diffuse from bulk media to the cell surface. For surface delivery, complexes are immobilized to the surface and cells are plated after complexes are present, presenting a high local concentration of DNA which can enhance delivery and pattern transfection.

The immobilization of DNA to the substrate may seem counterintuitive given the need for cellular internalization to achieve expression; however, natural and synthetic corollaries exist for growth factors and viral vectors. Growth factors associate with the extracellular matrix, functioning directly from the matrix or upon release (32-34). Additionally, many viral vectors associate with the extracellular matrix as a means to facilitate cellular binding and internalization (35,36). In substrate-mediated delivery, DNA is concentrated at the delivery site and targeted to cells adhered to the substrate (2,5,6,37). Cells cultured on the substrate can internalize the DNA either directly from the surface, or by degrading the linkage between the vector and the material, which may be accomplished through specific or nonspecific mechanisms.

2.4.1 DNA immobilization through specific interactions

DNA complexes can be immobilized on the substrate through specific interactions introduced through complementary functional groups on the vector and surface, such as antigen-antibody or biotin-avidin, to control vector binding to the substrate (5,37). The effective affinity of vector for substrate is determined by the strength of the specific interactions, which may also be influenced by environmental conditions (e.g., ionic strength, pH), binding-induced conformational changes, or vector unpacking. In the first studies on specific attachment of nonviral vectors, two cationic polymers, PLL and PEI, were modified with biotin residues for subsequent complexation with DNA and binding to a neutravidin substrate (5,6). Complexes were formed with mixtures of biotinylated and non-biotinylated cationic polymer at a constant N/P ratio. Release studies demonstrated only 25% of immobilized DNA complexes were released over an 8-day period, with approximately 15% released within the first 24 hours. For complexes formed with PLL, the number of biotin groups and their distribution among the cationic polymer were critical determinants of both binding and transfection. The number of biotin groups in the complex was manipulated through the fraction of biotinylated PLL used for complex formation and the number of biotin residues per PLL. Increasing the number of biotin groups per complex led to increased binding (5). However, *in vitro* transfection was maximal when complexes contained biotin residues attached to a small fraction of the cationic polymers (6). At this condition, less than 100 ng of immobilized DNA mediated transfection, which was increased 100 fold relative to bolus delivery of similar complexes (5). Additionally, transfection was observed only in the location to which complexes were bound, suggesting the possibility of spatially regulating DNA delivery. For complexes formed with PEI, substantial transfection was

observed *in vitro*, but was independent of the number of biotin groups present on the complex, suggesting that complex immobilization occurred through nonspecific interactions (6).

A specific interaction between cyclodextrin and adamantine was utilized to immobilize complexes of cyclodextrin-PEI with DNA on adamantine-functionalized surfaces by inclusion complex formation (38). However, transfection of these complexes was not investigated (38). Complexes have also been specifically immobilized to biomaterials for tissue engineering. DNA complexes were immobilized using the biotin-avidin strategy to hyaluronic acid-collagen hydrogels, and resulted in spatially controlled gene transfer by topographical patterning (22). Disulfide crosslinked peptide-DNA complexes were covalently immobilized into fibrin matrices by factor XIII activity and led to increased transfection efficiencies in 2D and comparable levels in 3D, when compared to transfection by PLL complexes (39).

2.4.2 DNA immobilization through nonspecific interactions

DNA complexed with cationic polymers or lipids can also interact with substrates through non-specific, noncovalent mechanisms, including hydrophobic, electrostatic, and van der Waals interactions. These interactions have been well-characterized for adsorption and release of proteins from polymeric systems (40,41). Nonspecific binding depends upon the molecular composition of the vector (e.g., lipid versus polymer) and the relative quantity of each (e.g., N/P), as well as surface properties. Polyplexes and lipoplexes non-specifically immobilized to serum-coated substrates have been shown to enhance the extent of transgene expression in both cell lines and primary human-derived cells, along with an increased cellular viability (2). This enhancement was dependent on both the properties of the complex (e.g., complexation agent,

N/P ratio), and substrate treatment (e.g. serum-coating vs. none). The properties of the surfaces and vectors were further shown to be critical determinants of cellular association of immobilized DNA (3). Serum coating of the substrate did not affect the quantity immobilized, but increased the amount of DNA released from the substrate and the number of cells internalizing plasmid, which paralleled an enhanced number of cells expressing transgene. Polyplexes delivered from coated substrates associated nearly 3-fold more readily with cells, but had decreased efficacy relative to bolus delivered polyplexes. The quantity of cell-associated DNA using lipoplexes was less for substrate-mediated delivery, yet still provided similar levels of transgene expression (3). Further studies were performed to identify the specific components within the serum, which could be contributing to the enhancement of substrate-mediated transfection by complexes nonspecifically immobilized on coated surfaces. Fibronectin coating, at intermediate densities, was determined to mediate the highest levels of transgene expression, potentially by targeting internalization through caveolae-mediated endocytosis (4).

DNA has also been nonspecifically immobilized to substrates through polyelectrolyte films that promote localized delivery to cells, though cells were not able to adhere to the films (42). The films consisted of alternating layers of a hydrolytically degradable synthetic polycation and DNA, which upon incubation with cells, undergo significant rearrangement to present condensed plasmid DNA particles to cells placed in contact with the film (42). This layer-by layer approach has also been used for delivery of lipoplexes from gold surfaces for stent-assisted gene transfer (43).

Furthermore, DNA has been co-precipitated with inorganic minerals (calcium phosphate) onto cell culture surfaces, which supported cell adhesion and enhanced transfection (44), but

required more DNA than typically required for bolus delivery. PEI-DNA complexes have also been freeze-dried onto polystyrene wells and resulted in enhanced cell monolayer formation and transfection upon seeding of a retinoblastoma cell line that is notoriously difficult to transfect (45).

Nonspecific binding of DNA complexes has been extended to mediate delivery from biomaterials for tissue engineering applications. Poly(lactide-co-glycolide) (PLGA) and collagen membranes were coated with phosphatidyl glycerol (1-5%) to support binding of complexes formed with polyamidoamine (PAMAM) dendrimers (46). Vectors were slowly released from this scaffold, yielding transfection *in vitro* comparable to bolus transfection controls. In vivo studies demonstrated a six to eight-fold enhancement in transfection relative to plasmid DNA delivery. Plasmid DNA has also been incorporated into inorganic calcium phosphate co-precipitates adsorbed onto PLGA matrices, which are mostly released by 48 hours and resulted in transfection in cells seeded on the scaffold (47). PEI-DNA complexes nonspecifically adsorbed to PLGA scaffolds resulted in robust substrate-mediated gene delivery, with orders of magnitude less DNA than required for similar transfection levels with bolus delivery (48). PEI-DNA complexes have been seeded on collagen films through deposition and it was determined that varying the thickness of the films, the volume of the deposition solution, the pH of that solution, and the crosslinking densities, varied the levels of transfection efficiency (49).

An alternative strategy to nonspecifically immobilize DNA to substrates or biomaterials is to attach cationic groups to the material to promote naked DNA binding, rather than adsorption of entire complexes. Collagen was cationized through modification with amino groups or

polylysine (50) and degradation of the collagen led to release of the bound DNA. Alternatively, PEI or PLL was bound or blended with PLGA or collagen (51,52), resulting in DNA binding and cellular transfection in vitro. Similarly, plasmid DNA adsorbed onto PLG microparticles coated with the cationic surfactant, cetyltrimethylammonium bromide, was able to transfect dendritic cells in vitro (53). However, plasmid DNA binding to a cationic material may exhibit limited cellular internalization due to strong interactions between the DNA and the material and therefore immobilization of whole complexes to surfaces appears to be a more effective strategy.

2.4.3 Substrate-mediated delivery with viral vectors

While the studies presented in this thesis focus on using nonviral delivery strategies, substrate-mediated delivery of viral vectors has been achieved through both specific and non-specific binding of the virus to the surface. Polystyrene beads and microspheres bind adenovirus vectors non-specifically, which increased transduction efficiency relative to free vector delivery and targeted gene expression in cells in contact with the spheres in vitro and in vivo (54,55). Specific interactions of viral particles with the surface of biomaterials have been incorporated through modification of the biomaterial or virus with functional groups, such as antibodies or biotin residues. Collagen gels modified with antibodies to immobilize vectors localized transduction in vivo relative to control conditions (37,56,57). Alternatively, adenovirus vectors have been chemically modified with biotin groups that are then bound to avidin-conjugated microspheres (58). This approach transduced cells immediately adjacent to the beads in vitro, and enhanced transgene expression for cells that are not readily transduced with adenovirus (58). Adenoviral vectors were also attached to solid surfaces through the biotin-avidin interaction, and

resulted in transduction efficiencies similar to those reported for bolus delivery (59). Recently, viruses have been engineered with functional groups in the viral shell, which would enable binding without chemical modification that can inactivate the virus (60-62).

For substrate-mediated gene delivery of either viral or nonviral vectors, the properties of the surface are critical to both immobilization strategies and transfection efficiencies. However, the properties of the substrate that mediate gene transfer remain poorly understood. Surfaces with controlled chemistries were explored in this thesis as a means to study the effect of the surface properties on substrate-mediated gene delivery and to use those findings to enhance and pattern delivery.

2.5 Self-assembled monolayers for substrate-mediated gene delivery

Delivery of DNA complexes from a substrate is dependent on the interactions between the surface and the complexes. Self-assembled monolayers (SAMs) can be used to study these interactions, as their flexibility in surface chemistry allows preparation of substrates with varying degrees of surface charge and wettability, which are hypothesized to play significant roles in substrate-mediated transfection of nonspecifically immobilized complexes. A SAM is a single layer of molecules on a substrate, which exhibit a high degree of orientation, molecular order, and packing. SAMs form by chemisorption and self-organization of functionalized, long-chain organic molecules onto surfaces of appropriate substrates. The well-defined monolayer forms by noncovalent forces upon exposure of the substrate to a solution or vapor containing the molecules (63). The final monolayer structure is near thermodynamic equilibrium and therefore forms spontaneously and rejects defects (63). SAMs have a dense and stable structure, which

makes them useful for studies of physical chemistry (63). The ability to tailor both the head and tail groups of the functionalized, long-chain organic molecules makes SAMs excellent model systems for the elucidation of interactions on surfaces and at interfaces (63). They are biocompatible and have been used in numerous cell adhesion and protein adsorption studies (64,65).

There are many different choices of chemistries to form SAMs of organic molecules. Monolayers of fatty acids (n-alkanoic acids) on metal oxides occur through an acid-base reaction, forming a surface salt between the carboxylate anion (of the fatty acid) and a surface metal cation (63). Monolayers of organosilicon derivatives (alkychlorosilanes, alkyalkoxysilanes, alkylaminosilanes) on hydroxylated surfaces occur by forming polysiloxane at the surface, connected to surface silanol groups (-SiOH) via Si-O-Si bonds (63). Monolayers of organosulfur adsorbates on metal and semiconductor surfaces rely on the affinity of sulfur compounds to transition metal surfaces and the possibility to form multiple bonds with surface metal clusters (63).

The best characterized organosulfur adsorbates used in SAMs are alkanethiolates on Au surfaces [reviewed in (63)]. Alkanethiols chemisorb to gold, with the loss of dihydrogen to form adsorbed alkanethiolates (66). The nature of the gold bond is not completely understood, though the generally assumed equation is $R\text{-}SH + Au(0)_n \rightarrow RS\text{-}Au(I)Au(0)_{n-1} + \frac{1}{2} H_2\uparrow$ (67). When gold substrates are immersed in ethanolic solutions of low alkanethiol concentration (Figure 2-4), two distinct adsorption kinetics are observed. The first step involves the adsorption of alkanethiol to gold, which occurs in a matter of seconds or minutes. Within this time, contact angles are close to limiting values and the thickness is 80-90% of maximum. This step is

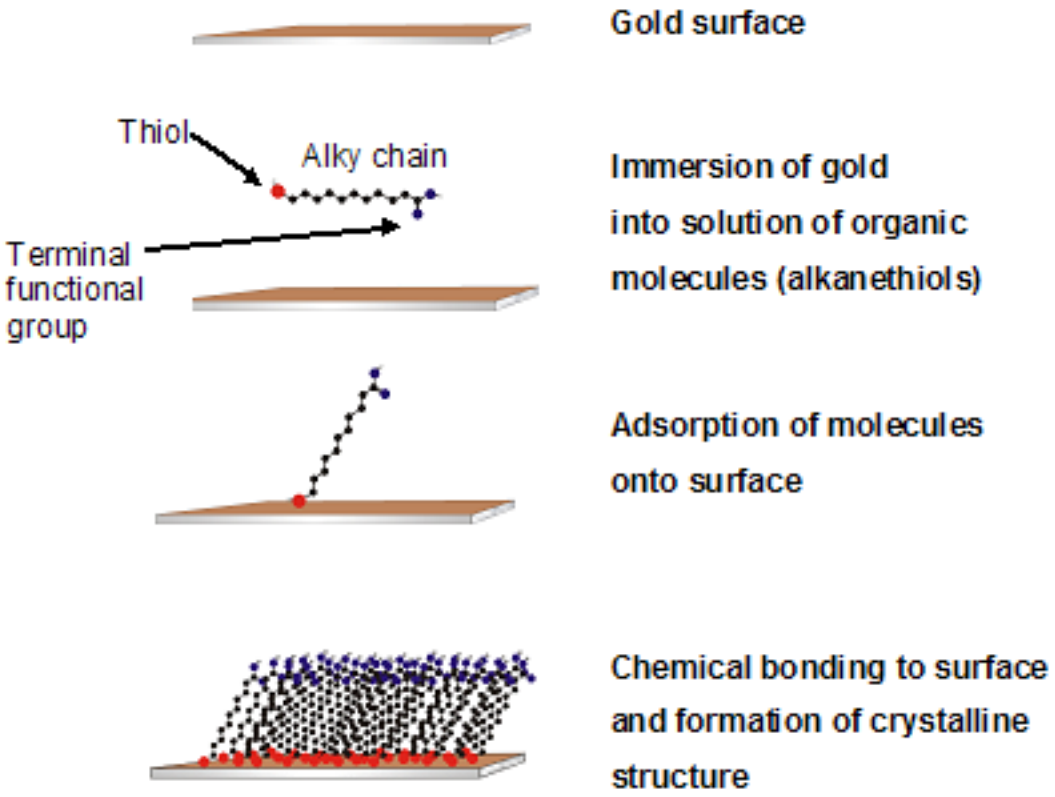

Figure 2-4 Formation of SAM of alkanethiols chemisorbed to Au substrate. Gold surface is immersed into an ethanolic solution containing organic molecules, which contain a head group (thiol) capable of chemisorbing to the surface, an alkyl chain, and a terminal functional (tail) group that confers properties to the surface. Organic molecules adsorb to the surface quickly, and then bond to the surface and form characteristic crystalline structure.

dependent on the concentration of alkanethiols. The second step involves surface crystallization and is relatively slow, lasting several hours. At the end of this step, the SAM thickness and contact angles reach their final values (63).

Alkanethiols with different terminal functional groups can be used to generate SAMs with different surface properties (Figure 2-5). The three alkanethiols most commonly used

throughout the studies presented in this thesis include 1-decanethiol (DT10), mercapto-1-undecanol (MUOH), and 11-mercaptoundecanoic acid (MUA). Surfaces with SAMs of DT10 are hydrophobic (contact angles greater than 100°), surfaces with SAMs of MUOH are uncharged and hydrophilic (contact angle <20°), and surfaces with SAMs of MUA are charged and hydrophilic (contact angle <10°). The formation of the MUA monolayer is very rapid, within 10-30 minutes, but formation of DT10 monolayers may take 6-12 hours to form. Mixtures of two alkanethiols can be used to generate more complicated surface chemistries, and typically do not result in phase-separated islands (68). SAMs of alkanethiols on gold can be used in cell culture for periods of days (67) and have been used in many cell culture studies, particularly to understand molecular surface determinants required for adhesion dependent cell growth and proliferation (69-71).

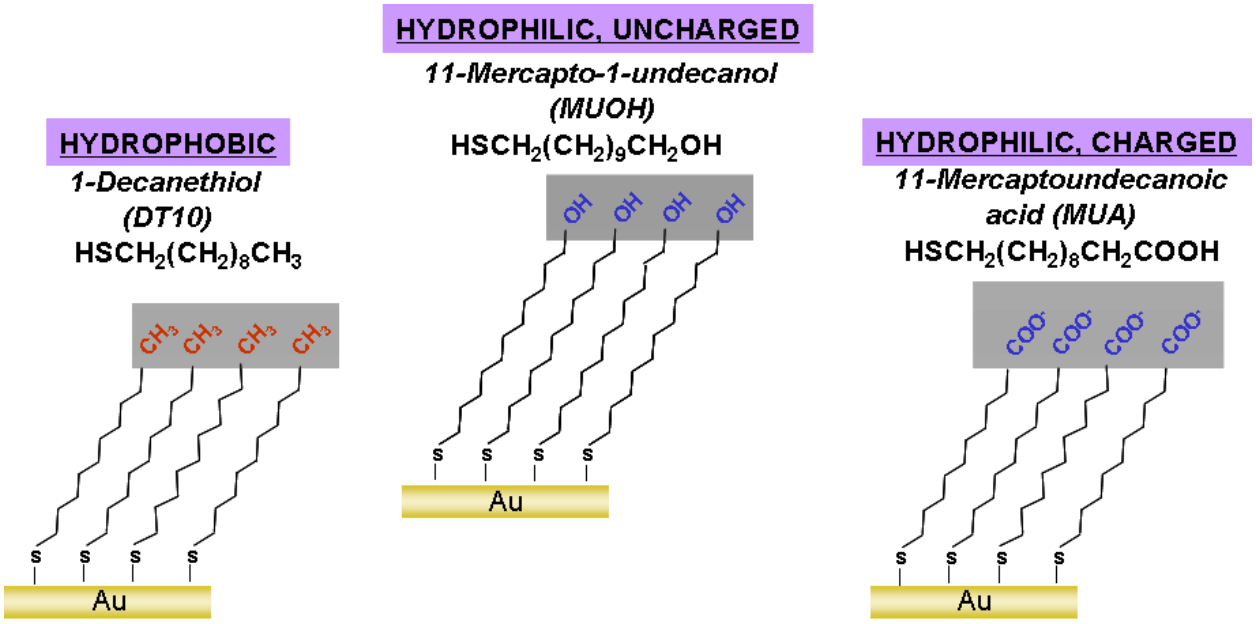

Figure 2-5 Commonly used alkanethiols for SAM formation.

2.5.1 Microcontact printing

Microcontact printing (μCP), a soft lithographic technique, can be used to imprint gold substrates with specific patterns of SAMs using an elastomeric stamp (65,72,73), reviewed in (74). The flexibility in surface chemistry of SAMs permits preparation of patterned surfaces with varying degrees of surface charge, wettability, and resistance to protein adsorption. Typically a polydimethylsiloxane (PDMS) stamp is used to pattern the adsorption of alkanethiols in SAMs on gold. The PDMS stamp can be polymerized against a large feature mold or a mold prepared using standard lithographic techniques, depending on required feature size. Stamps are loaded with alkanethiols through ink pads, cotton-tips swabs, or immersion of the stamp in the desired alkanethiol. The stamp is then brought into contact with the gold, resulting in patterned adsorption of the first alkanethiol. The remaining bare regions of gold are then derivatized with a second alkanethiol, which adsorbs to the non-stamped regions (Figure 2-6).

SAM surfaces patterned in regular arrays of hydrophilic regions amongst a background of hydrophobic regions can result in the formation of condensation figures (CFs) (Figure 2-6), water droplets formed from regions with different wettabilities (75,76). CF formation is both temperature and humidity dependent (75). The formation of these CFs, created by simply pipeting water onto the stamped surface, was traditionally used as a method to detect contamination on a homogeneous surface, to image surfaces, or as microreactors. These hydrophilic/hydrophobic arrays have since been used to anchor droplets, concentrating a sample during evaporation, to prepare protein samples for MALDI-MS (77), for pinning of aqueous solutions of DNA at specific array locations for microarray fabrication (78,79), and for DNA deposition by CFs on the hydrophilic regions (80), for subsequent chemical attachment of the

DNA to the surface. In the work presented in this thesis, these CFs were utilized to confine droplets containing DNA complexes to certain regions of a surface, resulting in patterned DNA deposition or immobilization on a surface.

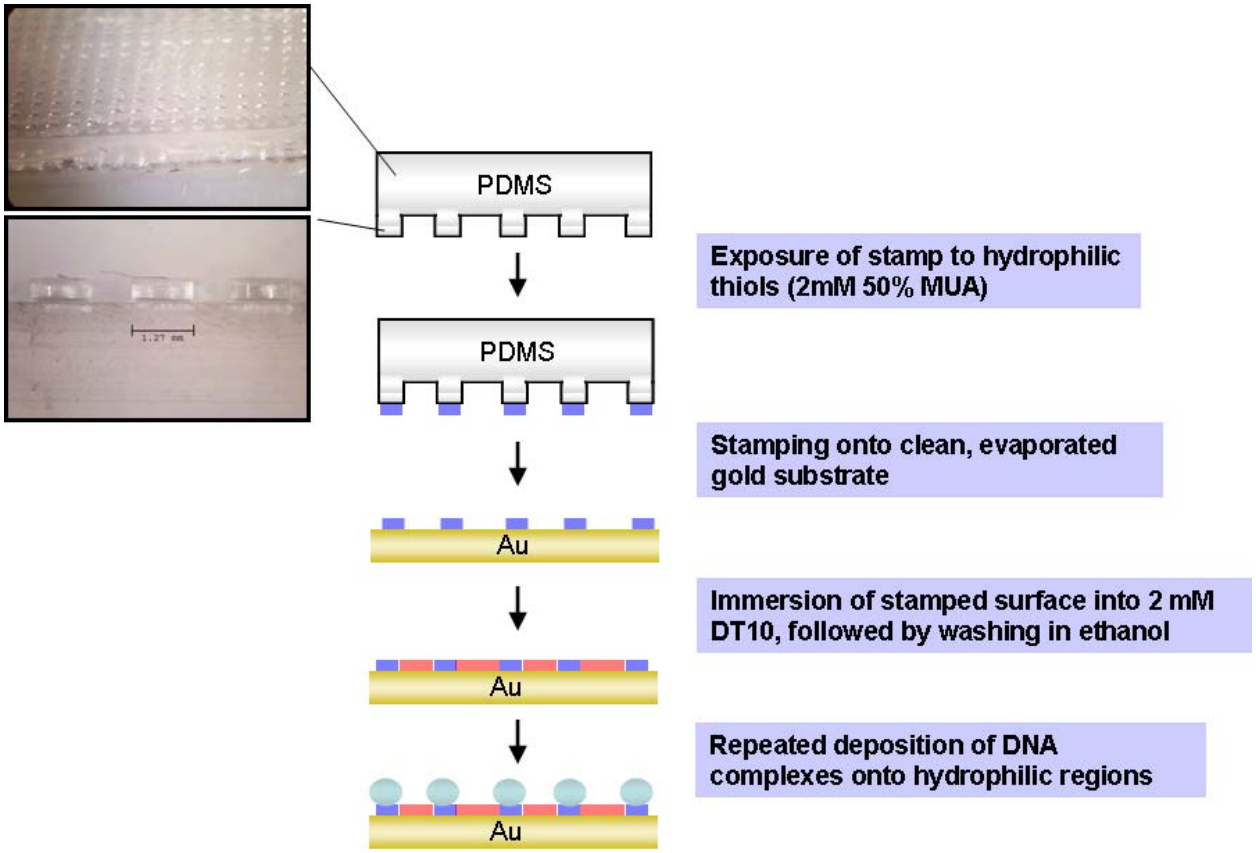

Figure 2-6 Microcontact printing of SAMs to create regions of hydrophilic spots in a background of hydrophobic alkanethiols, which support formation of condensation figures upon addition of aqueous solution containing DNA complexes.

Chapter 3

Applications of Substrate-Mediated Gene Delivery

3.1 Introduction

Controlled release systems typically employ biomaterials that deliver vectors according to two general mechanisms: i) polymeric release in which the DNA is released from the polymer or ii) substrate-mediated in which DNA is retained at the surface (81). In comparison to traditional gene delivery systems, controlled release can enhance gene delivery to cells within or adjacent to the biomaterial and increase the extent and duration of transgene expression, while reducing the need for multiple interventions. Additionally, localized vector delivery to specific tissues can avoid distribution to distant tissues, decrease toxicity to non-target cells, and reduce the immune response. These controlled release-based gene delivery systems capitalize on both specific and non-specific interactions between the biomaterial and vector, to achieve either release into the extracellular space or immobilization at the surface. While the potential to use these polymeric systems has been established, the design parameters by which to optimize or control gene transfer are not well understood. Vector and biomaterial development, combined with studies that correlate system properties with the quantity and duration of protein production, and the number and location of cells expressing the transgene will lead to molecular scale design of delivery systems. The development of these systems may increase the efficacy within current gene therapy trials, but may more importantly extend the applicability of gene delivery to other areas such as tissue engineering and functional genomics.

3.2 Tissue engineering

While there have been a multitude of polymeric release systems designed to incorporate DNA or DNA complexes within polymeric tissue engineering scaffolds (reviewed in (81)); the potential for substrate-mediated gene delivery to be extended to tissue engineering applications is just beginning to be explored. In these tissue engineering applications, the scaffold provides the structural support for cell adhesion and gene delivery from the surface of the scaffold provides a method to stimulate cellular pathways in tissue regeneration (82). Implantable biomaterials with immobilized DNA or DNA complexes could promote localized gene delivery, by maintaining elevated DNA concentrations in the cellular microenvironment, which improves gene delivery (30). Additionally, viral and non-viral vectors may have a relatively short half-life (83-85), and release systems, such as substrate-mediated gene delivery, could prevent their degradation and/or provide a sustained release.

As described in the previous chapter, substrate-mediated gene delivery has been adapted to tissue engineering scaffolds, including hyaluronic acid-collagen hydrogels (22), PLGA scaffolds (46-48) and collagen films (49). While these studies demonstrate the potential for using substrate-mediated gene delivery in tissue engineering applications, no specific in vivo application or tissue formation was reported in any of the studies. Application of fibrin matrices, loaded with covalently attached DNA-peptide complexes encoding for hypoxia-inducible factor-1α, to a dermal wound site resulted in increased angiogenesis (86), but these complexes, which were released upon degradation of the fibrin matrix, may be considered to be delivered via a polymeric release approach.

Most tissue engineering applications of substrate-mediated gene delivery involve localized gene transfer to the cardiovascular system (87). The potential to treat heart valve disease was explored using polyurethane prosthetic heart valve leaflets with immobilized adenoviral vectors tethered specifically through antibody attachment strategies (88). In vivo reporter gene expression was localized to cells attached to the leaflets with no detectable vector DNA in blood or distal organs. Viruses have also been tethered to endovascular microcoils (56) used in procedures to treat cerebral aneurysms and in vivo reporter gene expression was localized to cells adjacent to the implant, without evidence of DNA delivery to distal sites. Intravascular stents with immobilized plasmid DNA (43,89-91) or adenoviral vectors (37,57,92) were studied for their ability to locally deliver genes to the arterial wall for the treatment of coronary artenery disease to relieve atherosclerotic obstruction, in particular to prevent in-stent restenosis. While several studies demonstrated that cells adjacent to the stent expressed a reporter gene in vivo (37,57,90-92), stent-based delivery of a therapeutically relevant gene has yet to be realized.

The challenge of tissue engineering lies in creating an environment that provides the appropriate combination of signals to induce proper cell function and restore normal tissue function. The scaffold serves as a support for cell growth and localized DNA delivery can provide the signals to direct progenitor cell differentiation. Adapting the delivery strategies to control transgene expression spatially (μm to mm) or temporally (days to months) may recreate the environmental complexity present during tissue formation (93). The ability to regulate expression of one or more factors in time and space may be critical to the engineering of complex tissue architectures, such as those found in vascular networks and the nervous system.

Although several fundamental requirements for the scaffold structure have been identified (94), the design principles underlying gene delivery in tissue regeneration remain to be identified.

3.3 Transfected cell arrays

Perhaps the most reported application of substrate-mediated gene delivery is the ability to use the delivery technique in functional genomics studies, in particular the transfected cell array. Transfected cell arrays represent a high throughput approach to correlate gene expression with functional cell responses, based on gene delivery from a surface (95). While traditional cDNA microarrays can quantitatively compare the expression level of thousands of genes under controlled conditions, understanding the cellular responses of human disease requires more than just knowledge of gene expression profiles; one must understand the cellular and physiological context in which the gene expression is acting (96). Transfected cell arrays present a powerful approach to study gene function in the context of a living cell, allowing proteins to be translated and folded naturally and interact within the environment of the cell. Transfected cell arrays offer compact, economical, and high-throughput analysis in living cells that provides greater consistency across assays and facilitates comparisons between conditions, while reducing the amount of reagents and cell numbers required, which is an important factor for difficult to prepare cell types (97,98). Methods to use mammalian cells as suitable screening systems, like transfected cell arrays, need to be developed to elucidate gene function and cellular pathways responsible for diseases (99). A transfected cell array could provide a method to link gene expression to functional cell responses and to detect genes that are truly responsible for a cellular

effect, with the potential to impact nearly all aspects of medicine, such as determining molecular markers or targets, prior to the costly development of novel diagnostic and therapeutic strategies.

The first transfected cell array was published by Sabatini's group in 2001 (95). The reverse transfection cell-based microarray was created by printing mixtures of different DNA plasmids and gelatin into specific domains onto a substrate. A lipid-based transfection agent was then floated over the surface of the array, and HEK293T cells were seeded onto the array, forming a living cell microarray of locally transfected cells in a lawn of nontransfected cells. The array was used to analyze gene functions for phosphotyrosine activity and six genes were identified to be associated with this activity; five genes encoded known tyrosine kinase proteins and one encoded a protein of unknown function (95).

Since the original paper, the transfected cell array has been adapted to a variety of applications, to study signaling pathways (100), screen antibody fragments (101), identify possible new lysophosphatidic acid receptors (102), perform protein localization studies (103,104), screen for proapoptotic genes (105,106), and annotate protein function (107). The transfected cell array has also been adapted to high-throughput RNAi studies (108), specifically for analysis of spindle formation (109), secretory pathways (110), and chromosome segregation and nuclear structure in a time-lapse system (111).

Transfected cell microarray studies that offer technological improvements on the basic reverse transfection principle have been published. Efforts to improve transfected cell arrays have included incorporating fibronectin (112), atelocollagen (113), and recombinant proteins (114) with plasmid DNA or DNA complexes to mediate high transfection in the array. Studies have also investigated the effect of surface properties of the slide, including substrate

hydrophobicity on transfection efficiency in array (115), as well as the effect of coating cationic polymer and collagen onto surfaces prior to transfection (116). Micropatterning strategies have been used to create arrays of transfection using self-assembled monolayers to pattern DNA (117,118) or siRNA (119) complex immobilization on gold slides, as well as electrodes to deliver plasmids through electroporation (120,121). Micropatterning has been extended to hydrogels (122) for array fabrication. Arrays have also been formed with dendrimers (123), magnetic beads (124) and viral vectors (59,125,126), for Drosophila cells (127) and nonadherent cells (128).

While there have been technical advances in transfected cell arrays, further development of a well-characterized, substrate-mediated approach for transfected cell arrays requires the development of a cost-effective delivery system that efficiently transfects a wide variety of primary cells and cell lines, while allowing for spatially-controlled DNA within the different domains (95,129,130). Furthermore, improvements are needed to this technology to accommodate issues with transfection efficiency, normalization, post-transfection processing, sensitivity, image acquisition and quantification, as well as expanding the biological endpoints examined, in particular to elucidate gene function and cellular pathways responsible for diseases (96-98).

3.3.1 Transfected cell arrays to monitor estrogen receptor in breast cancer

Oncogenic state is a complex process and development involves the accumulation of multiple independent mutations that lead to deregulation of cell signaling pathways central to the control of cell growth and fate (131,132). The activity of various pathways within cancer cells

could be used to link molecular observations with the cellular basis of disease. A transfected cell array could be used to report on the activity of multiple signal transduction pathways and be used as a screen to identify which signal pathways are active within cancer cells**.** Using cancer cells from a biopsy, the transfected cell array could thus identify patient-specific expression patterns to tailor therapies for more effective treatment regimes.

The American Cancer Society estimates that in 2006, 214,640 American women will have been diagnosed with breast cancer, and an estimated 41,430 women will have died from the disease (133), second only to lung cancer. In the next 10 years, 5 million women worldwide are expected to be affected by breast cancer (133), and thus further advancements in early diagnosis and treatment are needed. While therapeutic targets are now being identified for both cancer prevention and treatment, individualization of treatment regimens to maximize response, to minimize morbidity and mortality, and to prevent the occurrence of a second breast cancer, has become the new therapeutic goal.

Estrogen is a known mammary epithelial cell carcinogen (134). Estrogenic control over several G1 cell-cycle regulators and growth factors has been demonstrated both in vivo and in vitro (135,136). Estrogenic promotion of cellular proliferation in particular, is believed to put responsive ductal cells at risk for carcinogenesis by facilitating or even inducing the acquisition of genetic changes during cell cycle progression (135,137). The specific action of estrogen is mediated by the estrogen receptors (ER) α and β (138). These steroid hormone receptors are members of the nuclear receptor superfamily of transcription factors and regulate transcription of target genes in an estrogen-dependent manner, through binding of the ligand, estradiol (E_2) (138,139). The ligand E_2, a hydrophobic molecule, readily diffuses across the plasma and

nuclear membranes and once inside the nucleus, binds to the ligand binding domain of the ER, which undergoes a crucial conformational change. The receptor then homodimerizes with another ER and they then interact with the estrogen response element (ERE) in promoters of estrogen-responsive genes (139). Through regulation of transcription, ERs modulate physiological processes, including reproductive organ development and function, bone density, and also contribute to the growth and development of breast and endometrial cancers (138).

The two estrogen receptors (α and β) are encoded by separate genes and are distinct. While they share 53% sequence identity in their ligand binding domains, the two receptors exhibit subtle differences in ligand binding specificity (138) and targets. In women, ERα is expressed in the brain, cardiovascular system, uterus, bone, breast and liver (138,139). ERα is the predominant ER expressed in breast cancer, while the function of ERβ and its role in breast cancer remains unclear (139). Estrogens, via ERα, act as potent mitogens of ER-positive breast cancer (140) and ERα expression is one of the most important biomarkers for determining treatment course for clinical breast cancer (138). ERα expression was originally used to determine clinical outcome of tumor therapy (141), and can now be used to select patients with ERα-positive breast tumors, which increases their chance of responding to endocrine therapy (139). The presence of ERα is not only an important predictive test for success of any endocrine treatment of breast cancer, but the functional significance of ERα in breast cancer has made it a predominate target of therapies aimed at the prevention and treatment of this disease (138,139,141). Selective estrogen receptor modulators, like tamoxifen, are competitive

inhibitors of E_2 at the ERα (138), and have been shown to be effective therapies, preventing the interaction of estrogen with ERα and therefore decreasing proliferation of target cells.

While microarrays have enabled high throughput gene expression profiling of breast cancer cells and tumors (142,143) to classify breast tumors into molecular subtypes, traditional cDNA and tissue microarrays use cell lysates or fixed tissue to provide a snapshot of the intracellular composition (i.e. mRNA or protein content). However, linking these expression profiles to functional endpoints is limited by the complexity and interconnectedness of the intracellular signaling network. We hypothesize that the interface between genotypic abnormalities and the phenotype lies not in the mRNA or protein content, but in the activity of the signal transduction pathways and gene regulation. Simple expression of transcription factors like ERα does not necessarily reflect pathway activation, as transcription factor activity is regulated through diverse mechanisms (144), including heteromeric complexes, ubiquitination, methylation, acetylation, and phosphorylation. Transfected cell arrays represent an approach to enable the high throughput analysis of cellular activity within a cellular context to investigate the genotype-phenotype interface. Through this novel technology, molecular observations could be linked to the cellular basis of disease, which may lead to more effective and tailored therapies.

Chapter 4

Substrate-Mediated Delivery from Self-Assembled Monolayers: Effect of Surface Ionization, Hydrophilicity, and Patterning

4.1 Introduction

Gene transfer has many potential applications in basic and applied sciences, including functional genomics, gene therapy, and tissue engineering. Although plasmid DNA provides transfection in vivo, complexing DNA with nonviral vectors, cationic lipids or polymers, can facilitate internalization and transfection in vitro and in vivo (7-9). Controlled delivery systems, including polymeric release in which the DNA is released from the polymer, or substrate-mediated delivery, in which DNA is retained at the surface, have the potential to overcome extracellular barriers that limit gene transfer, as well as enhance gene delivery relative to more traditional delivery methods (81). In substrate-mediated delivery, also termed reverse transfection or solid-phase delivery, plasmid DNA or DNA complexes are immobilized to a surface or biomaterial that supports cell adhesion. Placing the DNA directly in the cellular microenvironment increases its local concentration, which has been shown to enhance gene delivery (30). Cells cultured on the substrate can internalize the DNA either directly from the surface, or after release of the DNA from the surface.

DNA complexes can be immobilized on the substrate through specific or nonspecific interactions for delivery from the surface. Specific interactions can be introduced through complementary functional groups on the vector and surface, such as antigen-antibody or biotin-

avidin (5,37). Poly(L-lysine) (PLL) and polyethylenimine (PEI), modified with biotin residues, were complexed with DNA and bound to a neutravidin substrate (5,6), resulting in 100-fold increased transgene expression from the immobilized complexes relative to bolus delivery of complexes (5). Additionally, transfection was observed only in the location to which complexes were bound, suggesting the possibility of spatially regulating DNA delivery.

Plasmid DNA or DNA complexed with cationic polymers or lipids can also interact with substrates through non-specific, noncovalent mechanisms (2,46,145-147), including hydrophobic, electrostatic, and van der Waals interactions. These interactions have been well-characterized for adsorption and release of proteins from polymeric systems (40,41). Polyplexes and lipoplexes non-specifically immobilized to substrates have been shown to enhance the extent of transgene expression in both cell lines and primary human-derived cells, along with an increased cellular viability (2). This enhancement was dependent on both the properties of the complex (e.g., complexation agent, N/P ratio), and substrate. However, the properties of the substrate that mediate gene transfer remain poorly understood.

In this chapter, self-assembled monolayers (SAMs) of alkanethiols on gold were used to investigate substrate-mediated transfection by non-specifically immobilized complexes. SAMs provide a flexible system to regulate the terminal functional group chemistry to examine the complex-substrate interactions (63,148,149). Hydrophilic substrates with varying densities of ionic functional groups, as well as hydrophobic substrates, were examined for their ability to bind and release complexes, and to subsequently support transfection. Furthermore, the flexibility in surface chemistry of SAMs permits preparation of patterned surfaces with varying degrees of surface charge and wettability. Microcontact printing (μCP), a soft lithographic

technique, was used to imprint gold substrates with specific patterns of SAMs using an elastomeric stamp (65,72-74), creating regions of different surface properties. Here we demonstrate the ability to use micropatterning to pattern DNA complex immobilization and transfection.

4.2 Material and methods

4.2.1 Gold slide preparation and monolayer self assembly

Gold-coated glass slides, composed of a titanium adhesion layer and 100 – 500 Å of gold, were prepared using e-beam evaporation (Edwards Electron Beam Evaporator, Wilmington, MA). The gold-coated slides were then cut into smaller pieces with a diamond-tipped glass cutter, so that pieces fit into standard 48-well tissue culture plates. These gold pieces were prepared for SAM formation by treatment with oxygen plasma (Harrick Scientific, Ossining, NY), followed by sonication in ethanol, or alternatively cleaned in acetone and ethanol, with subsequent drying under a stream of nitrogen.

SAMs were formed by immersion of the clean gold substrates into 2 mM ethanolic solutions of alkanethiols for 30 minutes to overnight in the dark, depending on monolayer characteristics. Monolayers were formed with three different alkanethiols and combinations thereof, including 1-decanethiol (DT10), 11-mercapto-1-undecanol (MUOH), and 11-mercaptoundecanoic acid (MUA) (Aldrich, St. Louis, MO). Alkanethiol solutions were (freshly) prepared in filtered, degassed ethanol. After monolayer formation, SAM samples were rinsed in pure ethanol and dried with nitrogen before further use.

4.2.2 Verification of surface chemistry

X-ray Photoelectron Spectroscopy (XPS) was used to analyze the surface functional groups of the SAMs to verify successful modification. XPS spectra were recorded using an Omicron ESCA Probe system with an Al/Mg anode X-ray source. A single survey scan spectrum (range 20 - 1000 eV) and 3-5 narrow scans for C1s (275-295 eV) and O1s (525-550 eV) were recorded for each sample. Analysis of the data was performed using Multipak software (Physical Electronics, Inc, Eden Prairie, MN). Chemical shifts were referenced to C1s at 285 eV. Surface modification by SAM formation was also analyzed by the measurement of contact angles of water in air on the various SAMs at room temperature with a goniometer (Ramé-Hart; Mountain Lakes, NJ).

4.2.3 Quantification of DNA complex immobilization and release

Plasmid DNA encoding for luciferase (LUC) and enhanced green fluorescent protein (EGFP) with a CMV promoter was purified from bacteria culture using Qiagen (Santa Clara, CA) reagents and stored in Tris-EDTA buffer (10 mM Tris, 1 mM EDTA, pH = 7.4) for binding, release and transfection experiments. For DNA complex formation, Lipofectamine 2000 (Life Technologies, Gaithersburg, MD) in serum-free cell growth media (DMEM, Life Technologies) was added drop wise to DNA in serum-free cell growth media, mixed by gentle pipetting, and incubated for 20 minutes.

The binding and release of DNA complexes from various SAMs was monitored using plasmid DNA radiolabeled with α-^{32}P dATP. Briefly, a nick translation kit (Amersham Pharmacia Biotech; Piscataway, NY) was used following the manufacturer's protocol with minor

modifications (6). The labeled DNA was diluted with unlabeled DNA to a final concentration of 1% and this mixture was then used to form DNA complexes. After SAM preparation, digital photographs of each sample were taken before complex immobilization, and analyzed with ImageJ (NIH) to determine the area of each surface. Complexes (1 μg of DNA at a DNA (μg):lipid (μL) ratio of 1:2) were immobilized by incubation on SAMs for 2 hours, followed by two wash steps with serum-free cell growth media. The quantity of DNA immobilized was determined by immersing individual SAM samples in scintillation cocktail (5 mL, ScintiVerse II) for measurement with a scintillation counter. The counts were correlated to DNA mass using a standard curve. The density of DNA immobilized to each SAM sample was determined by normalizing the amount bound to area and reported as the mean ± s.e.m. of three replicates.

The release profiles from SAMs with immobilized DNA complexes were determined by incubation with serum-containing cell growth media at 37°C in a humid chamber. At predetermined time points, half of the media was removed and replaced with fresh media. The activity of the collected sample was measured in a scintillation counter. At the final time point, the counts remaining on the SAM samples were also determined. The percentage of DNA released was calculated as the ratio of the cumulative counts released through a given time divided by the total counts initially on the substrate, thus, the release curves represent the percentage of DNA released relative to the initial amount bound to each surface.

4.2.4 Transfection on SAMs

Transfection studies were performed with NIH/3T3 (ATCC; Manassas, VA) cells cultured at 37°C and 5% CO_2 in DMEM supplemented with 1% sodium pyruvate, 1%

penicillin-streptomycin, 1.5 g/L $NaHCO_3$ and 10% fetal bovine serum. After complex formation and immobilization as described above, SAMs were immediately seeded with 15,000 cells in 48-well plates. Transfection was analyzed following a 48-hour culture, characterized through the extent of transgene expression, which was quantified by measuring the luciferase activity using the Luciferase Assay System (Promega, Madison, WI). Cells were lysed and assayed for enzymatic activity after 48 hours. The luminometer (Turner Designs, Sunnyvale, CA) was set for a 3 second delay and an integration of the signal for 10 seconds. Luciferase activity was normalized to the total protein amount determined with the BCA protein assay (Pierce, Rockford, IL). The effect of SAMs on cell morphology and adhesion was determined by cell seeding on SAMs, as described above, in the absence of DNA complex immobilization.

4.2.5 Patterned SAMs and complex deposition

Microcontact printing (μCP) with a polydimethylsiloxane (PDMS) stamp was used to imprint gold surfaces with specific patterns of hydrophilic alkanethiols, which could be used to regulate the location of DNA deposition and subsequent delivery from the surface. For stamp fabrication, PDMS was prepared in a 10:1 (v:v) ratio of Silicone Elastomer-184 and Silicone Elastomer Curing Agent-184 (Sylgard 184, Dow Corning, Midland, Michigan) by mixing the base and curing agent at least 50 times using a syringe mixing system. After allowing all air bubbles to escape, the PDMS was poured directly into a metal mesh master mold, situated between two blocks of polyethylene with neoprene spacers, and cured at room temperature for approximately 3 days. The stamp was then removed from the mold, and washed with ethanol and dried under nitrogen before each use. This master produced stamps with approximately 1-

mm features. Alternatively, PDMS stamp molds were also fabricated by spin coating SU-8 negative photoresist (MicroChem, Newton, MA) onto a silicon wafer, exposing photoresist to UV through a mask for 10 seconds, and then developing the photoresist following the manufacturer's instructions. The mask was prepared using a computer drawing program to create a pattern that was printed onto a transparency (67,74), also with 1-mm features. PDMS (5.5 g) was poured onto the photolithographic mold, cured at 60°C for 1-3 hours, and then carefully peeled away from mold. The stamp was cleaned in an oxygen plasma cleaner, rinsed in acetone and methanol, and dried under nitrogen before each use.

For μCP of alkanethiols, the PDMS stamp was inked with a 2 mM solution of 50% MUA/50% MUOH thiols and then dried under nitrogen. The stamp was then placed in contact with a gold substrate for 1-5 minutes. The stamped substrate was then carefully peeled from the stamp and immersed into a 2 mM solution of DT10 for 15-60 minutes. After derivatization with the secondary thiol, the stamped surface was washed twice in ethanol and dried under nitrogen.

Secondary Ion Mass Spectrometry (SIMS) was used to verify the spatial distribution of SAMs on the stamped surface by imaging the two-dimensional distribution of chemical species on the submicron scale. SIMS spectra and images for bulk and patterned surfaces were recorded using PHI TRIFT III ToF-SIMS system (Physical Electronics, Inc, Eden Prairie, MN). The two dimensional distribution was obtained using stage raster imaging techniques, scanning specifically for OH, S, $C_2H_2O_2$, Au, CHO_2, $C_2H_3O_2$, and C_2H chemical species in negative mode. Furthermore, water droplets termed condensation figures (CFs), which form from regions with different wettabilities (76), were used as an additional method to verify and image SAM patterns on the surface, by simply pipeting MilliQ water onto the stamped surfaces.

Plasmid DNA (pEGFP-LUC) was labeled with tetramethyl rhodamine (Label IT Nucleic Acid Labeling Kit, Mirus, Madison, WI). This DNA was used to form complexes with Lipofectamine 2000, as described above. Complexes were then deposited onto patterned SAM surfaces in CFs formed on the hydrophilic areas. Complexes were allowed to deposit for a period of one hour, in humid conditions, and then visualized with fluorescence microscopy. Control deposition studies were performed with rhodamine-labeled DNA complexes immobilized on uniform 50% MUA/50% MUOH and DT10 SAMs.

4.2.6 Patterned transfection

On a patterned SAM surface, 0.5 μg of plasmid DNA (pEGFP-LUC) complexed with lipid (1:2.5, DNA to lipid ratio) in a total volume of 50 μl, was deposited in CFs that formed on the hydrophilic regions over the entire surface for one hour, in humid conditions. The droplets were then removed with a stream of nitrogen and deposition was repeated for up to five times, with freshly prepared complexes using the same conditions as above. The patterned surface was then washed with media and NIH/3T3 cells were seeded as described above. Transfection was analyzed following a 48-hour culture and characterized through the number of transfected cells, using GFP expression. Transfected cells were visualized and manually counted using an epifluorescence microscope (Leica; Bannockburn, IL) with a FITC filter and equipped with a digital camera. The percentage of transfected cells was calculated as the ratio of the number of transfected cells divided by total cell number, which was determined by manual counting of phase images. Control transfection studies were performed on uniform 50% MUA/50% MUOH and DT10 SAMs.

4.2.7 Statistics

Statistical analysis was performed using JMP software (SAS Institute, Inc., Cary, NC). Comparative analyses were completed using one-way ANOVA with Tukey post-tests, at a 95% confidence level. Mean values with standard error of the mean are reported and all experiments were performed in triplicate.

4.3 Results and discussion

4.3.1 Surface characterization

SAM formation was confirmed with XPS and contact angle measurements. The XPS spectra (Figure 4-1) indicated that while the gold substrate showed minimal carbon, oxygen, or sulfur peaks, the MUA SAM sample containing carboxylic acid groups had a peak at binding energy ~289 eV, characteristic of the carbon in the COOH groups (150). Additionally, the O1s peak intensity further verified the presence of carboxylic acid groups in the MUA sample. The low sulfur intensity was similar to XPS spectra previously reported (150). Spectra for other SAMs also indicated successful modification (data not shown). Substrate modification by SAM formation was further confirmed by the measurement of contact angles of water droplets in air on the various SAMs. The wettability of the surfaces indicated that the DT10 SAMs were hydrophobic (angles greater than 110 degrees), while surfaces with SAMs of MUOH and MUA were hydrophilic (angles less than 30 degrees), as expected (148,150,151). Additionally, contact angles for all SAMs were different than that of gold, indicating surface modification.

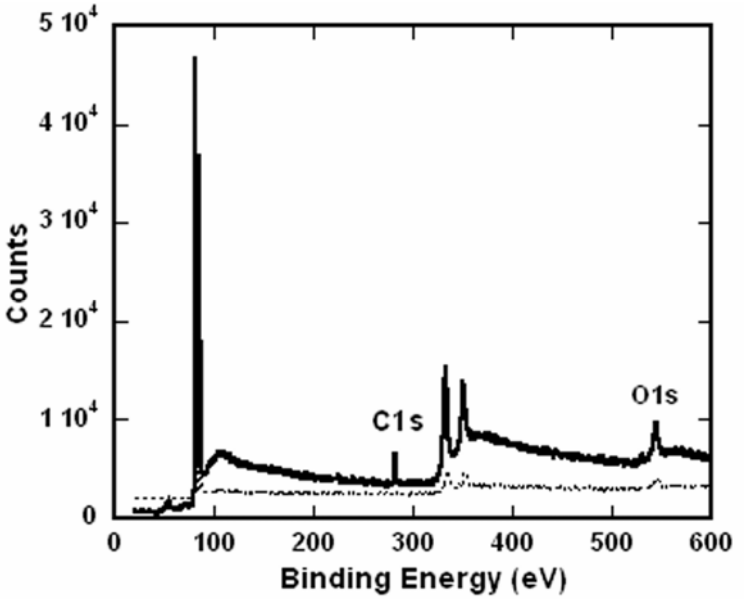

Figure 4-1 XPS verification of SAM formation. XPS spectrum of a MUA surface (solid line) relative to a gold surface (dashed line) indicated increases in carboxylic acid groups at binding energy ~289 eV, characteristic of the carbon in the COOH groups. The O1s peak intensity further verified the presences of the carboxylic acid groups in the MUA sample.

4.3.2 Quantification of complex immobilization

SAMs of alkanethiols on gold were used to investigate the relationship between surface properties and nonspecific immobilization of DNA complexes. Both hydrophilic and hydrophobic surfaces were investigated, including hydrophilic substrates with varying densities of charged, carboxylic acid groups. The amount of DNA immobilized to the surfaces ranged from 63 ng/cm^2 to 29.5 ng/cm^2, as the percentage of carboxylic acid functional groups decreased from 100% (100% MUA) to 0% (0% MUA, 100% MUOH) (Figure 4-2A). Binding of DNA complexes on 100% MUA surfaces was significantly greater than 50% MUA SAMs ($p < 0.01$), as well as 10% MUA, 1% MUA, and 0% MUA SAMs ($p < 0.001$). Surfaces containing 50 %

carboxylic acid groups resulted in statistically greater binding than substrates with 10% ($p < 0.01$) or 1% ($p < 0.001$) charged groups.

In addition to the percentage of carboxylic acid groups, the hydrophobicity of the SAMs also affected the amount of immobilized DNA complexes (Figure 4-2B). While complex binding was statistically greater on a hydrophilic SAM containing 100% carboxylic acid functional groups as compared to a hydrophobic DT10 SAM (49.4 ng/cm^2, $p < 0.01$), the opposite was true for hydrophilic surfaces with few or no charged functional groups. DNA complex adsorption was statistically greater on a hydrophobic substrate (Figure 4-2B) than hydrophilic surfaces containing 10% ($p < 0.01$) or fewer ($p < 0.001$) carboxylic acid groups (Figure 4-2A and B). For any SAM substrate, the amount bound corresponded to less than 4% of DNA initially added to the surface, which is less than previously reported for similar deposition schemes (2).

Surface ionization and hydrophobicity were both found to mediate complex immobilization. Increasing the density of charged functional groups on the surface increased complex immobilization, suggesting that electrostatic interactions play a major role in binding. However, statistically greater adsorption to a hydrophobic substrate (DT10) as compared to a nonionic, hydrophilic surface (100% MUOH) suggests that immobilization can also be mediated by hydrophobic interactions. Substrate hydrophobicity has previously been shown to play a significant role in relative local DNA plasmid concentration within deposited spots of an array (115,148,149,152), with higher surface immobilization on hydrophobic polystyrene substrates as compared to more hydrophilic, treated surfaces. DNA polyplex adsorption was also found to be higher on polystyrene substrates, as compared to more hydrophilic, serum-modified surfaces (2).

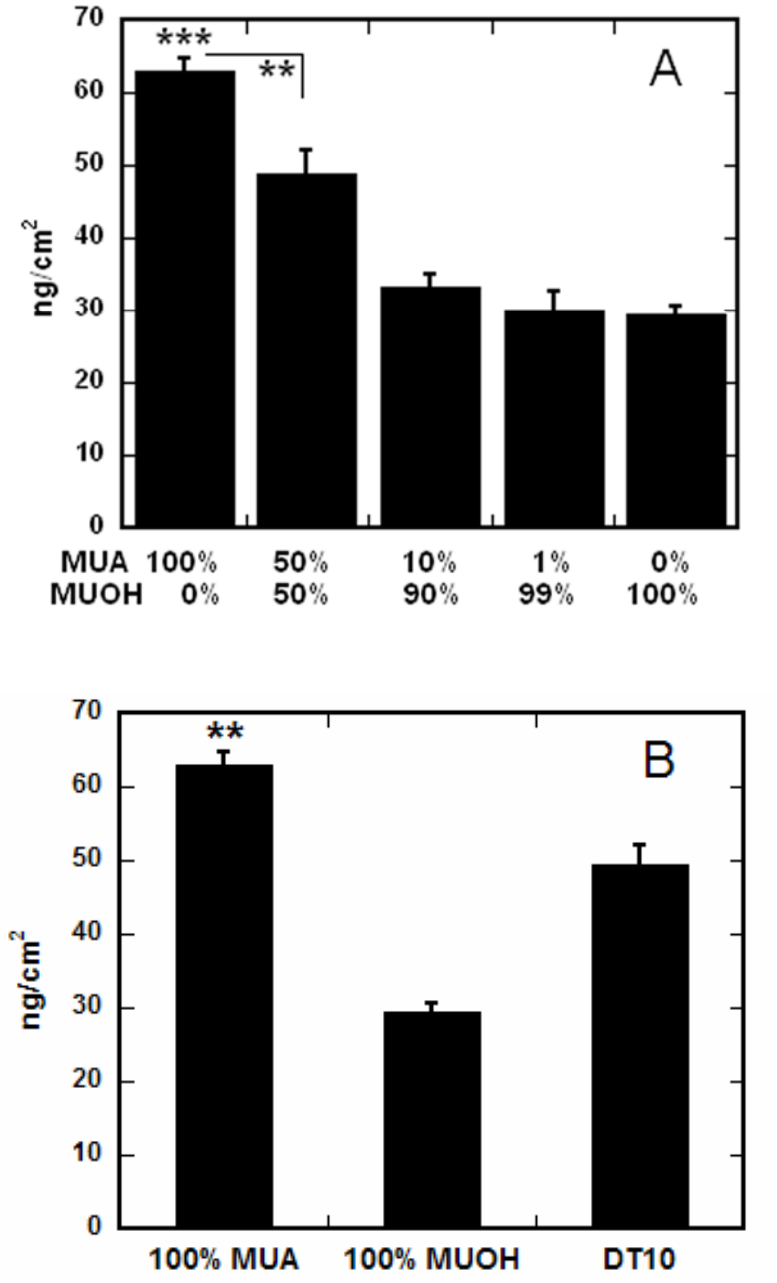

Figure 4-2 DNA-complex binding on SAMs. The amount of immobilized radiolableled DNA was determined for varying densities of carboxyl groups (A) and surface hydrophobicity (B). Percentage of carboxyl groups (A) refer to a background of MUOH SAMs. All values are reported as the mean ± s.e.m. *(**$p < 0.01$, *** $p < 0.001$).*

SAMs present an opportunity to dissect the contributions of specific surface functional groups on complex immobilization and substrate-mediated transfection. Our findings reveal that nonspecific DNA complex adsorption is mediated by at least two mechanisms: adsorption by charge-charge interactions and adsorption by hydrophobic interactions, two mechanisms which have been shown to be involved in nonspecific protein adsorption (148,149,152). However, like protein adsorption (148,153), DNA complex immobilization is presumably also affected by properties of the complexes themselves (2,6). In contrast to our findings, a study by Yamauchi and colleagues (118) reported that immobilization of DNA complexes on SAMs was independent of surface chemistry, yet indicated that electrostatic interactions were most important for DNA complex immobilization. In addition, hydrophobic regions were shown to have tight interactions (118), which is similar to our finding that surface hydrophobicity and ionization affect DNA complex immobilization.

4.3.3 Quantification of complex release

The stability of the interaction between the complexes and surface was investigated through release studies (Figure 4-3). Release rates and total amount of DNA complexes released from SAMs was independent of surface chemistry (Figure 4-3). Most release occurred by 24 hours and after 8 days 70-85% of complexes were released. The release of DNA complexes increased from 73% for hydrophilic, ionic surfaces (100% MUA), 77% for hydrophobic surfaces (DT10), to 84% and 85% for 0% (100% MUOH) and 50% MUA, respectively. Similarly, Yamauchi and colleagues (118) found at high surface densities that surface chemistry did not affect the release rates of DNA complexes from SAMs. In contrast, they found that lower

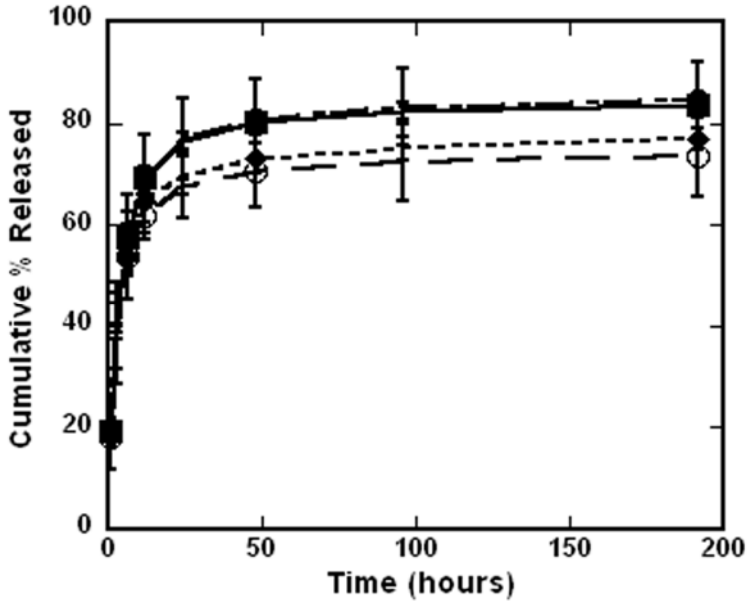

Figure 4-3 Surface chemistry and release. Radiolabeled DNA was used to quantify the amount of DNA released from each type of SAM (● 50% MUA, ○ 100% MUA; ■ 100% MUOH, ♦ DT10) into serum-containing media. All values are reported as cumulative percentage released, reported as the mean ± s.e.m. at each time point.

densities of immobilized complexes resulted in highest release on hydrophilic substrates, containing either carboxylic acid or hydroxyl terminal groups, whereas release was limited on hydrophobic surfaces due to tight interactions (118). However, their release profiles were determined in PBS, which presumably only disrupted electrostatic interactions (118). In this chapter, release profiles were performed in serum-containing growth media. The presence of serum has been shown to significantly enhance the release of non-specifically immobilized complexes relative to incubation with PBS (2). This enhanced release from the substrate is presumably mediated by competitive binding of serum that displaces the complexes and

components. Additionally, serum-containing media represents the most stringent release conditions, as it also contains salts that could disrupt electrostatic interactions, and also best emulates cell culture conditions. Our finding that release is independent of surface chemistry suggests that complex release from the substrate is mediated by competitive binding of serum that displaces the complexes, and components within the serum can bind through both electrostatic and hydrophobic interactions to the underlying SAMs.

4.3.4 Transfection on bulk SAMS on gold

Substrate-mediated delivery is based on the immobilization of DNA complexes to the culture substrate (2,5,6), resulting in elevated DNA concentrations in the cellular microenvironment, which has been shown to enhance gene delivery (30,31). While immobilizing DNA to a substrate may seem counterintuitive as cellular internalization is necessary for expression, viral vectors have been shown to associate with the extracellular matrix to facilitate cellular binding and internalization (35,36). The properties of the substrate are critical determinants of the interaction strength between the complexes and the surface, which subsequently affects the extent of transfection. SAMs were explored to examine the relationship between surface chemistry and substrate-mediated transfection. SAMs of alkanethiols on gold can be used in cell culture for periods of days (67) and have been used in many cell culture studies, particularly to understand molecular surface determinants required for adhesion dependent cell growth and proliferation (69-71).

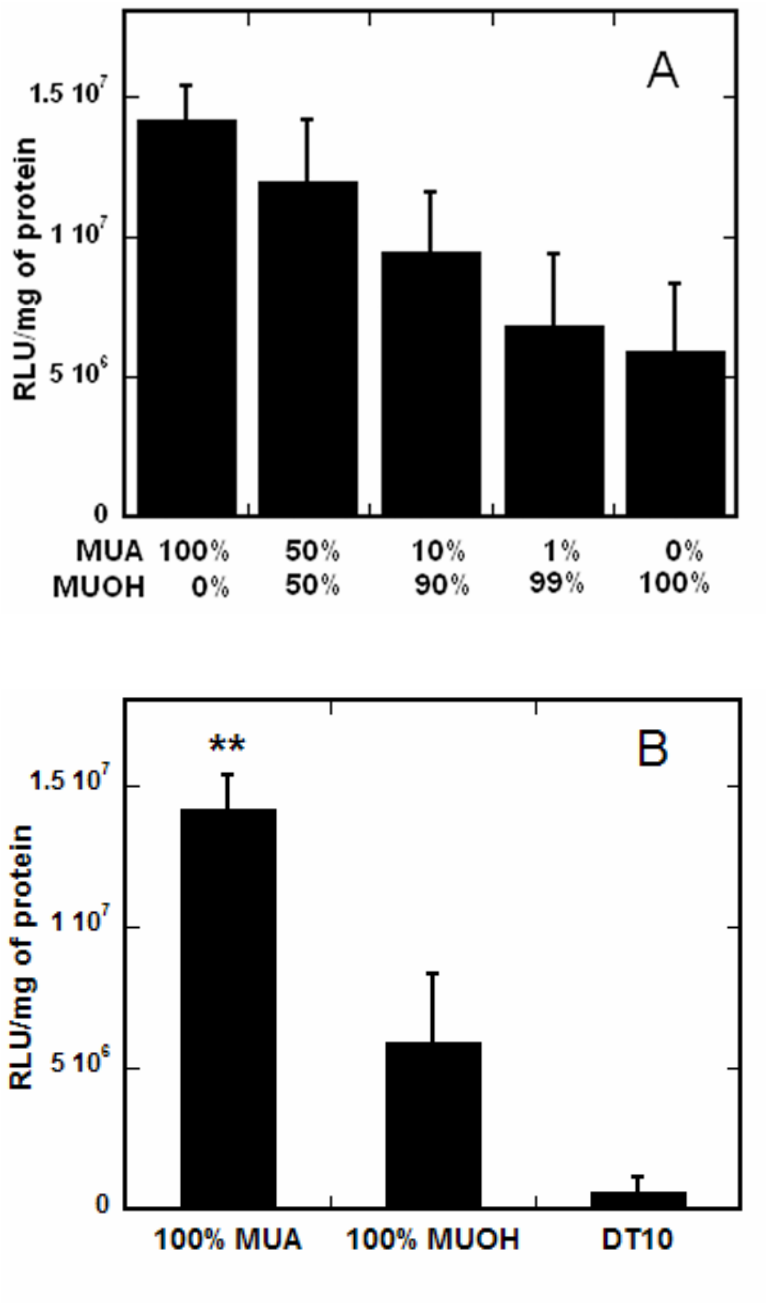

Figure 4-4 Surface chemistry and substrate-mediated transfection. SAMs were formed with an increasing density of carboxyl groups (A) and varying hydrophobicity (B). All values are reported as the mean ± s.e.m *(**$p < 0.01$).*

Transfection, like immobilization, was affected by both surface hydrophilicity and ionization (Figure 4-4), with the greatest transfection on surfaces containing 100% carboxylic acid functional groups. Increasing the percentage of ionic functional groups presented at the surface increased the extent of transfection, with 2.4-fold greater transfection on 100% MUA surface as compared to a nonionic hydrophilic substrate (100% MUOH) (Figure 4-4A), similar to previous reports (118). The trend for increased transfection mirrored that of DNA immobilization (Figure 4-2A), as over 2-fold more DNA complexes were bound to the 100% MUA surfaces as compared to 100% MUOH. Delehanty and colleagues (115) also found that an increase in the amount of deposited DNA resulted in a corresponding increase in transfection efficiency.

Complexes immobilized on hydrophilic, ionic surfaces (100% MUA) resulted in statistically greater transfection ($p < 0.01$) than hydrophobic substrates (Figure 4-4B). While DNA complex immobilization was less than 1.5-fold greater on 100% MUA than hydrophobic surfaces (Figure 4-2B), transfection was over 2.5-fold lower on the hydrophobic substrate (DT10). Additionally, transfection was greater on all hydrophilic surfaces, including 0-10% MUA, compared to the DT10 surface, in contrast to statistically greater immobilization of DNA complexes on the hydrophobic surface (Figure 4-2B). Low transfection on the DT10 substrates could be due to a combination of factors, including insufficient cell adhesion (70) or complex conformation changes induced upon binding, which have been shown to contribute to irreversible binding of proteins to hydrophobic surfaces (154). Total protein amount on the hydrophobic surfaces, as determined by the BCA assay, was similar or greater than all other surfaces, indicating that low transfection on these substrates was not due to insufficient cell

numbers (data not shown). Additionally cell morphology and adhesion were similar on hydrophilic and hydrophobic surfaces (Figure 4-5). Yamauchi and colleagues have proposed

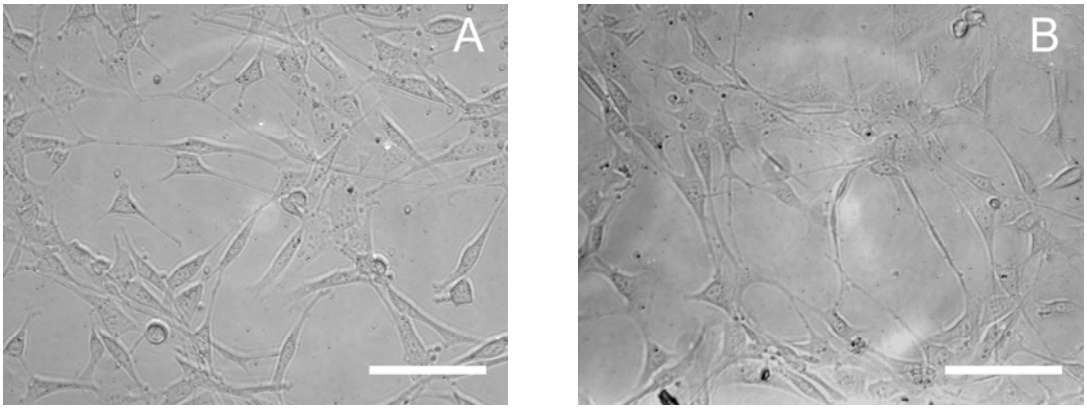

Figure 4-5 Cell adhesion on SAMs. The morphology and adhesion of cells was observed 24 hours after seeding cells on SAMs of (A) 50% MUA and (B) DT10, both lacking immobilized DNA complexes. Scale bars correspond to 200 μm.

that tight interactions of the DNA complexes with hydrophobic substrates can lead to lower transfection efficiencies (118). For DNA polyplexes or lipoplexes adsorbed to serum-modified, hydrophilic surfaces, the amount bound was similar as to those immobilized on hydrophobic, polystyrene surfaces, however the extent of transfection was greater on the hydrophilic substrates (2), consistent with results reported here.

Charged, hydrophilic substrates, which may provide reversible interactions between the substrate and complex, provides the most efficient gene delivery, requiring orders of magnitude less DNA on the surface as compared to previous reports (2). Transfection was highest on the

hydrophilic substrates, and transgene expression was significantly increased on hydrophilic substrates with similar or less amounts of DNA relative to hydrophobic substrates. The conformation of the DNA complexes may be altered upon binding to hydrophobic surfaces and explain low transfection levels. Thus, variability in the type of interactions between the complexes and substrate, mediated by changes in hydrophobicity and ionization, result in the different transfection levels observed on SAMs of varying surface chemistries.

4.3.5 Patterned SAMs and complex deposition

SAMs can be used in conjugation with μCP, a soft lithographic technique, to imprint substrates with specific patterns of SAMs (65,72,74). A PDMS stamp was used to imprint gold surfaces with specific patterns of hydrophilic alkanethiols (50% MUA) in a background of methyl-terminated alkanethiols (DT10). Secondary Ion Mass Spectrometry (SIMS) verified the

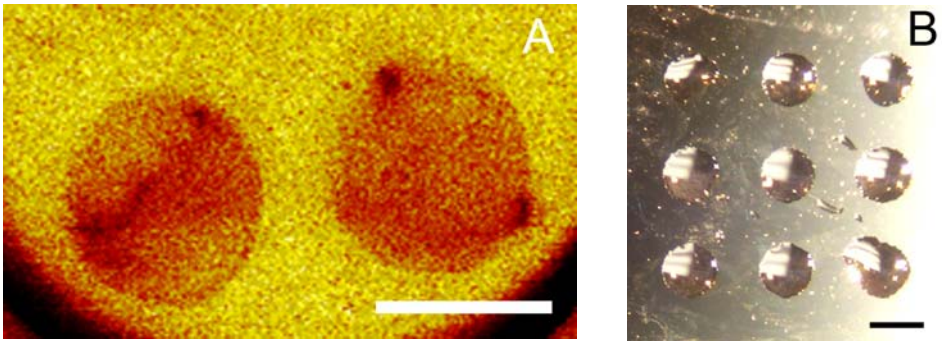

Figure 4-6 Microcontact printing on SAMs. (A) Secondary Ion Mass Spectrometry (SIMS) of stamped surface imaged the relative concentration of the mapped molecules, with red referring to higher concentrations of the hydrophilic alkanethiols. (B) Condensation figures created by pipeting water onto the stamped surface, which quickly collected in the hydrophilic regions. Gold-coated glass slides were used to prepare SAMs (Platypus Technologies, Madison, WI). Scale bars correspond to 1 mm**.**

spatial distribution of SAMs on the stamped surface (Figure 4-6A). The image brightness at each point is a function of the relative concentration of the mapped molecules, with red regions indicating higher concentrations of the carboxylic acid-terminated alkanethiolates. Additionally, the formation of CFs, created by simply pipeting water onto the stamped surface, was used as a method to verify and image SAM patterns on the surface (Figure 4-6B). These CFs were also utilized to confine droplets containing DNA complexes to specific regions of the surface, resulting in patterned DNA immobilization on a surface. Rhodamine-labeled DNA complexes were deposited on patterned surfaces in CFs formed on the hydrophilic areas (Figure 4-7). Complexes were seen to be confined to the circular patterns created by stamping, with relatively even distributions over the entire circular hydrophilic region (Figure 4-7, A-D), in contrast to unpatterned surfaces (Figure 4-7,E-F).

4.3.6 Patterned transfection

SAM surfaces patterned in regular arrays of hydrophobic and hydrophilic regions result in water condensation preferentially on the hydrophilic regions (75,76). These hydrophilic/hydrophobic arrays can be used to anchor droplets for concentrating a sample during evaporation, to prepare protein samples for MALDI-MS (77), or to pin aqueous solutions of DNA at specific array locations (78-80). Additionally, DNA complexes can be deposited in CFs on the hydrophilic regions to spatially regulate immobilization and upon seeding of cells, to pattern transfection. In this chapter, expression was examined by quantifying the percentage of transfected cells within the patterns (Figure 4-8). GFP expression was assayed at 24 and 48 (data not shown) hours using fluorescence microscopy. Transfection was confined to the patterns at

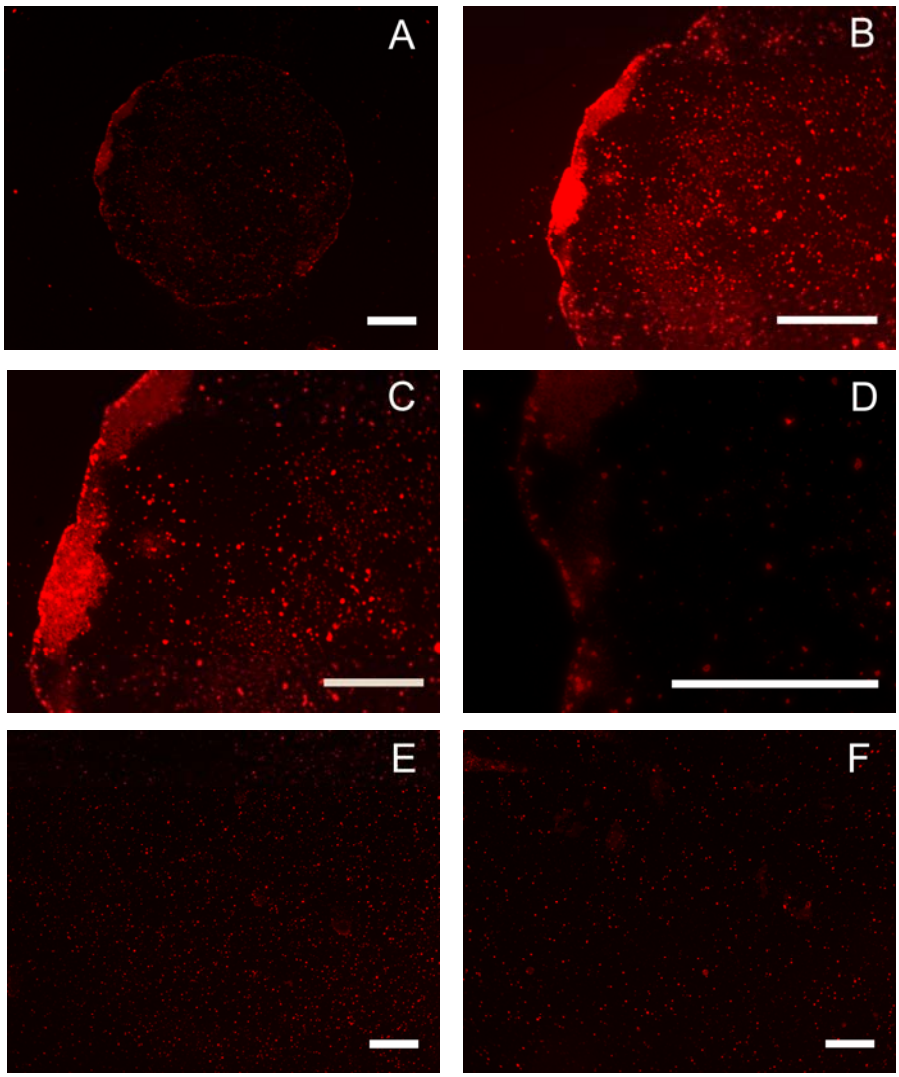

Figure 4-7 Patterned complex deposition. Condensation figures were utilized to confine droplets containing rhodamine-labeled DNA complexes to hydrophilic regions of a patterned surface, resulting in patterned DNA immobilization (A-D). Complexes were allowed to deposit for one hour, in humid conditions, and then visualized with fluorescence microscopy. Control complex deposition was performed on unpatterned 50% MUA (E) and DT10 (F) SAMs. Scale bars correspond to 200μm (A, B, E, F) and 100 μm (C, D)**.**

both time points and cells in these patterns exhibited transfection efficiencies near 40% (Figure 4-8A), similar to unpatterned substrates (Figure 4-8, C-F). Cellular adhesion was also patterned, as adhesion was greater on carboxyl-terminated SAMs (Figure 4-8B). This finding supports previous studies reporting the inability of cells to adhere to methyl-terminated SAMs in the presence of serum (69-71,155). Selective cellular adhesion suggests that hydrophilic/hydrophobic patterning strategies not only aid in the placement of complexes (78,79,118) but also the attachment of cells (69-71), resulting in patterns of transfection. In a similar study, micropatterned SAMs greatly facilitated regionally defined loading of DNAs and their expression in mammalian cells (118), however cellular adhesion was not patterned, presumably due to choice of cell type. We have found that on our patterned substrates, the hydrophilic regions support cell adhesion and high transfection, while the hydrophobic regions limit cellular attachment, properties which could be important to the fabrication of a transfected cell array.

Patterned gene delivery from a surface can be translated to a transfected cell array, which represents a high throughput approach to correlate gene expression with functional cell responses (95). Transfected cell arrays have been formed using a substrate-mediated approach in which plasmids or adenoviruses were mixed with collagen and spotted onto glass slides or into wells (95,113,126). Plated cells were transfected and could be analyzed for cellular responses using a variety of imaging or biochemical techniques. These systems have also been used for transfection of siRNAs, which were printed in cationic lipid/Matrigel mixtures (108). Alternatively, Chang et al.(116) developed a technology they refer to as “surfection”, in which a cationic polymer (PEI) and collagen are coated onto a surface. Plasmid DNA is then mixed with

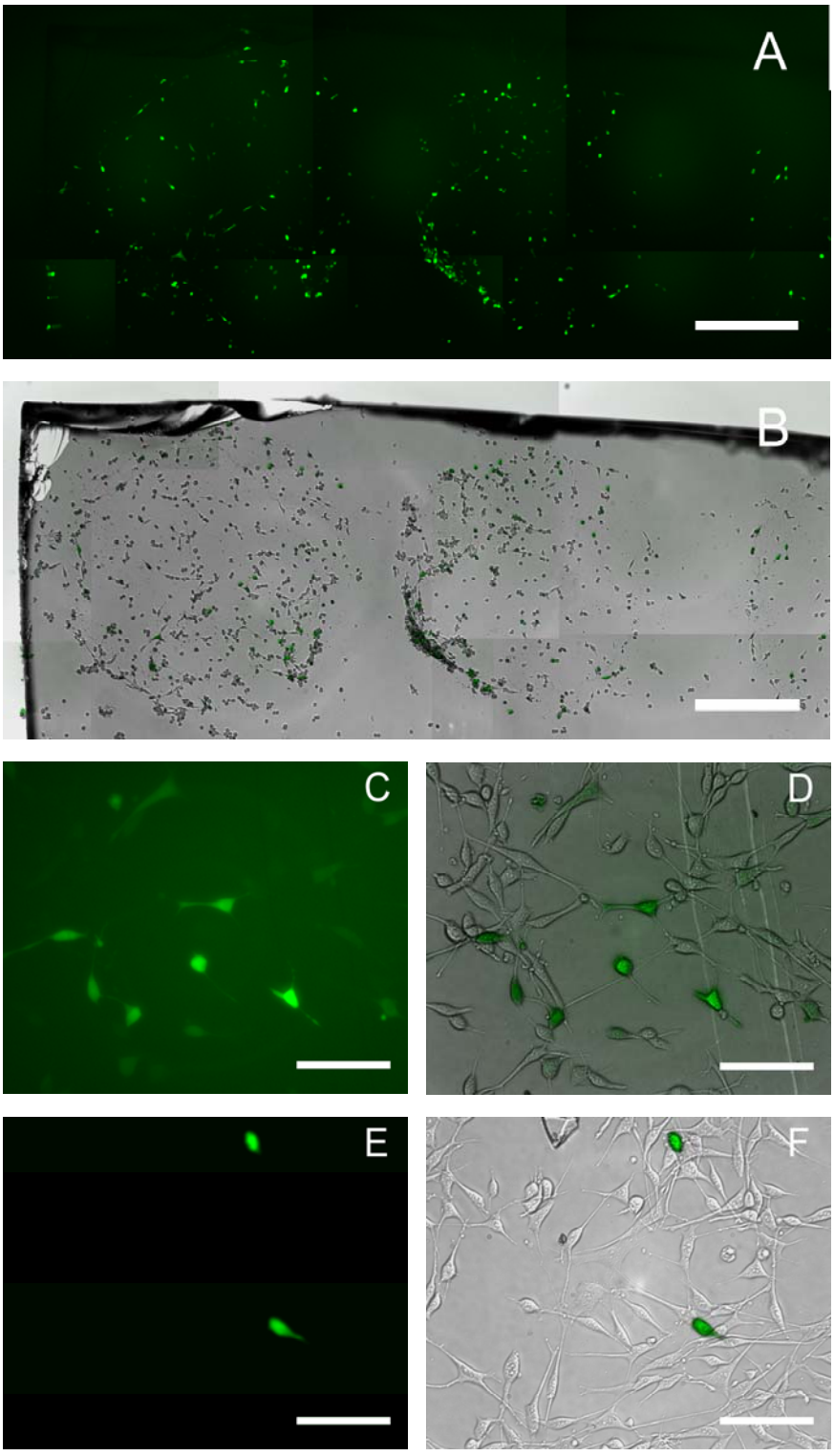

Figure 4-8 Patterned gene expression. Fluorescence and phase images were acquired and assembled to represent the entire patterned region (A, B). Transfection was confined to patterns

and transfection efficiency within patterns was over 30%. Control transfections were performed on uniform 50% MUA (C, D) and DT10 (E, F) SAMs. Gold-coated glass slides were used for SAM preparation (Platypus Technologies). Scale bar corresponds to 500 μm (A,B) and 200 μm (C-F).

cells that are plated onto this surface, which is divided up into wells by a silicone rubber sheet, to pattern transfection. Also, DNA complexes have been mixed with fibronectin and spotted onto glass slides for arrayed transfection of human mesenchymal stem cells (112). While transfected cell arrays hold great potential (95,108,112,113,116,126), further development of a substrate-mediated delivery system that efficiently transfects a wide variety of primary cells and cell lines, while allowing for spatially-controlled delivery within the different domains is required (95,129,130). Using SAMs on gold to form transfected cell arrays can allow precise control over surface chemistries, interactions between the substrate and DNA complexes, transfection efficiencies, and pattern sizes to create a well-characterized and efficient array delivery system.

4.4 Conclusions

In substrate-mediated delivery, DNA is immobilized to a substrate for delivery to cells that adhere to the substrate (5,37). Efficient delivery of DNA complexes from a surface is dependent on balancing the interactions between the substrate and the complexes. SAMs provide a versatile and flexible system to correlate surface chemistry to DNA complex binding, release and transfection. Surface hydrophobicity and ionization were found to mediate both complex immobilization and transfection, while release was independent of substrate properties.

Increasing the density of carboxylic acid groups on the surface increased complex immobilization and transfection, suggesting that electrostatic interactions contribute to efficient gene delivery from a substrate. Additionally, μCP was used to imprint substrates with specific patterns of SAMs, creating hydrophilic regions within a hydrophobic background. Condensation figures containing DNA complexes formed preferentially on the hydrophilic regions, resulting in patterned complex immobilization and transfection. The ability to control the interactions between complexes and substrates, combined with patterning strategies, has multiple applications, such as scaffolds for tissue engineering and functional genomic screens in cell-based assays.

Chapter 5

Substrate-mediated gene delivery of tethered complexes from self-assembled monolayers

5.1 Introduction

Efficient, controlled gene delivery is a fundamental goal in biotechnology, but can be limited by both extracellular and intracellular barriers that prevent efficient gene transfer. Extracellular barriers to gene delivery include mass transport limitations, cytotoxicity, degradation, and aggregation (1), as well as cell targeting and uptake. Intracellular barriers to gene transfer include release from the endosomal/lysosomal compartments into the cytoplasm, subsequent delivery to the nucleus and expression of the transgene (16). Methods, such as complexing DNA with nonviral vectors, as well as delivery mechanisms such as controlled release systems, have been developed to overcome both intracellular and extracellular barriers. Complexation with cationic lipids or polymers can facilitate internalization and transfection (7-9), by enhancing interactions between positively charged DNA complexes and the negatively charged cellular membrane, in addition to providing stability against degradation (13) and facilitating intracellular trafficking (7,14). Controlled release systems for DNA delivery have the potential to overcome extracellular barriers that limit gene transfer (81) and include delivery through polymeric release in which the DNA is released from a polymer scaffold or substrate-mediated delivery, in which DNA is retained at the surface of a substrate.

The substrate-mediated delivery strategy is based on the immobilization of DNA, complexed with nonviral vectors, to a biomaterial or substrate that supports cell adhesion (82).

Substrate-mediated gene delivery maintains elevated DNA concentrations in the cell microenvironment, increasing its local concentration, which has been shown to enhance transgene expression. DNA complexes can be immobilized on the substrate through specific interactions introduced by means of complementary functional groups on the vector and surface or through nonspecific interactions.

Specific interactions, including antigen-antibody or biotin-avidin (5,6,22) have been used to immobilize DNA complexes. Poly(L-lysine) (PLL) or polyethylenimine (PEI) modified with biotin residues for subsequent complexation with DNA and binding to a neutravidin substrate (5,6) resulted in 100-fold increased transfection from the immobilized PLL complexes relative to bolus delivery of complexes (5). For PEI, biotinylation did not affect the amount of complexes bound or subsequent transfection, indicating that transfection was most likely mediated by nonspecifically bound complexes (6).

Nonspecific mechanisms have been used to immobilize plasmid DNA or DNA complexed with cationic polymers or lipids on substrates (2,45,46,117,145-147,156,157). Polyplexes and lipoplexes non-specifically immobilized to serum-coated polystyrene have been shown to enhance the extent of transgene expression in both cell lines and primary human-derived cells, along with an increased cellular viability (2). Self-assembled monolayers (SAMs) of alkanethiols on gold have been used to study the mechanisms of transfection by complexes nonspecifically immobilized on chemically specific substrates, to determine appropriate biomaterial surface properties for efficient gene delivery (117, Chapter 4). SAMs are homogenous, highly ordered films of organic molecules anchored to a surface that provide a flexible system to regulate terminal functional group chemistry to examine the complex-substrate

interactions (63,148,149). DNA, complexed with cationic lipids, was immobilized through nonspecific mechanisms to SAMs presenting various combinations of hydrophilic and charged, hydrophilic and uncharged, and hydrophobic terminal functional groups (117, Chapter 4). Surface hydrophilicity and ionization were found to mediate both immobilization and transfection, with highest levels on hydrophilic, charged SAMs relative to uncharged or hydrophobic surfaces. However, modulating the surface chemistry had no effect on complex release.

While nonspecific immobilization strategies have been used to enhance transfection in vitro, translating the substrate-mediated delivery approach to biomaterials for the localized, controlled, and efficient delivery of DNA in vivo requires that the complexes be retained at the biomaterial surface, with tunable release profiles. Previous studies with nonspecifically immobilized complexes have demonstrated a rather fast release of complexes, independent of immobilization strategy or surface chemistry (2,6,117). In the studies reported in this chapter, SAMs of alkanethiols on gold were used to investigate substrate-mediated transfection by covalently tethered complexes to determine the effect of immobilization strategy on complex binding, release and transfection.

In our approach presented here, the ability of specifically tethered complexes to mediate transfection was investigated. DNA, complexed with PEI, was covalently linked to SAMs presenting appropriate functional groups through a fraction of the functional groups available on the PEI present in the complex. Preformed complexes were immobilized through direct covalent attachment or via crosslinkers (homobifunctional or heterobifunctional), both with and without the ability to be degraded. The tethering strategies investigated were based on well-known

coupling chemistries, which have previously been used to attach proteins and other biomolecules to SAMs and other substrates. Proteins have been tethered to SAMs via carbodiimide chemistry (158-161) or Schiff base formation (153). Direct coupling strategies have also been used to attach PEI to SAMs via formation of an interchain carboxylic anhydride intermediate (162). Homobifunctional crosslinkers have been used to crosslink proteins (163) to SAMs, as well as PEI to a biodegradable polymer for subsequent delivery of DNA for transfection of cells adjacent to polymer (51). Similarly, proteins (78) and thiolylated oligonucleotides (164) have been crosslinked to SAMs via heterobifunctional crosslinkers. Similar attachment strategies were investigated for complex tethering.

Our goal was to directly attach unmodified complexes to substrates, rather than attaching moieties to PEI prior to complexation or after, to avoid complications with complexation and complex activity. SAMs were again used as model substrates, in that they present a uniform, defined surface chemistry and offer laterally well-defined sites at which biomolecules can be covalently attached to specific functional elements. Oligo(ethylene glycol) (EG) –terminated alkanethiols (165,166) were incorporated into the SAMs presenting the appropriate functional groups for the covalent tethering strategies, to limit nonspecific complex adsorption, which has plagued previous attempts of specific immobilization (6). These EG-terminated SAMs have been shown to resist nonspecific protein adsorption (166,167) and have previously been incorporated into SAMs for subsequent immobilization of proteins and ligands with sensitive functional groups (159,160), to prevent the adhesion of the protein of interest to all but the exposed functional groups on the surface. For our study, the percentage of EG incorporated was low so as not to prevent cell adhesion.

Covalently tethered complexes provide an approach to extend the retention of complexes at the surface, especially in serum-containing environments, including in vivo conditions. These covalent tethering strategies have the potential to be translated to biomaterial surfaces, for use in tissue engineering applications. Furthermore, the covalent immobilization of functional, biological molecules onto defined and conductive surface provides the basis for sophisticated biomolecular architectures with numerous applications for in vitro studies and in vivo translation.

5.2 Material and methods

5.2.1 Gold slide preparation and monolayer self assembly

E-beam evaporation (Edwards Electron Beam Evaporator, Wilmington, MA) was used to prepare gold-coated glass slides consisting of a 5 nm titanium adhesion layer and 50 nm of gold. These gold-coated slides were cut into smaller pieces that fit into standard 48-well tissue culture plates with a diamond-tipped glass cutter. To prepare for SAM formation, gold was extensively washed in acetone and ethanol, with subsequent drying under a stream of nitrogen.

SAM formation was accomplished by immersion of the clean gold substrates into 2 to 10 mM ethanolic solutions of alkanethiols for 3 to 18 hours in the dark, under argon. Monolayers were formed with combinations of four different alkanethiols, including 11-mercaptoundecanoic acid (MUA, COOH-terminated), 1,8-octanedithiol (O8SH, SH-terminated) (Aldrich, St. Louis, MO), 2-hydroxypentamethylene sulfide (HPMS, C=O-terminated) (Toronto Research Chemicals, Ontario, Canada) and $HS(CH_2)_{11}(OCH_2CH_2)_6OH$, an oligo(ethylene glycol)-terminated alkanethiols (EG) (ProChimia, Gdansk, Poland). The combination of thiols used for

monolayer formation was determined by the immobilization chemistry utilized. Alkanethiol solutions were freshly prepared in filtered, degassed ethanol. After monolayer formation, SAM samples were rinsed in pure ethanol and dried with nitrogen before further use.

5.2.2 Cellular adhesion on SAMs

Cell morphology and adhesion studies were performed on SAMs with increasing percentages of EG-terminated alkanethiols in a background of MUA, prepared as described above. NIH/3T3 cells (ATCC; Manassas, VA), cultured at 37°C and 5% CO_2 in DMEM supplemented with 1% sodium pyruvate, 1% penicillin-streptomycin, 1.5 g/L $NaHCO_3$ and 10% fetal bovine serum, were seeded at a density of 15,000 cells per SAM. Cellular morphology and adhesion were analyzed after 24 and 48 hours using phase microscopy.

5.2.3 DNA complex formation

Plasmid DNA was purified from bacteria culture using Qiagen (Valencia, CA) reagents and stored in Tris–EDTA buffer solution (10 mM Tris, 1 mM EDTA, pH 7.4) at −20 °C. Plasmid pEGFP-LUC encodes both the enhanced green fluorescent protein (EGFP) and firefly luciferase protein (LUC), under the direction of a CMV promoter and was used for all binding, release and transfection experiments. For DNA complex formation, branched PEI (25 kDa, Aldrich, St. Louis, MO) was diluted in an appropriate buffer (see immobilization chemistries below) and then added dropwise to DNA in the same buffer, vortexed for 10 seconds, and incubated for 15 min at room temperature. All complexes were formed at N/P ratios of 25, and 3

μg of DNA (300 μl final volume of complexes) was added to each SAM for all binding, release and transfection studies.

5.2.4 Complex immobilization

DNA complexes, formed as described above, were immobilized to SAMs using six different tethering strategies. Direct coupling was accomplished through carbodiimide chemistry (EDC/NHSS) or Schiff base formation. Crosslinking was accomplished through a homobifunctional crosslinker (glutaraldehyde) or heterobifunctional crosslinkers (sulfo-SMCC, AEDP, sulfo-LC-SMPT).

5.2.4.1 Direct coupling

For direct coupling of complexes, carbodiimde chemistry was used to attach amine-containing PEI-DNA complexes to COOH-terminated SAMs. Specifically, 1-Ethyl-3-(3-Dimethylaminopropyl) carbodiimde Hydrochloride (EDC, Pierce, Rockford, IL) with N-hydroxysulfosuccinimide (NHSS, Pierce, Rockford, IL) coupling was performed by first forming SAMs with various amounts of COOH-terminated alkanethiols in a background of EG-terminated alkanethiols, to prevent nonspecific adsorption. These SAMs were then activated for complex attachment by equilibration with 1X PBS (phosphate-buffered saline, pH 7.4) for 2 minutes, followed by a second incubation in a solution of EDC and NHSS (0.4 M and 0.1 M, respectively) in MilliQ water for 10 minutes. Complexes, formed as described above in 25 mM sodium phosphate buffer (pH 6.5), were then added to these activated SAMs for 2 hours, in the presence of EDC and NHSS (final concentrations, 0.2 M and 0.05 M, respectively). After the

immobilization period, the complex solution was removed and the SAMs were washed twice with PBS. For control studies, MilliQ water was added to the surfaces in place of the EDC and NHSS solution.

A second type of direct covalent attachment was performed through Schiff base/amine bond tethering of PEI-DNA complexes to aldehyde-terminated SAMs. Specifically, coupling was performed by first forming SAMs with various amounts of aldehyde-terminated alkanethiols (HPMS) in a background of EG-terminated alkanethiols, to prevent nonspecific adsorption. Complexes, formed as described above in 100 mM HEPES buffer (pH 6.5) or 0.2 M sodium bicarbonate (pH 9.6), were added directly to these SAMs for 2 hours, or further reduced in the presence of sodium cyanborohydride (10 μl of 5 M $NaCNBH_3$ per mL of reaction solution, ICN Biomedicals Inc., Aurora, OH). After the immobilization period, the complex solution was removed and the SAMs were washed twice with the corresponding complex formation buffer.

5.2.4.2 Homobifunctional crosslinking

Glutaraldehyde was used to crosslink PEI-DNA complexes to SAMs. A homobifunctional crosslinker, glutaraldehyde contains aldehyde groups on either end that can react with hydrazide groups and amines on SAMs and PEI of the complexes, respectively. Specifically, SAMs with 60% COOH-terminated alkanethiols in a background of EG-terminated alkanethiols were modified with adipic acid dihydrazide (AAD, Sigma, St. Louis, MO) to present hydrazide groups. AAD was attached to COOH SAMs through EDC/NHSS chemistry, as described above. Briefly, 32 mg/ml AAD solution in 0.1 M sodium phosphate, 0.15 M NaCl (pH 7.2) was added to the surface in the presence of EDC and NHSS (final concentrations, 0.2 M

and 0.05 M, respectively) for 16 hours with mixing. The AAD/EDC/NHSS solution was then removed and surfaces were thoroughly rinsed with sodium phosphate buffer. Glutaraldehyde (10% in sodium phosphate buffer, Fisher Chemical, Fair Lawn, NJ), was added to the AAD-modified surfaces, either in the absence or presence of $NaCNBH_3$ for further reduction of the Schiff base (10 µl of 5 M per mL of reaction solution) for one hour. After this period, surfaces were again rinsed in sodium phosphate buffer and complexes, formed as described above in sodium phosphate buffer, were added directly to these SAMs for 2 hours, or further reduced in the presence of sodium cyanborohydride, as described above. After the immobilization period, the complex solution was removed and the SAMs were washed twice with sodium phosphate buffer. For control studies, complexes were immobilized in the absence of glutaraldehyde.

5.2.4.3 Heterobifunctional crosslinking

Complexes were also crosslinked to SAMs using sulfosuccinimidyl 4-(N-maleimidomethyl)cyclohexane-1-carboxylate (sulfo-SMCC, Pierce, Rockford, IL), a noncleavable, heterobifunctional crosslinker that contains an NHS ester on one end and a maleimide group on the other. Specifically, SAMs with SH-terminated alkanethiols (O8SH) (168-170) were formed either homogeneously or in a background of EG-terminated alkanethiols to prevent nonspecific binding of complexes. PEI-DNA complexes, formed as described above in sodium phosphate buffer, were incubated with sulfo-SMCC, at 40-fold molar excess of crosslinker over that of PEI, for 15 minutes to 1 hour at room temperature. These maleimide-activated complexes were then added to the sulfhydryl-containing SAMs (O8SH) for 4 hours at room temperature. After the immobilization period, the complex solution was removed and the

SAMs were washed twice with sodium phosphate buffer. For control studies, complexes were immobilized in the absence of sulfo-SMCC.

5.2.4.4 Cleavable heterobifunctional crosslinking

A cleavable, heterobifunctional crosslinker, 3-[(2-Aminoethyl)dithio]propionic acid – HCL (AEDP, Pierce, Rockford, IL) was also used to tether complexes to SAMs. AEDP contains an amine on one end and a carboxylic acid group on the other end and can be used with carbodiimide chemistry to conjugate with amines on PEI of the complexes and carboxylic acid groups on SAMs. The disulfide cross-bridge of AEDP may be cleaved using disulfide reducing agents like dithiothreitol (DTT, Sigma, St. Louis, MO). Specifically, AEDP crosslinking was performed by first forming SAMs with COOH-terminated alkanethiols, either homogeneously or in a background of EG-terminated alkanethiols to prevent nonspecific adsorption. These SAMs were then activated for complex attachment by equilibration with 1X PBS for 2 minutes, followed by a second incubation in a solution of 0.2 M EDC, 0.05M NHSS, 8 mM AEDP in water for 2 hours. The EDC/NHSS/AEDP solution was then removed and these AEDP-activated SAMs were rinsed twice in MilliQ water and once in 1X PBS. Complexes, formed as described above in 25 mM sodium phosphate buffer (pH 6.5), were then added to these activated SAMs for 2 hours, in the presence of EDC and NHSS (final concentrations, 0.2 M and 0.05 M, respectively). After the immobilization period, the complex solution was removed and the SAMs were washed twice with PBS. If cleaving of the crosslinker was desired for binding studies, 50 mM DTT was added in sodium phosphate buffer to the SAMs with tethered complexes and incubated for 4 hours at 37°C. After this period of reduction, the DTT solution

was removed and SAMs were rinsed with sodium phosphate buffer. Cleaving of the crosslinker for transfection studies was performed as just described, but 24 hours after cell seeding (see below). For control studies, MilliQ water was added to the surfaces in place of the EDC and NHSS solution, for each of the carbodiimide steps.

A second, cleavable heterobifunctional crosslinker was used to tether PEI-DNA complexes to SAMs. Sulfosuccinimidyl 6-[α–methyl-α-(2-pyridulditho)toluamido]hexanoate (sulfo-LC-SMPT, Pierce, Rockford, IL) contains one end with a pyridyl disulfide derivative that is sulfhydryl-reactive, while the other end is an amine reactive-NHS ester. This crosslinker, like AEDP, contains a disulfide bridge that is cleavable using disulfide reducing agents like DTT. Specifically, sulfo-LC-SMPT crosslinking was performed by first forming SAMs with SH-terminated alkanethiols (O8SH), either homogeneously or in a background of EG-terminated alkanethiols to prevent nonspecific binding of complexes. PEI-DNA complexes, formed as described above in 50 mM sodium phosphate, 0.1 M NaCl (pH 7.2), were incubated with sulfo-LC-SMPT, (4 mM in MilliQ water, final concentration), for 30 minutes to 1 hour at room temperature. These activated complexes were then added to the sulfhydryl-containing SAMs (O8SH), which had been rinsed in 1X PBS, 10 mM EDTA, and incubated overnight at room temperature. After the immobilization period, the complex solution was removed and the SAMs were washed twice with sodium phosphate buffer. If cleaving of the crosslinker was desired for binding studies, 50 mM DTT was added in sodium phosphate buffer to the SAMs with tethered complexes and incubated for 4 hours at 37°C. After this period of cleavage, the DTT solution was removed and SAMs were rinsed with sodium phosphate buffer. For control studies, complexes were immobilized in the absence of sulfo-LC-SMPT.

5.2.5 Quantification of DNA complex immobilization and release

Plasmid DNA was radiolabeled with α-^{32}P dATP to measure the immobilization and release of DNA complexes tethered to SAMs through direct and crosslinking strategies, as described above. Briefly, a nick translation kit (Amersham Pharmacia Biotech; Piscataway, NY) was used following the manufacturer's protocol with minor modifications (6). The labeled DNA was diluted with unlabeled DNA to a final concentration of 1% and this mixture was then used to form DNA complexes, as described above. After SAM preparation, digital photographs of each sample were taken prior to complex tethering and analyzed with ImageJ (NIH) to determine the area of each surface. The quantity of DNA immobilized was determined by immersing individual SAM samples in scintillation cocktail (5 mL, BioSafe II, Research Products International Corp., Mount Prospect, IL**)** for measurement with a scintillation counter. The counts were correlated to DNA mass using a standard curve. The density of DNA immobilized to each SAM sample was determined by normalizing the amount bound to area.

Release profiles were determined for SAMs with immobilized DNA complexes, by incubation with serum-containing cell growth media at 37°C in a humid chamber. At predetermined time points, half of the media was removed and replaced with fresh media. The activity of the collected sample was measured in a scintillation counter. At the final time point, the counts remaining on the SAM samples were also determined. The percentage of DNA released was calculated as the ratio of the cumulative counts released through a given time divided by the total counts initially on the substrate, thus, the release curves represent the percentage of DNA released relative to the initial amount bound to each surface. Release

profiles were not determined for all tethering strategies, but only for those for which more extensive analysis was deemed necessary.

5.2.6 Transfection on SAMs

Transfection studies were performed with NIH/3T3 cells, cultured as described above, on SAMs with complexes immobilized through direct and crosslinking coupling strategies. After complex formation and immobilization as described above, SAMs were seeded with 15,000 cells in 48-well plates. Transfection was analyzed following a 48-hour culture, quantified by measuring the luciferase activity using the Luciferase Assay System (Promega, Madison, WI). The luminometer (Turner Designs, Sunnyvale, CA) was set for a 3 second delay with an integration of the signal for 10 seconds. Luciferase activity (RLU) was normalized to the total protein amount determined with the BCA protein assay (Pierce, Rockford, IL). Transfection studies were not performed for Schiff base or sulfo-LC-SMPT tethering strategies, as these were not further analyzed due to the amount of DNA complexes bound and/or ease of preparation (see section 5.3).

5.2.7 Statistics

JMP software (SAS Institute, Inc., Cary, NC) was used to perform all statistical analysis. Comparative analyses were completed using one-way ANOVA with Tukey post-tests, at a 95% confidence level. Mean values with standard deviation are reported and all experiments were performed in triplicate.

5.3 Results and discussion

Covalent coupling of DNA complexes to a substrate functions to place and maintain the DNA within the cell microenvironment. Tethering could also provide an approach to extend the retention of complexes at the surface, especially in serum-containing environments, including in vivo conditions. Coupling to chemically defined SAMs as model substrates are advantageous in that they offer laterally well-defined sites at which biomolecules can be covalently attached to specific functional elements.

5.3.1 Direct coupling

For direct coupling of complexes, carbodiimde chemistry to attach amine-containing biomolecules to COOH-terminated SAMs is well characterized (159,161) and easily adapted to preformed complexes, with only a small fraction of free amino groups on PEI expected to react with surface (171). In our studies, EDC was used to react with carboxylic acid groups present in the SAM to form an amine-reactive intermediate, an O-acylisourea. As this intermediate is unstable in aqueous solutions, it was stabilized using NHSS, which forms an amine-reactive NHS ester (Figure 5-1). Primary amines within the PEI-DNA complexes were then reacted with the activated SAMs presenting NHS esters, forming a stable peptide (amide) bond between the surface and complex. Complexes were tethered to SAMs with varying densities of COOH groups, in a background of EG-terminated alkanethiols (Figure 5-2), which were also included in the monolayers as they are widely used to prevent nonspecific adsorption of proteins in covalent coupling strategies (159,160), and were hypothesized to limit nonspecific complex immobilization. The effect of EG-containing SAMs on cell morphology and adhesion was

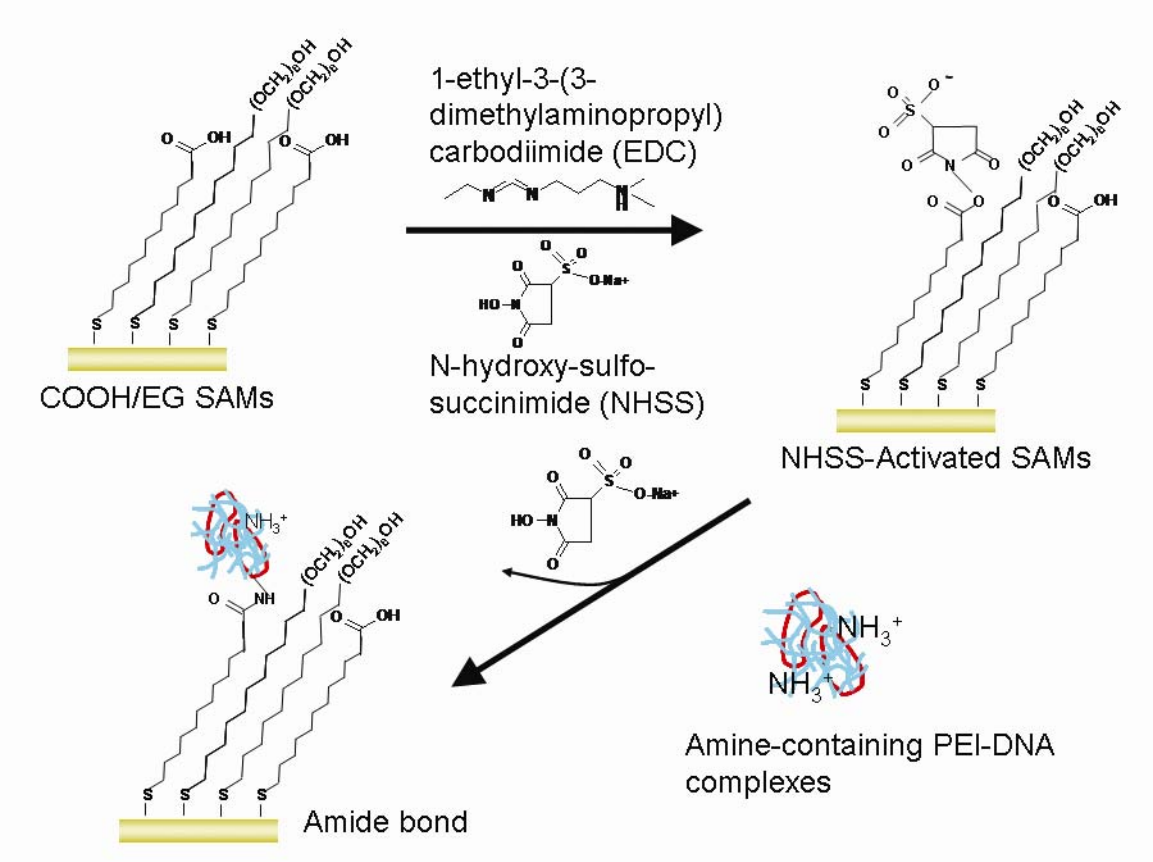

Figure 5-1 Direct coupling of PEI-DNA complexes to COOH/EG SAMs via EDC/NHSS chemistry.

determined by cell seeding on SAMs with increasing percentages of EG-terminated alkanethiols in a background of MUA (COOH). A monolayer containing no EG thiols resulted in a robust cell monolayer and increasing the percentage of EG groups did not appreciably affect cellular adhesion until EG groups constituted 40% or more of the monolayer (see Chapter 6, Figure 6-1). Therefore 40% EG SAMs were used in all tethering studies, except in control conditions.

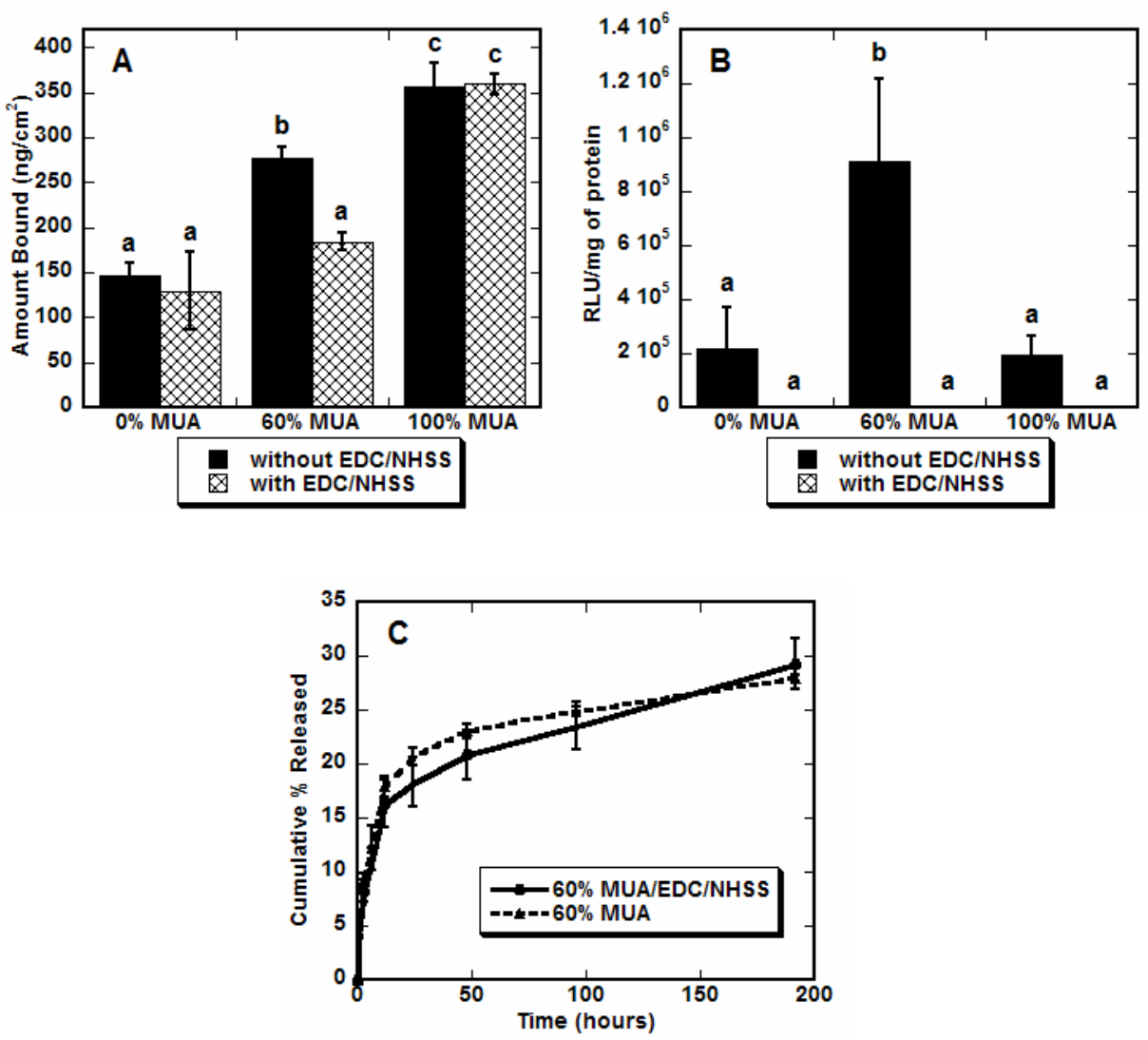

Figure 5-2 EDC/NHSS coupling of complexes on SAMs. The amount of immobilized radiolableled DNA was determined for SAMs with increasing percentages of COOH (MUA) groups in a background of EG (A) in the presence or absence of the coupling reagents (EDC/NHSS). Transfection was assayed from the same conditions (B). Radiolabeled DNA was used to quantify the amount of DNA released (C) from tethered complexes (● 60 % MUA with EDC/NHSS, ▲ 60 % MUA) into serum-containing media. All values are reported as the mean ± s.d. and release values are reported as cumulative percentage released at each time point. *(Columns labeled with same letter designate conditions not statistically different; all other comparisons, $p < 0.01$ for (A), $p < 0.001$ for (B)).*

For surfaces with no or only COOH groups (0% and 100% MUA, respectively) the amount of DNA immobilized to the surfaces was not affected by the addition of the EDC/NHSS (Figure 5-2A), suggesting that nonspecific binding may be prevailing, similar to previous results (6). Binding was statistically greater ($p < 0.01$) on surfaces containing only COOH-terminated alkanethiols (100% MUA), similar to previous studies (Chapter 4, 117) that showed increasing the percentage of carboxylic acid groups on the surface increases binding of nonspecifically immobilized DNA complexes.

For SAMs containing both COOH- and EG-terminated alkanethiols (60% MUA), the addition of EDC/NHSS resulted in statistically less DNA bound ($p < 0.01$), which could indicate successful tethering, in that one might expect covalent coupling to limit the interactions of the complexes with the surface, thereby reducing the amount of DNA immobilized (Figure 5-2A). Binding on 60% MUA SAMs, without the addition of EDC/NHSS, was significantly greater than binding on 0% MUA, and lower than binding on 100% MUA, again supporting previous studies demonstrating the effect of electrostatic interactions between the surface and complexes (Chapter 4). All binding densities are much greater than previous reports of lipoplexes binding to SAMs (Chapter 4, 117), but are consistent with binding densities for PEI-DNA complexes on hydrophilic, serum-coated polystyrene substrates (2). However, there was sufficient binding to 0% MUA surfaces (100% EG), which was unaffected by the addition of EDC/NHSS, suggesting that a sufficient amount of nonspecific binding exists and was not prevented by the addition of the EG groups in the SAMs. This nonspecific binding could therefore be contributing to all binding densities for this coupling strategy (see Chapter 6 for more analysis and explanation).

Transfection levels on all SAMs to which EDC/NHSS was added were zero (Figure 5-2B), indicating that complexes were not available or viable for transfection. For the 60% MUA and 100% MUA SAMs, the addition of EDC/NHSS would be expected to couple the complexes to the surfaces, which would then make them not available for internalization by cells, and would thus validate our system's ability to tether complexes. However, the addition of EDC/NHSS to SAMs containing no COOH groups (0% MUA), also resulted in no transfection. On these surfaces, where the SAMs contained only EG groups, the complexes have nothing to tether to, and a complete lack of transfection most likely indicates an inactivation of the complexes. The amines of the PEI within the complexes could be activated by the addition of the NHSS, but that in turn could be prohibiting successful cellular internalization and/or transfection.

Transfection by nonspecifically immobilized complexes, when no EDC/NHSS was added (Figure 5-2B), was statistically greater ($p < 0.001$) on SAMs containing both COOH- and EG-terminated alkanethiols (60% MUA). These findings are in contrast to previous studies, where surfaces with 100% carboxylic acid functional groups resulted in highest transfection levels, presumably due to high binding efficiencies (Chapter 4, 117). This enhancement in transfection by SAMs containing EG groups is further explored in Chapter 6.

Release studies were used to investigate the presence of a covalent tether between the complexes and surface (Figure 5-2C). Release rates and total amount of DNA complexes released from SAMs were independent of the addition of EDC/NHSS. For both conditions (60% MUA, with or without EDC/NHSS) most release occurred by 24 hours and after 8 days, less than 30% of the complexes were released, regardless of addition of the coupling reagents. These release rates are substantially lower than profiles previously determined for lipoplexes from

SAMs (117), but similar to release curves obtained from PEI-DNA complexes on hydrophilic, serum-coated polystyrene substrates (2). Our finding that release was not affected by the addition of EDC/NHSS provides even more evidence that the complexes were not successfully tethered to the SAMs, and all DNA immobilization and release measured was that from nonspecifically immobilized complexes.

Direct coupling to SAMs via EDC/NHSS chemistry has been used to immobilize antibodies for the formation of an antibody array (161), proteins and ligands on mixed SAMs containing EG-terminated alkanethiols and COOH-terminated thiols for AFM studies (159), and nitrilotriacetic acid groups for immobilizing His-tagged proteins onto surfaces (172). Furthermore, NHS-terminated alkanethiols have been used to form SAMs that covalently tether proteins (158,160). We chose to explore the ability of EDC/NHSS coupling to tether PEI-DNA complexes given its extensive use in protein tethering and the ability to use "standard" SAMs and subsequently perform reactions on them to modify the surface chemistry. Performing reactions on SAMs permits the properties of the surface to be tuned at the molecular level, but due to the tightly packed nature of the SAMs, the choice of reaction is important (173). The NHS functionality is often used to introduce a variety of amine-terminated molecules to SAMs under mild conditions. The reaction proceeds quickly, giving high yields and is compatible with a wide range of functional groups (173). While it is believed that most types of reactions can be performed on SAMs, multistep synthesis of complex molecules on SAMs has not been widely explored and our studies indicate that further modifications and refinements may be required, including carefully selecting the ionic strength and pH of conjugation buffer, which have been shown to affect protein tethering via EDC/NHSS (159).

A second type of direct covalent attachment was performed through Schiff base/amine bond tethering of PEI-DNA complexes to aldehyde-terminated SAMs (Figure 5-3). Aldehydes react directly with amines to form a Schiff base, which is rather labile, but can be chemically stabilized by reduction to form a covalent, secondary amine linkage. The aldehyde-terminated monolayer was formed by exploiting the equilibrium between 2-hydroxypentamethylene sulfide (HPMS) and its open chain aldehyde isomer in solution (174). Adsorption of the ring-opened, aldehyde-terminated thiol on gold generates an aldehyde-terminated monolayer. This monolayer has been shown to bind primary amine-containing polymers (174) and proteins (153) and could directly react with amines on PEI-DNA complexes to form Schiff base without the use of other reagents. The Schiff base, in turn, can be further reduced to an amine bond using sodium cyanborohydride, $NaCNBH_3$.

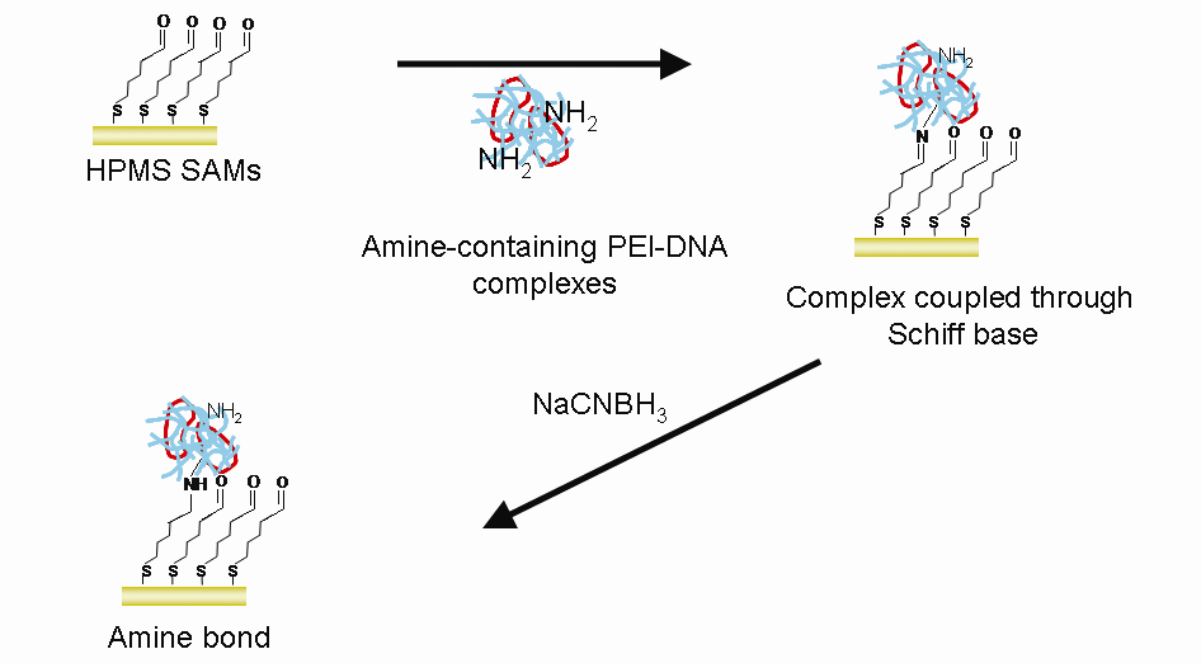

Figure 5-3 Direct coupling of PEI-DNA complexes to aldehyde-terminated SAMs (HPMS) via Schiff base formation followed by reduction to amine bond.

Complex immobilization to SAMs with deceasing percentages of the aldehyde-terminated thiols (HPMS), in a background of EG-terminated alkanethiols included to limit nonspecific complex immobilization, was not affected by the composition of the surface or the presence of the reduction agent, when complexes were deposited in high pH (9.6) (Figure 5-4A). All conditions resulted in binding efficiencies less than 50 ng/cm^2, which is lower than previous reports of lipoplexes binding to SAMs (Chapter 4, 117), and binding densities for PEI-DNA complexes on hydrophilic, serum-coated polystyrene substrates (2).

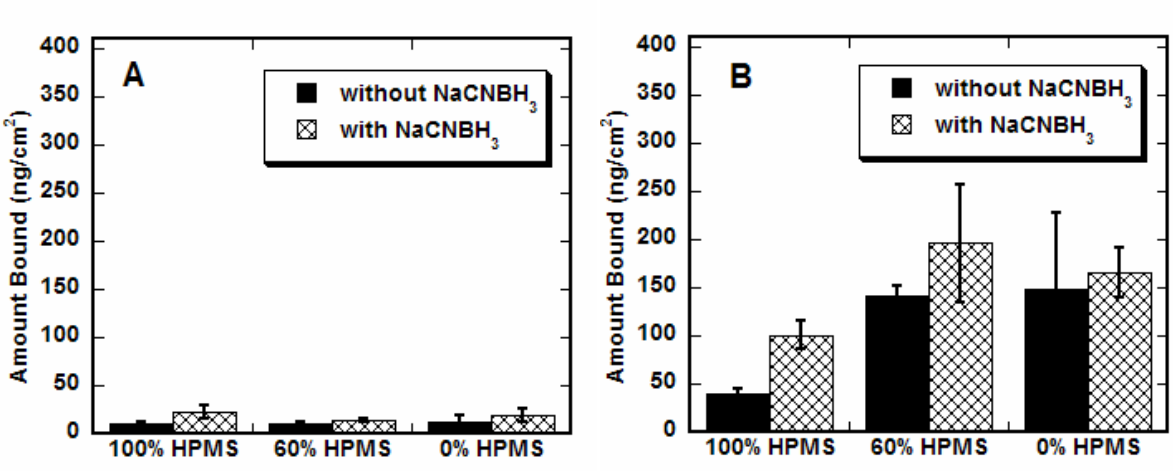

Figure 5-4 Schiff base coupling of complexes on SAMs. The amount of immobilized radiolableled DNA was determined for SAMs with decreasing percentages of aldehyde (HPMS) groups in a background of EG in the presence of absence of the reducing reagent ($NaCNBH_3$). Complexes were immobilized in buffers of high pH, 9.6 (A) and low pH, 6.5 (B).

For immobilization at lower pH (6.5) (Figure 5-4B), binding densities were again not affected by surface chemistry or the reduction of the Schiff base, as there was no statistical significance between any conditions at this pH. For surfaces containing only aldehyde groups (100%

HPMS), complex binding was higher (though not significantly) when the reducing agent was present, which could verify greater binding when complexes were presumably covalently tethered, which is in opposition to our results with EDC/NHSS. However, Schiff base formation is known to proceed more efficiently at alkaline pH (175), and the much lower binding densities for complexes deposited in pH 9.6 (Figure 5-4A) than in pH 6.5 (Figure 5-4B) could be attributed to more effective covalent tethering, and thus less DNA bound, similar to results with EDC/NHSS. However, for immobilization in both pHs, sufficient complex binding on surfaces containing no aldehyde-terminated alkanethiols (0% HPMS) as compared to SAMs with increasing percentage of HPMS, suggests nonspecific interactions might be the predominate immobilization mechanism. Transfection studies were not performed for the Schiff base tethering strategy, given the low complex binding densities, high amounts of nonspecific binding, and lack of statistical significance between conditions, as well as problems with monolayer formation.

5.3.2 Homobifunctional crosslinking

Glutaraldehyde was used to crosslink PEI-DNA complexes to SAMs (Figure 5-5). A homobifunctional crosslinker, glutaraldehyde contains aldehyde groups on either end that can react with hydrazide groups or amines. This crosslinker is very widely used for proteins (163) in that it allows for specific mild covalent coupling (if further reduced) that is not appreciably degraded. While Schiff base formation is typically thought of as a bond between aldehyde- and amine-containing molecules, aldehyde-containing molecules will also react with hydrazide compounds to form hydrazone linkages, which is a form of a Schiff base, but more stable than

one between an amine and aldehyde. This bond can also be further reduced in the same way. To capitalize on this more stable Schiff base, SAMs were modified with hydrazide groups to crosslink to PEI-DNA complexes with glutaraldehyde.

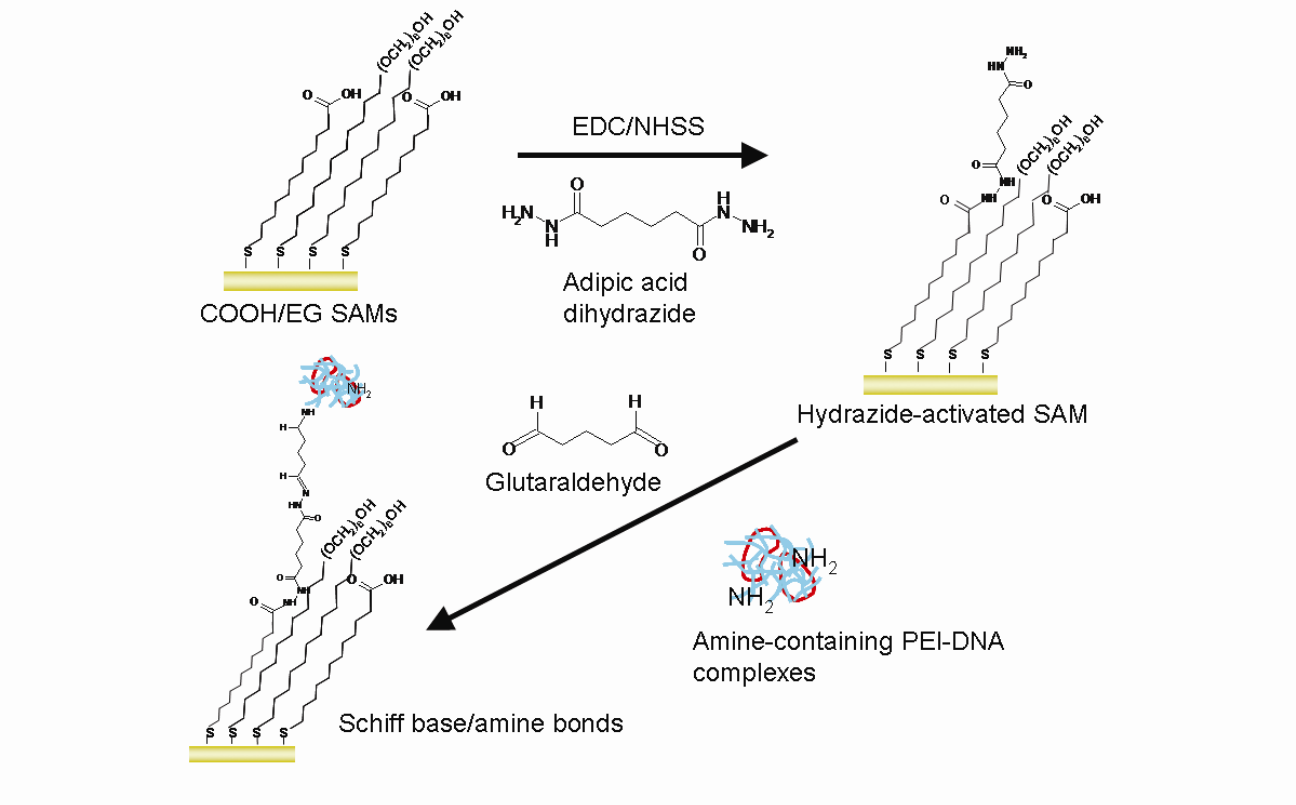

Figure 5-5 Homobifunctional crosslinking of PEI-DNA complexes to hyrazide-modified SAMs via glutaraldehyde.

Complex immobilization in the absence of the crosslinker resulted in high binding densities that were not affected by the absence or presence of reducing agent (Figure 5-6A), as expected. These high binding efficiencies are much greater than previous reports of lipoplexes

binding to SAMs (Chapter 4, 117), and PEI-DNA complexes on hydrophilic, serum-coated polystyrene substrates (2), indicating that SAMs presenting hydrazides support high levels of DNA immobilization. The amines on the hydrazides would not be expected to attract the positively-charged complexes, though incomplete complexation could result in loops of DNA extruding form the complexes, which could in turn interact with the hydrazide surfaces. When glutaraldehyde was added to the SAMs but not the reducing agent, binding was similar to those conditions without the crosslinker. However, complex immobilization was statistically lower ($p < 0.001$) on surfaces where the presumed hydrazone and Schiff base linkages were further reduced by $NaCNBH_3$, again providing evidence for lowered binding for covalently tethered complexes.

Transfection was nearly nonexistent on all surfaces (Figure 5-6B), in the absence or presence of the crosslinker and the reducing agent. Cells were found to be dead on all surfaces (data not shown), and apparent transfection on SAMs without glutaraldehyde with $NaCNBH_3$ can be attributed to a few remaining cells in a single replicate, given the large error bars and extremely low RLU/mg of protein values reported. While supporting high levels of complex binding, hydrazide-terminated SAMs may be toxic to cells or prevent cellular adhesion altogether. Alternatively, high concentrations of complexes in the cell microenvironment could have contributed to the cell morbidity. Additionally, homobifunctional crosslinkers, including glutaraldehyde, can have inherent problems in that both ends can react with surface (or complexes), forming loops and leaving no group to react with complexes (or surface), and can also result in a broad range of poorly defined aggregates that were not competent for transfection.

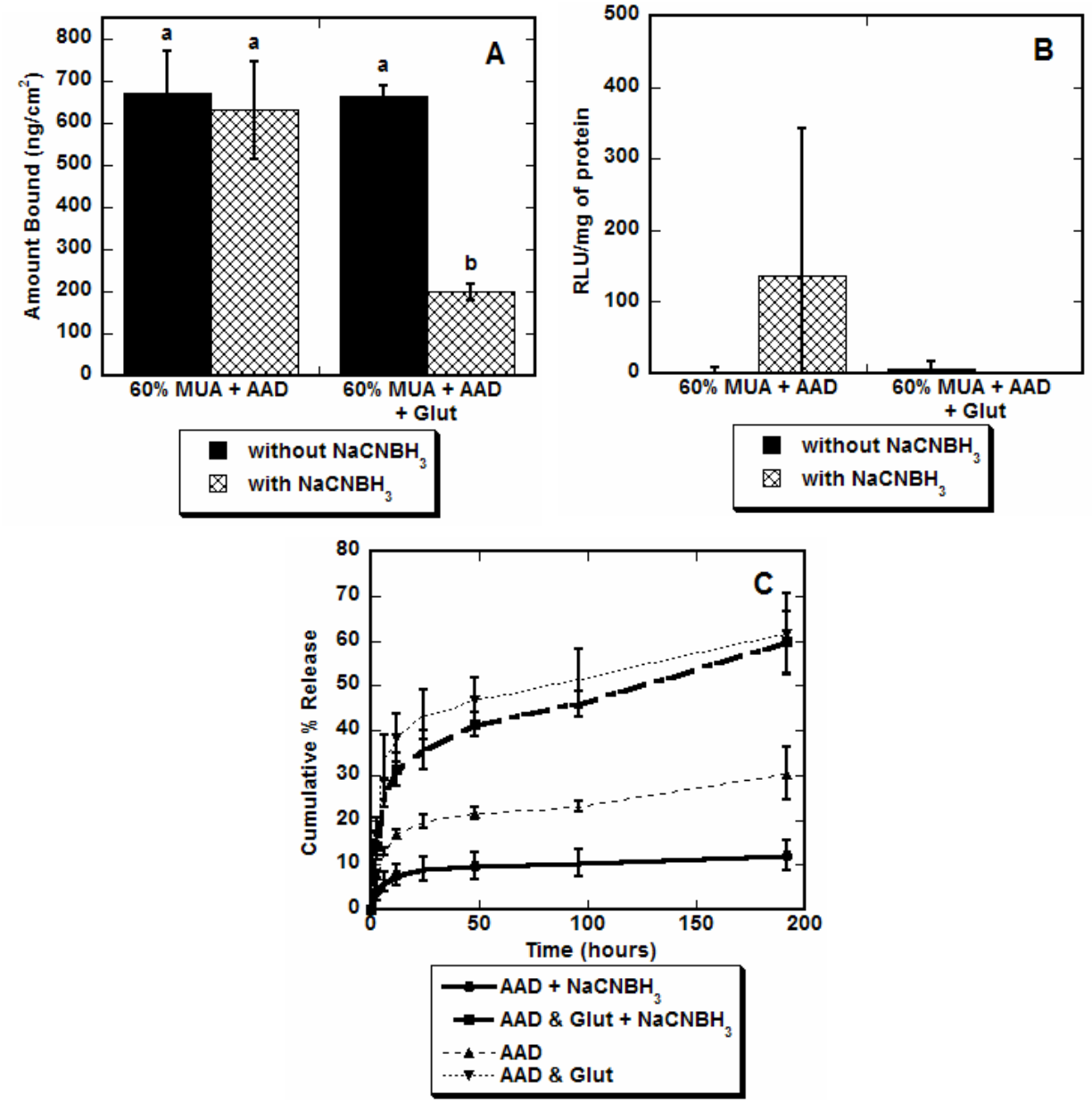

Figure 5-6 Glutaraldehyde crosslinking of complexes on SAMs. The amount of immobilized radiolableled DNA was determined for SAMs with 60% COOH (MUA) groups in a background of EG (A) in the presence or absence of the crosslinker (Glut) and reducing agent ($NaCNBH_3$). Transfection was assayed from the same conditions (B). Radiolabeled DNA was used to quantify the amount of DNA released (C) from tethered complexes (● 60 % MUA with EDC/NHSS/AAD and $NaCNBH_3$, ■ 60% MUA with EDC/NHSS/AAD and Glut and $NaCNBH_3$, ▲ 60 % MUA with EDC/NHSS/AAD, ▼ 60% MUA with EDC/NHSS/AAD and Glut) into serum-containing media. All values are reported as the mean ± s.d. and release values are reported as cumulative percentage released at each time point. *(Columns labeled with same letter designate conditions not statistically different; all other comparisons, $p < 0.001$ for (A)).*

Release profiles were used to investigate the presence of a covalent tether between the complexes and surface (Figure 5-6C). Release rates and total amount of DNA complexes released from SAMs was dependent on the coupling conditions. Release profiles were nearly identical for conditions in which glutaraldehyde was added to the surfaces, both with and without $NaCNBH_3$, with nearly 60% of the complexes released. However, for control conditions which did not contain glutaraldehyde, release rates were much slower, with less than 30% of complexes released. For all conditions most release occurred by 24 hours. Our finding that release is faster for complexes presumably tethered to the SAMs than for complexes nonspecifically immobilized, suggests that the tethering was either incomplete or degraded by some component in the media, which would make glutaraldehyde an interesting crosslinker to explore, if issues with the cytotoxicity associated with this tethering strategy could be eliminated.

5.3.3 Heterobifunctional crosslinking

Complexes were also crosslinked to SAMs using sulfo-SMCC, a noncleavable, heterobifunctional crosslinker that contains an NHS ester on one end and a maleimide group on the other (Figure 5-7). The NHS esters can react with primary amines to form covalent amide bonds, as described above, and maleimide groups can react with sulfhydryl groups to form stable thioether bonds. This crosslinker is often used for antibody-enzyme preparation and has been used with SAMs to attach biomolecules (78,164). In our studies, PEI-DNA complexes were added to SAMs with SH-terminated alkanethiols (O8SH) (168-170), formed either homogeneously or in a background of EG-terminated alkanethiols to prevent nonspecific binding of complexes. Complex binding was exceptionally high on O8SH SAMs in the absence of the

sulfo-SMCC crosslinker (Figure 5-8A), higher than densities reported in this study or elsewhere (2,117), suggesting that thiol-terminated SAMs promote nonspecific complex binding. However, complex immobilization was statistically lower when the sulfo-SMCC crosslinker was added to the surface ($p < 0.001$), again providing evidence for lowered binding for covalently tethered complexes.

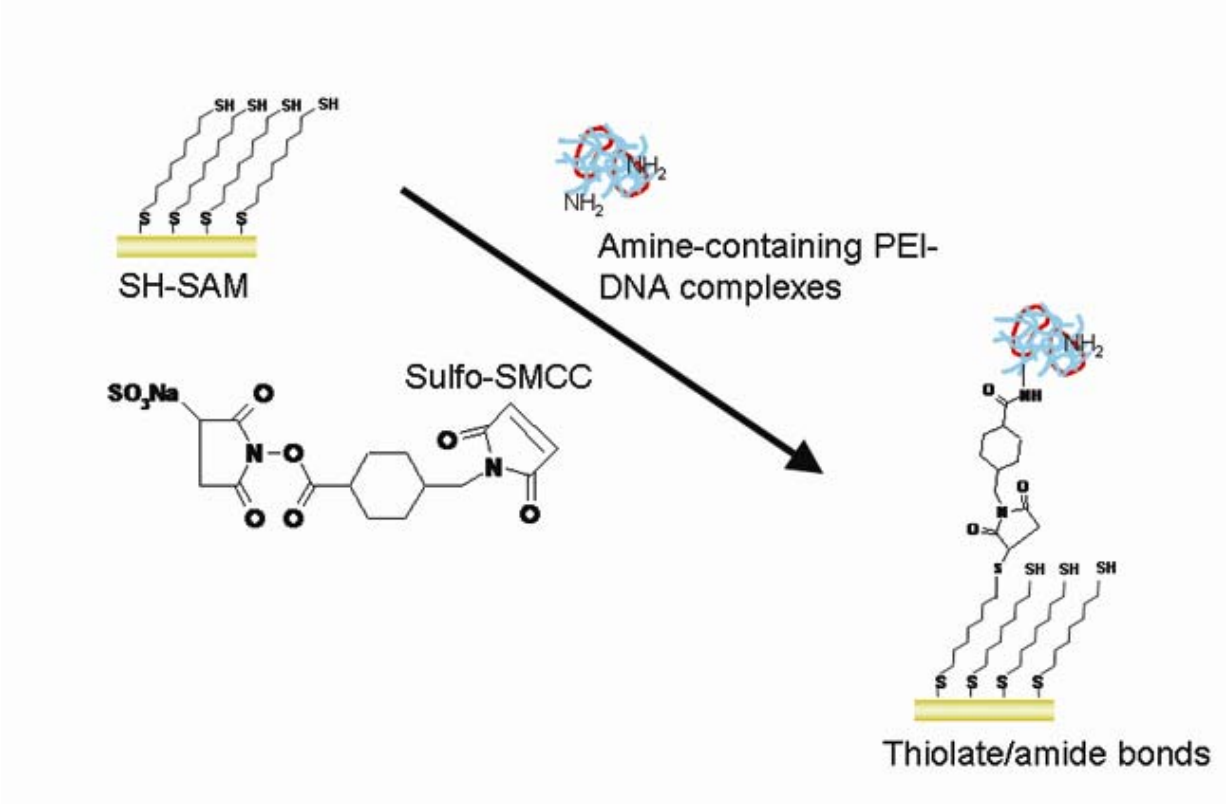

Figure 5-7 Heterobifunctional crosslinking of PEI-DNA complexes to thiol-terminated SAMs via sulfo-SMCC schematic.

Transfection was only observed for conditions with nonspecifically immobilized complexes (Figure 5-8B) and is similar to reported levels (2, Chapters 4 and 6), even though the amount of complexes bound was high. Once again, transfection by these nonspecifically

immobilized complexes was higher from surfaces containing EG groups (60% O8SH). Transfection levels on all SAMs to which the sulfo-SMCC crosslinker was added were zero, indicating that complexes were not available or viable for transfection. The addition of sulfo-SMCC would be expected to couple the complexes to the surfaces, which would then make them not available for internalization by cells, and would thus further validate our system's ability to tether complexes. The amines of the PEI within the complexes could be activated by the

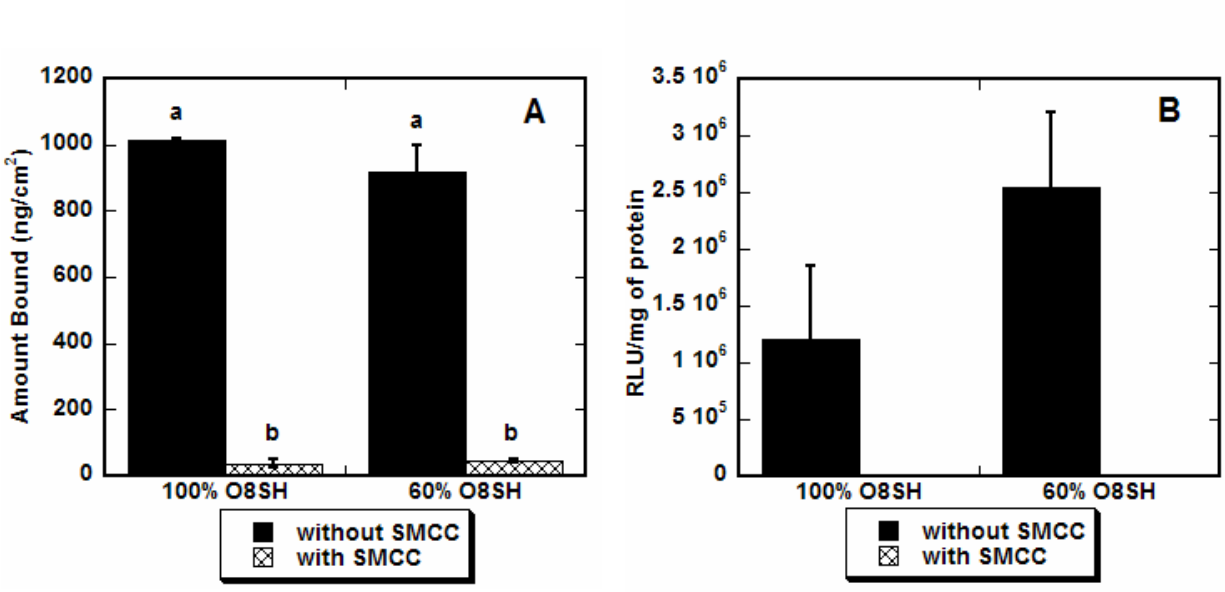

Figure 5-8 Sulfo-SMCC crosslinking of complexes on SAMs. The amount of immobilized radiolableled DNA was determined for SAMs with decreasing percentages of thiol (O8SH) groups in a background of EG (A) in the presence or absence of the crosslinker. Transfection was assayed from the same conditions (B). All values are reported as the mean ± s.d. *(Columns labeled with same letter designate conditions not statistically different; all other comparisons, $p < 0.001$ for (A)).*

addition of the NHS-containing crosslinker, but that in turn could be prohibiting successful cellular internalization and/or transfection. Furthermore, the activated complexes may not have been able to tether to the SAMs, as the O8SH monolayers are prepared from a dithiol, which could loop onto the gold substrate, where both thiol termini bond to the gold substrate or the

molecule itself lies flat on the surface (176). While there is little evidence of looping (169,170), the O8SH surface may need to be reduced to ensure the SH groups are reactive (168) in future studies.

5.3.4 Cleavable heterobifunctional crosslinking

AEDP, a cleavable, heterobifunctional crosslinker, was also used to tether complexes to SAMs (Figure 5-9). AEDP contains an amine on one end and a carboxylic acid group on the other end and can be used with EDC/NHSS chemistry to conjugate with amines on PEI of the complexes and COOH-terminated SAMs. The disulfide cross-bridge of AEDP can be cleaved using disulfide reducing agents like DTT to test the ability of a short degradable crosslinker, analogous to direct coupling with EDC/NHSS, to affect transfection of immobilized complexes.

Complex binding, in the presence or absence of AEDP with EDC/NHSS, was robust (Figure 5-10A), with binding densities similar to previous studies with presumed covalent tethering (Figure 5-2A in this chapter) or nonspecific binding of PEI-DNA complexes (2, Chapter 6). For surfaces with only COOH-terminated alkanethiols, there was no difference in binding between complexes nonspecifically immobilized in the presence of AEDP only (control conditions) and complexes presumably covalently tethered with the addition of EDC/NHSS to the AEDP crosslinker. For surfaces containing both COOH- and EG-terminated alkanethiols, complex binding was statistically lower in the presence of AEDP with EDC/NHSS ($p < 0.01$), again demonstrating lower binding for covalently tethered complexes, especially in the presence of the EG- thiols. One might expect that the presence of the EG groups within the SAM could separate the COOH groups, providing less contacts between the surface and the complexes and

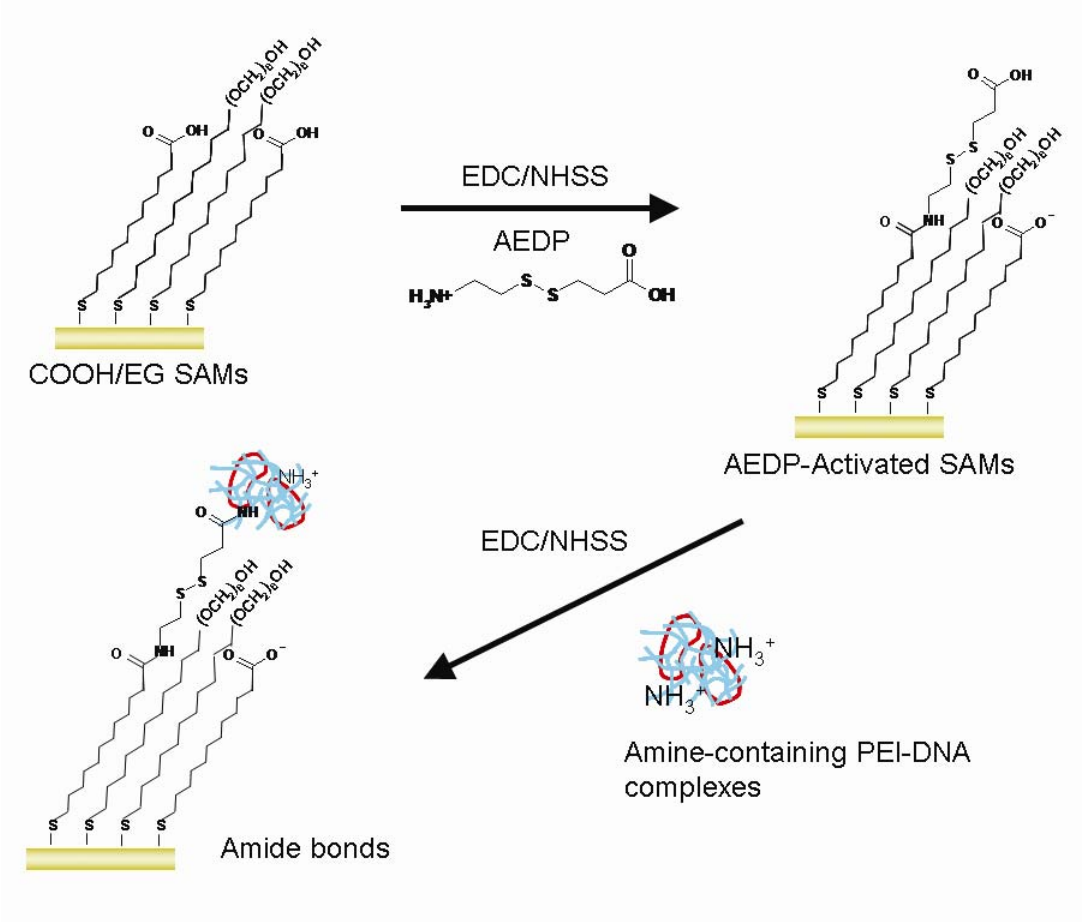

Figure 5-9 Heterobifunctional crosslinking of PEI-DNA complexes to COOH/EG SAMs via cleavable AEDP.

thus lowering the amount of DNA immobilized. However, for all conditions the addition of DTT, which should cleave the disulfide linkage within AEDP, did not affect complex binding. The inability of DTT to cleave the bond, which would be expected to be reflected in lowered DNA binding densities, could indicate that complexes were not successfully tethered. Alternatively, if the disulfide bond was at all hindered, DTT might not effectively cleave the bond. Furthermore, DTT may have been able to cleave the bond, but complexes may have

immediately rebound to the SAMs through nonspecific interactions, which have been prevalent throughout these studies.

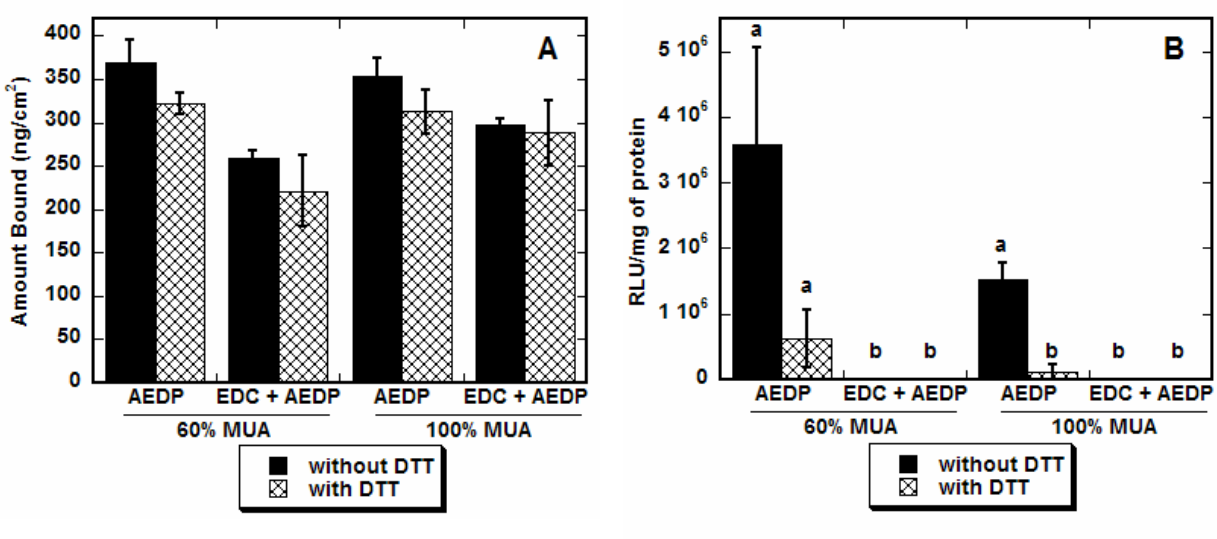

Figure 5-10 AEDP crosslinking of complexes on SAMs. The amount of immobilized radiolableled DNA was determined for SAMs with increasing percentages of COOH (MUA) groups in a background of EG (A) in the presence or absence of the coupling reagents (EDC/NHSS), both without and with the addition of DTT to cleave the disulfide bridge. Transfection was assayed from the same conditions (B). All values are reported as the mean ± s.d. *(Columns labeled with same letter designate conditions not statistically different; all other comparisons, $p < 0.01$ for (B)).*

Transfection levels did not correspond to complex binding efficiencies (Figure 5-10B). Transfection was only observed in the two conditions where only nonspecific immobilization was expected (60% MUA and 100% MUA with AEDP only), and was once again higher on SAMs containing EG groups (60% MUA). Surfaces to which EDC/NHSS was added to the AEDP crosslinker supported no transfection ($p < 0.01$), even though high amounts of complexes

were immobilized, which again could indicate successful covalent tethering. The addition of DTT would be expected to increase the level of transfection, as it would release covalently tethered complexes, making them available for internalization by cells. However, DTT addition to complexes resulted in lowered (60% MUA, AEDP only) or zero transfection levels. As cell morphology was unaffected by these conditions (data not shown), the inability of DTT to cleave complexes and increase transfection indicates a complete lack of covalent tethering, a shielding effect of the disulfide within the crossbridge, or inactivation of the complexes by these treatment schemes. Additionally, the cells themselves, attached to these surfaces, could prevent access of DTT to the disulfide bond, and thus prohibit cleavage of the complexes.

Finally, a second cleavable heterobifunctional crosslinker was used to tether PEI-DNA complexes to SAMs. Similar to sulfo-SMCC, sulfo-LC-SMPT contains a sulfhydryl-reactive end with a pyridyl disulfide derivative, while the other end is an amine reactive-NHS ester (Figure 5-11). This crosslinker, like AEDP, contains a disulfide bridge that is cleavable using disulfide reducing agents like DTT. PEI-DNA complexes were added to SAMs with SH-terminated alkanethiols (O8SH), formed either homogeneously or in a background of EG-terminated alkanethiols to prevent nonspecific binding of complexes, in the same manner as for its analogous crosslinker, sulfo-SMCC. Complex binding densities on O8SH SAMs in the absence of the sulfo-LC-SMPT crosslinker (Figure 5-12), were the highest ever observed by nonspecifically immobilized complexes on any surface, higher than densities reported in this study or elsewhere (2,117, Chapters 4 and 6), further suggesting that thiol-terminated SAMs promote nonspecific complex binding, similar to results with sulfo-SMCC. However, unlike

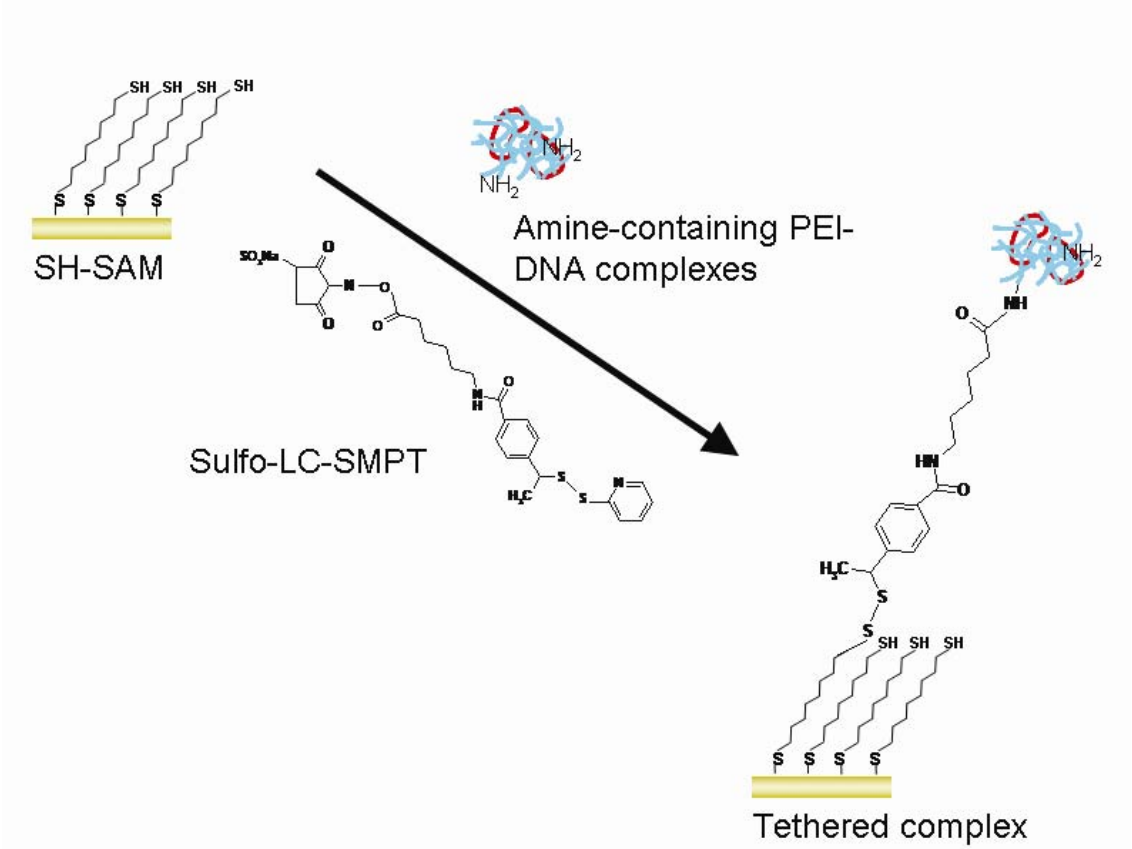

Figure 5-11 Heterobifunctional crosslinking of PEI-DNA complexes to thiol-terminated SAMs via cleavable sulfo-LC-SMPT.

other covalent tethering strategies reported in this chapter, complex immobilization was unaffected when the sulfo-LC-SMPT crosslinker was added to the surface. The addition of DTT, which would be expected to cleave the disulfide bridge within sulfo-LC-SMPT and release the complexes from the surface if they were tethered, had no effect on complex binding. While the disulfide bridge is cleavable, it is thought to be more slowly cleaved because of the hindered nature of the cross-bridge (175), and the inability of DTT to affect the complex binding densities may be attributed to inappropriate cleavage times. Transfection studies were not performed for the sulfo-LC-SMPT tethering strategy, given the extremely high complex binding densities,

which would be expected to be highly toxic, high amounts of nonspecific binding, and lack of statistical significance between conditions.

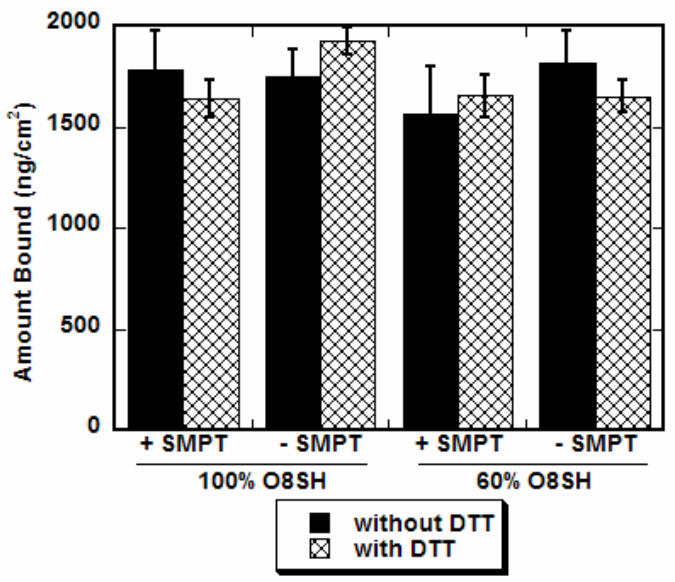

Figure 5-12 Sulfo-LC-SMPT crosslinking of complexes on SAMs. The amount of immobilized radiolableled DNA was determined for SAMs with decreasing percentages of thiol (O8SH) groups in a background of EG in the presence or absence of the crosslinker, both without and with the addition of DTT to cleave the disulfide bridge. All values are reported as the mean ± s.d.

5.4 Conclusions

Gene delivery has many potential applications in basic science (e.g., to study function and regulation of gene expression and proteins), therapeutics (e.g., gene therapy to treat genetic diseases), functional genomics (e.g., transfected cell arrays) and tissue engineering (e.g., to present factors in tissue regeneration matrices). The substrate-mediated delivery strategy is based on the immobilization of DNA complexes to a biomaterial or substrate that supports cell

adhesion (82). DNA complexes can be immobilized on the substrate through specific interactions introduced through complementary functional groups on the vector and surface or through nonspecific interactions.

In this chapter, strategies to covalently tether PEI-DNA complexes to SAMs were presented. Covalently tethered complexes provide an approach to extend the retention of complexes at the surface, especially in serum-containing environments, including in vivo conditions. These covalent tethering strategies have the potential to be translated to biomaterial surfaces, for use in tissue engineering applications. As summarized in Table 5.1, covalent tethering by EDC/NHSS, glutaraldehyde, sulfo-SMCC, and AEDP resulted in lower complex binding than corresponding conditions without the addition of crosslinker. In each of these cases, the presumed covalent tethering of complexes resulted in no transfection (Table 5.1),

Table 5-1 Summary of Tethering Strategies

Tethering Strategy	Binding		Transfection		Potential Problems with Strategy
	with crosslinker[a]	without crosslinker[b]	with crosslinker	without crosslinker	
EDC/NHSS	lower	same	none	highest on MUA/EG	inactivation of complexes
Schiff base	same	lower	N/A	N/A	low complex binding, monolayer formation issues
Glutaraldehyde	lower	higher	none	low	cell death on all surfaces
Sulfo-SMCC	lower	much higher	none	highest on SH/EG	inactivation of complexes
AEDP	lower	same	none	highest on MUA/EG	inactivation of complexes, shielding of disulfide bridge
Sulfo-LC-SMPT	same	much higher	N/A	N/A	high nonspecific binding

a. Compared to conditions without crosslinker.
b. Compared to densities reported elsewhere in thesis and literature.

which could be evidence of successful tethering, or more probably, inactivation of the complexes, as the addition of a reducing agent to cleavable crosslinkers (AEDP, sulfo-LC-SMPT) did not affect complex binding densities or transfection. Additionally, hydrazide and thiol-terminated SAMs appear to support high complex binding, which could contribute to cell toxicity and the lack of transfection.

When EG-terminated alkanethiols were incorporated into the monolayers, initially intended to eliminate nonspecific binding of complexes during studies where the complexes were to be tethered, control conditions indicated that monolayers containing 40% EG resulted in statistically greater transfection (Table 5.1). We hypothesize that the presence of EG groups in the monolayer may better preserve complex conformation upon binding to substrates, thereby enhancing the activity of substrate-mediated delivery of DNA complexes and this hypothesis is explored in Chapter 6. In the covalent coupling studies presented here, the lowered binding densities and complete lack of transfection may be evidence for tethering, verifying our system could be the foundation for further studies. In particular, studies aimed at controlling the extent of tethering (6), through modification of the amount of amines present within the complex (N/P ratio) and functional groups on surface (SAM composition, crosslinker concentration and conjugation times) will be important to modulate binding, release and transfection. However, the release profiles, toxicity issues, inability to cleave cleavable crosslinkers and vast amounts of nonspecific binding presented in this chapter suggest more work is needed to investigate covalent complex tethering.

Chapter 6

Incorporation of Polyethylene Glycol into Self-Assembled Monolayers Enhances Substrate-Mediated Gene Delivery by Nonspecifically- Bound Complexes

6.1 Introduction

Developing systems capable of controlled and efficient gene transfer is a fundamental goal of biotechnology, with applications including functional genomics, gene therapy, and tissue engineering. The primary challenge in applying gene delivery to these applications is inefficient delivery, with extracellular and intracellular barriers both limiting the efficiency. Controlled release systems for DNA delivery have the potential to overcome extracellular barriers that limit gene transfer and enhance gene delivery relative to more traditional delivery methods (81). These systems include delivery through polymeric release in which the DNA is released from a polymer scaffold or substrate-mediated delivery, in which DNA is retained at the surface of a substrate. Substrate-mediated delivery, also termed solid phase delivery or reverse transfection, involves the immobilization of DNA, complexed with nonviral vectors, to a biomaterial or substrate that supports cell adhesion (82). Cells cultured on the substrate are exposed to elevated DNA concentrations within the local microenvironment, which enhances transfection.

DNA complexes can be immobilized on the substrate through specific or nonspecific interactions for delivery from the surface. Specific interactions can be introduced through complementary functional groups on the vector and surface, such as antigen-antibody or biotin-avidin (5,6,22). Poly(L-lysine) (PLL) and polyethylenimine (PEI), modified with biotin residues,

were complexed with DNA and bound to a neutravidin substrate (5,6), resulting in 100-fold increased transgene expression from the immobilized complexes relative to bolus delivery of complexes (5). Plasmid DNA or DNA complexed with cationic polymers or lipids can also interact with substrates through non-specific mechanisms (2,45,46,117,145-147,156,157). Polyplexes and lipoplexes non-specifically immobilized to substrates enhanced transgene expression in both cell lines and primary human-derived cells, along with an increased cellular viability (2) and this enhancement was dependent on both the properties of the complex and substrate.

Surface chemistry has been shown to affect substrate-mediated delivery of non-specifically immobilized complexes, impacting both the initial binding and also subsequent transfection. Self-assembled monolayers (SAMs) of alkanethiols on gold were used to provide a flexible system for regulating surface chemistry (63,148,149) to examine complex-substrate interactions. DNA, complexed with cationic lipids, was immobilized through nonspecific mechanisms to SAMs presenting combinations of hydrophilic and charged (COO^-), hydrophilic and uncharged (OH), and hydrophobic terminal functional groups (CH_3) (Chapter 4, 117). Surface hydrophilicity and ionization were found to mediate both DNA complex immobilization and transfection, but had no effect on complex release. Greatest amounts of binding and transfection were observed on surfaces presenting charged, hydrophilic groups, suggesting that electrostatic interactions allow for reversible interactions between the substrate and complexes and result in efficient gene delivery (118). Hydrophobic substrates bound similar quantities of DNA as the hydrophilic surfaces, yet transfection was significantly reduced, suggesting the

conformation of the DNA complexes may be altered upon binding to hydrophobic surfaces and result in low transfection levels (2,117).

However, as in traditional gene delivery approaches, further improvements are still needed for substrate-mediated gene delivery to address issues that limit gene transfer, including complex size stability, complex aggregation, and strong interactions between the surface and complexes (2,22). Polyethylene glycol (PEG), which has the monomeric repeat unit [-CH_2-CH_2-O]- is widely used in drug and gene delivery and has been incorporated into DNA complexes of several cationic polymers, including polymethacrylate (177), PEI (27,178-185), PLL (186-188), and poly(amidoamine)s (189). PEG reduces the surface charge of the complexes (178,179,184,187), which in turn reduces cytotoxicity (178,180,184). The shielding effect of PEG also reduces the interaction between the complex and blood components (plasma proteins and erythrocytes) (178) and can prolong circulation of the complexes in the blood stream (178,185). Furthermore, PEGylation can prevent salt-induced aggregation through steric stabilization (178,179,182-184,186,187). Additionally, PEG is often used as a spacer for targeting ligands since the shielding effect of PEG is able to decrease nonspecific interactions with negatively charged cellular membranes, which results in reduction of nonspecific cellular uptake (190).

While some PEGylation strategies have had no effect on transfection efficiency in vitro (178,184,186) or in vivo (178), or even enhanced transfection (180,187), others have reported that PEGylation resulted in poor transfection (181,182,185), presumably due to interference with complexation (189). Further studies have probed the influence of the extent of PEGylation on PEI-DNA complexes and have found that increasing PEG incorporated within the complex

reduces cell binding and transfection (27,179) by more effectively shielding the surface charge of the DNA complexes (179). However, this appears to be polymer-specific, as transfection was enhanced with longer PEG chains conjugated to PLL (186,187), suggesting that PEG may induce leakage of endosomal membranes, resulting in improved cytoplasmic release of DNA or complexes.

In this chapter, SAMs of alkanethiols on gold were used to investigate substrate-mediated transfection by non-specifically immobilized complexes on surfaces containing varying densities of PEG functional groups. We hypothesize that rather than attach PEG to the complexes directly, its presence in a SAM could enhance substrate-mediated transfection by conveying the desired properties of PEG on gene delivery (reduced complex aggregation, complex size stability), and promote interactions between the complexes and cell membrane (Chapter 5). SAMs presenting oligo(ethylene glycol) (EG) groups (165,166) have previously been used to resist protein adsorption according to the length of the EG chain and percent composition within the monolayer (166,167), and are used here to modulate DNA complex adsorption for substrate-mediated gene delivery. In our studies, EG-terminated alkanethiols were incorporated into SAMs at concentrations that do not limit cell adhesion and combinations of EG- and COO^--terminated alkanethiols were examined for their ability to bind and release complexes and to subsequently support transfection. Complex morphology, a factor in gene delivery, was examined with atomic force microscopy on these surfaces. The correlation between surface chemistry and morphology of immobilized complexes must be a design consideration for translating substrate-mediated gene delivery to biotechnology applications.

6.2 Material and methods

6.2.1 Gold slide preparation and monolayer self assembly

Gold-coated glass slides were prepared using e-beam evaporation (Edwards Electron Beam Evaporator, Wilmington, MA), and consisted of a 5 nm titanium adhesion layer and 50 nm of gold. A diamond-tipped glass cutter was used to cut the gold-coated slides into smaller pieces that fit into standard 48-well tissue culture plates. Gold was prepared for SAM formation by extensive washing in acetone and ethanol, with subsequent drying under a stream of nitrogen. SAMs were formed by immersion of the clean gold substrates into 2 mM ethanolic solutions of alkanethiols for 18 hours in the dark, under argon.

Monolayers were formed with combinations of four different alkanethiols, including 1-decanethiol (DT10, CH_3-terminated), 11-mercapto-1-undecanol (MUOH, OH-terminated), 11-mercaptoundecanoic acid (MUA, COO^--terminated) (Aldrich, St. Louis, MO), and $HS(CH_2)_{11}(OCH_2CH_2)_6OH$, an oligo(ethylene glycol)-terminated alkanethiols (EG) (ProChimia, Gdansk, Poland). Alkanethiol solutions were freshly prepared in filtered, degassed ethanol. After monolayer formation, SAM samples were rinsed in pure ethanol and dried with nitrogen before further use.

6.2.2 Cellular adhesion on SAMs

Cell morphology and adhesion studies were performed on SAMs with increasing percentages of EG-terminated alkanethiols in a background of MUA, prepared as described above. NIH/3T3 cells (ATCC; Manassas, VA), cultured at 37°C and 5% CO_2 in DMEM supplemented with 1% sodium pyruvate, 1% penicillin-streptomycin, 1.5 g/L $NaHCO_3$ and 10%

fetal bovine serum, were seeded at a density of 15,0000 cells per SAM. Cellular morphology and adhesion were analyzed after 24 and 48 hours using phase microscopy. Adhesion studies were also performed on SAMs containing only EG-terminated alkanethiols, with immobilized PEI-DNA complexes (as described below) or by coating the EG-SAMs with free PEI, at a concentration equal to that added to complexes of various N/Ps (see below).

6.2.3 DNA complex formation

Plasmid was purified from bacteria culture using Qiagen (Valencia, CA) reagents and stored in Tris–EDTA buffer solution (10 mM Tris, 1 mM EDTA, pH 7.4) at −20 °C. Plasmid pEGFP-LUC encodes both the enhanced green fluorescent protein (EGFP) and firefly luciferase protein (LUC), under the direction of a CMV promoter and was used for quantification of binding, release, and transgene expression levels. Transfection efficiency was determined with plasmid pβGAL, which encodes for nuclear-targeted β-galactosidase, under the direction of a CMV promoter. For DNA complex formation, branched PEI (25 kDa, Aldrich, St. Louis, MO) was diluted in 25 mM sodium phosphate buffer, pH 6.5 and then added dropwise to DNA in sodium phosphate buffer, vortexed for 10 seconds, and incubated for 15 min at room temperature. Complexes were formed at N/P ratios of 10 or 25, and 3 μg of DNA (300 μl final volume of complexes) was added to each SAM for binding, release and transfection studies.

6.2.4 Quantification of DNA complex immobilization and release

Plasmid radiolabeled with α-^{32}P dATP was used to measure the immobilization and release of DNA complexes on SAMs with varying amounts of EG-terminated alkanethiols in a

MUA background. Briefly, a nick translation kit (Amersham Pharmacia Biotech; Piscataway, NY) was used following the manufacturer's protocol with minor modifications (6). The labeled DNA was diluted with unlabeled DNA to a final concentration of 1% and this mixture was then used to form DNA complexes, as described above. After SAM preparation as described above, digital photographs of each sample were taken prior to complex immobilization and analyzed with ImageJ (NIH) to determine the area of each surface. SAMs were activated for complex immobilization by equilibration with 1X PBS (phosphate-buffered saline, pH 7.4) for 2 minutes, followed by a second incubation in MilliQ water for 10 minutes. Complexes were immobilized by incubation on these activated SAMs for 2 hours. After the deposition period, the complex solution was removed and the SAMs were washed twice with PBS. The quantity of DNA immobilized was determined by immersing individual SAM samples in scintillation cocktail (5 mL, BioSafe II, Research Products International Corp., Mount Prospect, IL) for measurement with a scintillation counter. The counts were correlated to DNA mass using a standard curve. The density of DNA immobilized to each SAM sample was determined by normalizing the amount bound to area.

To determine the release profile, SAMs with immobilized DNA complexes were incubated with serum-containing cell growth media at 37°C in a humid chamber. At predetermined time points, half of the media was removed and replaced with fresh media. The activity of the collected sample was measured in a scintillation counter. At the final time point, the counts remaining on the SAM samples were also determined. The percentage of DNA released was calculated as the ratio of the cumulative counts released through a given time

divided by the total counts initially on the substrate, thus, the release curves represent the percentage of DNA released relative to the initial amount bound to each surface.

6.2.5 Transfection on SAMs

Transfection studies were performed with NIH/3T3 cells, cultured as described above, on SAMs with varying amounts of EG-terminated alkanethiols, in backgrounds of MUA, MUOH or DT10, as well as SAMs containing combinations of MUA, MUOH, and DT10 only. After complex formation and immobilization as described above, SAMs were immediately seeded with 15,000 cells in 48-well plates. Transfection was analyzed following a 48-hour culture, characterized through the extent of transgene expression, which was quantified by measuring the luciferase activity using the Luciferase Assay System (Promega, Madison, WI). The luminometer (Turner Designs, Sunnyvale, CA) was set for a 3 second delay with an integration of the signal for 10 seconds. Luciferase activity (RLU) was normalized to the total protein amount determined with the BCA protein assay (Pierce, Rockford, IL). Transfection efficiency was also analyzed following a 48-hour culture, characterized through the number of transfected cells using β-galactosidase expression visualized by staining with X-gal solution followed by imaging with a microscope (Leica; Bannockburn, IL) equipped with a color filter. The number of transfected cells was determined by counting 5 random fields on each SAM. The percentage of transfected cells was calculated as the ratio of the number of transfected cells divided by total cell number, determined by manual counting of phase images.

6.2.6 Atomic force microscopy of immobilized complexes

Atomic force microscopy (AFM) was used to examine complex morphology. SAMs for AFM studies were prepared on gold-coated mica substrates (150 nm of gold, Agilent Technologies AFM, Tempe, AZ). SAM formation and complex formation and immobilization were performed as described above. After immobilization, surfaces were rinsed with 1X PBS, as described above, with two additional washes in MilliQ water, to remove any traces of salt on the surface. Samples were allowed to dry in air before imaging. AFM experiments were carried out with a DI Multimode AFM (Digital Instruments, Houston, TX) with a Type J scanner controlled with a NanoScope IIIa controller (Digital Instruments). Images were collected in air at room temperature using contact AFM. Silicon nitride cantilevers (Veeco, Santa Barbara, CA) with a spring constant of 0.12 N/m were used for collection of all images. Images were collected at 256 x 256 pixel resolution at a scan rate of <2 Hz. Initial image collection utilized the DI software, NanoScope 5.03, version r1 (Digital Instruments) and images were filtered using a flattening analysis, and then further analyzed by WSxM, version 3.0 (Nanotec Electronica, Madrid, Spain) to generate height profiles, and compare surface roughness using root-mean-square (RMS) calculations. Area-perimeter ratios analysis was performed with a height cut off of 40 nm (for 0% EG, N/P 10 and 40% EG, N/P 25 conditions) in regions with large globular particles and 7 nm and 15 nm (0% EG, N/P 10 and 40% EG, N/P 25, respectively) in regions without these large globular structures, which resulted in a range of ratios reported for these two conditions. For area-perimeter analysis on all other images (40% EG, N/P 10 and 0% EG, N/P 25), the height cut off used was 7 nm.

6.2.7 Statistics

Statistical analysis was performed using JMP software (SAS Institute, Inc., Cary, NC). Comparative analyses were completed using one-way ANOVA with Tukey post-tests, at a 95% confidence level. Mean values with standard deviation are reported and all experiments were performed with a minimum sample size of three, in replicates.

6.3 Results and discussion

6.3.1 Cell adhesion on EG SAMs

The maximal amount of EG that could be incorporated into the monolayer without sacrificing cell morphology and adhesion (Figure 6-1) was initially determined. Cells were seeded on SAMs with increasing percentages of EG-terminated alkanethiols in a background of MUA (COO^-). A monolayer containing no EG thiols resulted in a robust cell monolayer (Figure 6-1A), similar to previous results on COO^--terminated SAMs (70,71). Increasing the percentage of EG groups to 40% (Figure 6-1B, 20% EG; Figure 6-1C, 40% EG) did not appreciably affect the cell morphology or the cell monolayer. Increasing the EG groups to 60% or more (Figure 6-1D, E) altered the cell morphology and produced a more sporadic cell distribution on the surface. A SAM consisting of only EG groups (Figure 6-1F) had no cells attached, which is expected due to the resistance of the surface to protein adsorption (166,167), that would be needed to support cellular adhesion. A complete elimination of cellular adhesion on SAMs containing 100% EG thiols indicates the robustness of the monolayers formed.

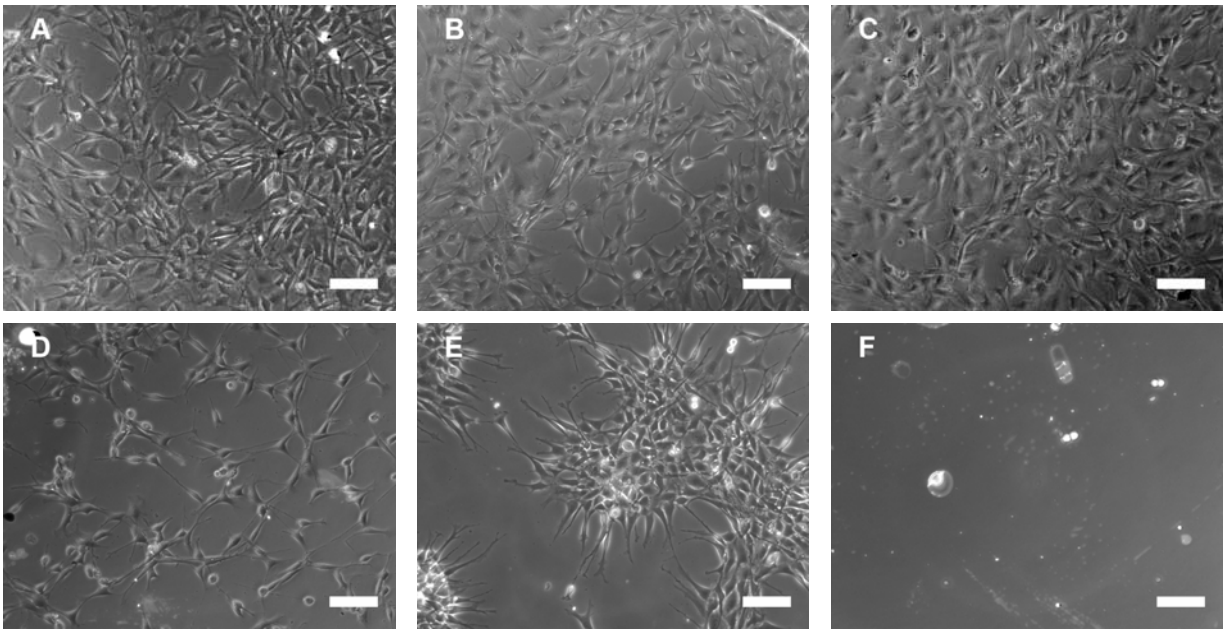

Figure 6-1 Cell adhesion on EG-containing SAMs. Images were captured 48 hours after seeding cells on SAMs (A) 0% EG/100% COO^-, (B) 20% EG/80% COO^-, (C) 40% EG/60% COO^-, (D) 60% EG/40% COO^-, (E) 80% EG/20% COO^-, and (F) 100% EG, all lacking immobilized DNA complexes. Scale bars correspond to 100 μm.

6.3.2 Quantification of complex immobilization

SAMs with varying densities of EG groups, in a background of MUA (COO^-) were subsequently employed to investigate the non-specific immobilization of complexes. The amount of DNA immobilized to the surfaces did not vary with monolayer composition (Figure 6-2), but was affected by the N/P ratio (Figure 6-2). For an N/P of 10 (Figure 6-2A), binding averaged approximately 0.35 μg/cm^2, whereas complexes at N/P of 25 averaged higher binding densities, approximately 0.5 μg/cm^2 (Figure 6-2B). These amounts are similar to, or much greater than previous reports of lipoplexes binding to SAMs (117,118, Chapter 4), but are

consistent with binding densities for PEI-DNA complexes on hydrophilic, serum-coated polystyrene substrates (2).

Previous studies suggest that nonspecific DNA complex adsorption is mediated by at least two mechanisms: electrostatic and hydrophobic interactions (Chapter 4, 117). Increasing the density of charged functional groups (COO^-) in a background of uncharged groups (OH) increased complex immobilization, suggesting that electrostatic interactions play a major role in binding (117). However, in this study, by decreasing the EG groups, and thus increasing the COO^- background, no differences in binding were observed. The larger EG headgroups could be shielding the presentation of the COO^- groups, similar to the shielding observed when PEG is incorporated into DNA-polymer complexes (179). Shielding by the EG groups within the SAM could limit the electrostatic interactions between the carboxylic acids groups within the SAM and complexes and thus reduce the effect of charged functional groups on binding. Additionally, free PEI in the complex solution, which would be more abundant at an N/P of 25, could be binding to the SAM and changing the surface properties, eliminating differences between surfaces. Although these EG-modified SAMs have substantially reduced protein adsorption (166,167), presumably through steric stabilization and excluded volume, they still adsorb serum proteins (191,192) and complexes may bind either to the adsorbed proteins or to the sites that mediate protein adsorption.

6.3.3 Quantification of complex release

Release studies were subsequently used to investigate the stability of the interaction between the complexes and surface (Figure 6-3). Similar to previous studies on SAMs (Chapter

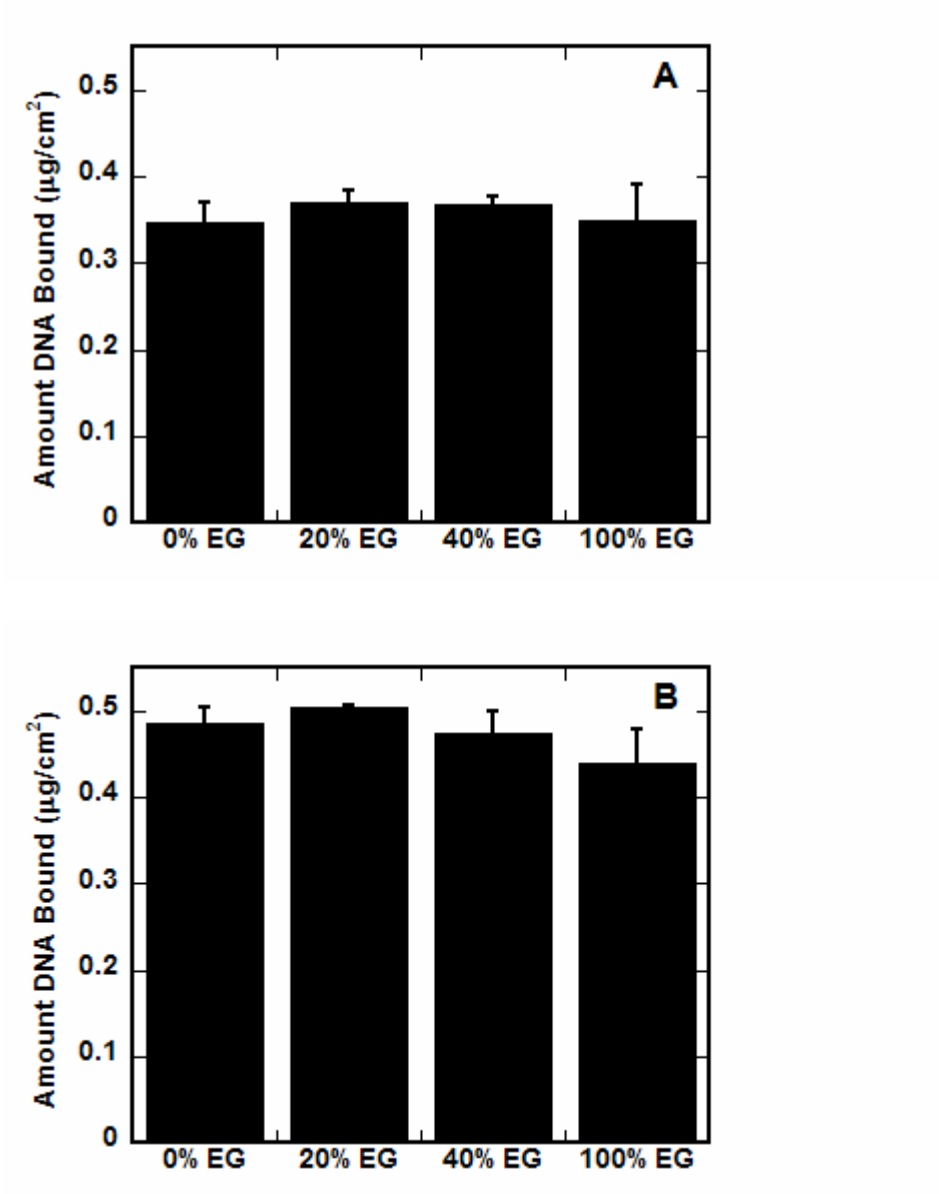

Figure 6-2 DNA complex immobilization on EG-containing SAMs. The amount of immobilized radiolableled DNA was determined for SAMs with increasing percentages of EG groups in a background of MUA (COO^-), for complexes formed at N/P of 10 (A) and 25 (B). Values are reported as the mean ± s.d.

4, 117,118), release rates and total amount of DNA complexes released from SAMs was independent of surface chemistry (Figure 6-3). For both N/P of 10 (Figure 6-3A) and 25 (Figure 6-3B), most of the DNA release occurred by 24 hours. After 8 days, less than 30% of the complexes were released, regardless of the composition of the SAM or complex. These release rates are substantially lower than profiles previously determined for lipoplexes from SAMs (Chapter 4, 117), but similar to release curves obtained from PEI-DNA complexes on hydrophilic, serum-coated polystyrene substrates (2). The presence of serum in the release media significantly enhances the release of non-specifically immobilized complexes relative to incubation with PBS (2). Our finding that release is independent of surface chemistry, both in this study and in previous reports (Chapter 4, 117), suggests that complex release from the substrate is mediated by competitive binding of serum components to the EG-containing SAMs, which can adsorb significant amounts of serum proteins (191).

6.3.4 Transfection on SAMS on gold

6.3.4.1 Transgene expression

SAMs with various densities of EG-terminated alkanethiols were explored to examine the ability of PEG on a surface to affect substrate-mediated gene delivery. While binding and release were not affected by the EG in the surface, expression levels increased with the percentage of EG alkanethiols in the SAM (Figure 6-4) up to 40% EG. For the lower N/P (Figure 6-4A), expression was significantly greater on 40% EG SAMs than surfaces containing no EG alkanethiols ($p < 0.05$) or surfaces containing only EG alkanethiols ($p < 0.01$); the latter

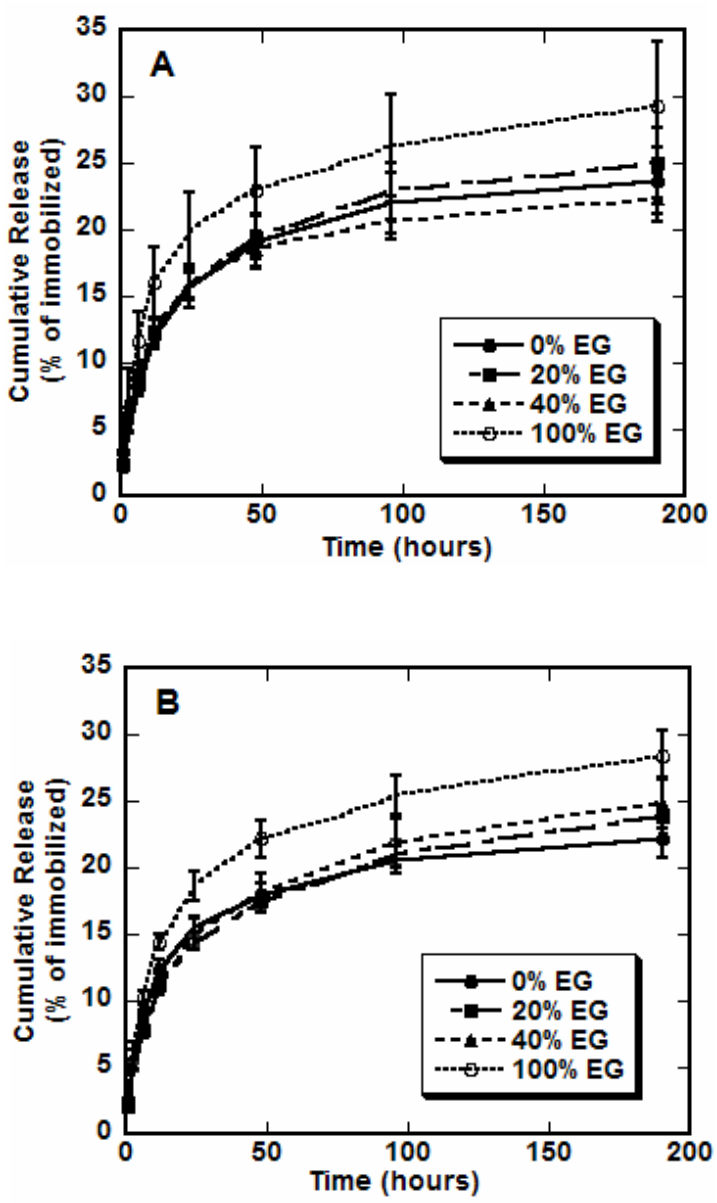

Figure 6-3 EG-containing SAMs and release. Radiolabeled DNA was used to quantify the amount of DNA released from each type of SAM (● 0% EG, ■ 20% EG, ▲ 40% EG, ○ 100% EG) into serum-containing media. Complexes formed at N/P 10 (A) and 25 (B). Values are reported as cumulative percentage released, reported as the mean ± s.d. at each time point.

observation presumably due to low cell binding. For complexes at the high N/P (Figure 6-4B), transfection was again significantly greater on SAMs containing 40% EG than surfaces with no EG ($p < 0.05$), however transfection was not statistically different between the 40% EG condition and SAMs with only EG alkanethiols, suggesting both significant cell adhesion and subsequent transfection on these surfaces. This issue of cell adhesion to complexes immobilized on EG-terminated alkanethiols is discussed in the next section. These findings, that increasing the percentage of EG groups, and thus decreasing the percentage of carboxylic acid groups increases transfection, are in contrast to previous studies, where surfaces with 100% carboxylic acid functional groups resulted in highest transfection levels, presumably due to high binding efficiencies (Chapter 4, 117). However, in the present study, the presence of EG in the surface did not affect complex immobilization, and therefore the amount of DNA bound did not contribute to enhanced transfection.

EG groups on the surface may enhance transfection through multiple mechanisms, including PEG-complex and PEG-cell interactions. PEG incorporated into DNA complexes of cationic polymers can reduce their surface charge (178,179,184,187), cytotoxicity (178,180,184), and interaction with blood components (178), as well as prevent aggregation through steric stabilization (178,179,182-184,186,187). Because of its ability to modulate the properties of complexes, PEG has been reported to enhance transfection when attached to polymer-DNA complexes directly (27,180,186,187) or simply added to transfection media containing lipoplexes (193). The enhancement of transfection by EG-containing SAMs could be attributed to the possible modulation of complex properties (surface charge, aggregation, complex-cell interaction), similar to the effects of PEG with soluble complexes, by mere association of the EG

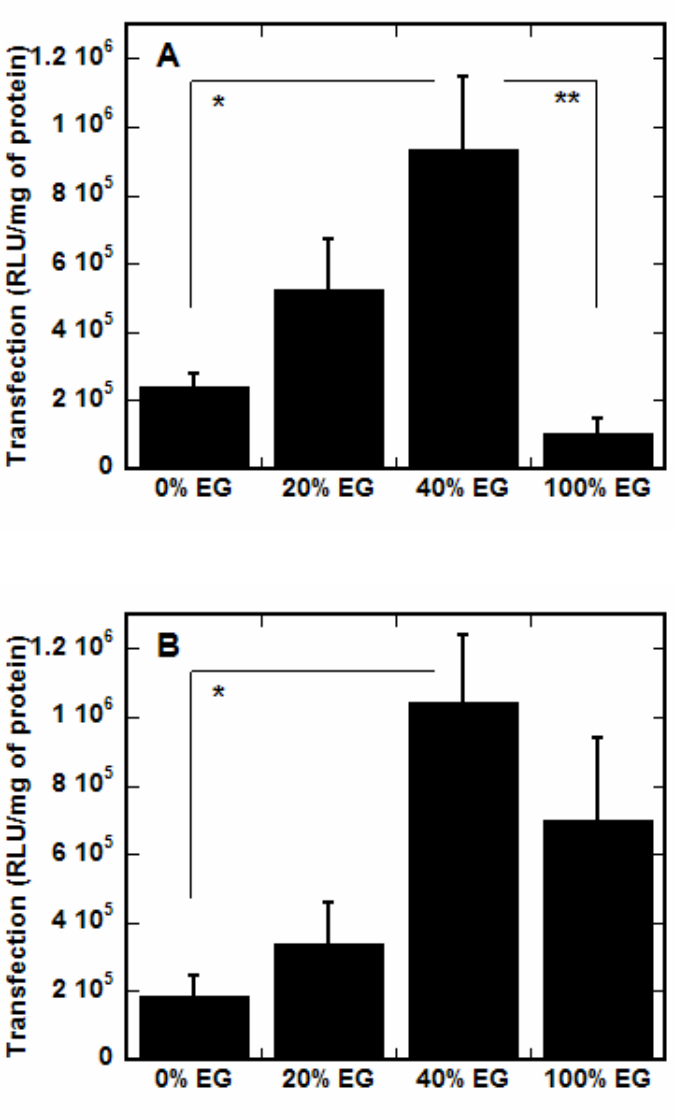

Figure 6-4 EG-containing SAMs and substrate-mediated transfection. SAMs were formed with increasing percentages of EG groups in a background of MUA (COO^-) and transfection was assayed for complexes formed at N/P of 10 (A) and 25 (B) by normalizing luciferase levels to total protein amounts. Values are reported as the mean ± s.d. *(*p < 0.05, **p < 0.01).*

groups with the complexes on the surface. Similarly, the addition of Pluronic, a block co-polymer of poly(ethylene oxide)-poly(propylene oxide)-poly(ethylene oxide), to microfluidic channels used for deposition of DNA complexes, enhanced substrate-mediated transfection within these channels possibly by preventing aggregation or enhancing complex association with the cells (157).

However, the association of the cell membrane with the SAMs containing EG groups could also contribute to an enhancement of transfection. PEG is known to induce association and fusion of phospholipid vesicles at high concentrations (194), widely used in the cell fusion required for formation of hybridomas. PEG, when added to transfection media of lipoplexes has been shown to increase the association of lipoplexes with the cell membrane up to 100 fold over controls without PEG (193). This enhanced association could occur through a depletion effect, which produces an attractive osmotic force due to a polymer depleted layer near the bilayer surface (193). Thus, EG groups on the surface of the SAMs may promote association of the DNA complexes with the cell membranes.

By incorporating PEG groups onto the SAM surface, complex properties and transfection can be enhanced, but the EG groups can not interfere with complexation. PEGylation of the polymer prior to DNA association can interfere with complexation (189), which can reduce transfection (181,182,185). Furthermore, in typical PEGylation strategies, the surface charge of polymer-DNA complexes decreases due to the shielding effect of PEG (179), with PEG side chains covering the surface of complexes and hindering the interaction between the complex and cell membrane. However, with EG present on the surface, complexes can be formed with the traditional procedures for subsequent immobilization. The presence of the EG groups on the

surface should not interfere with cellular association of the complexes as previously reported (27,179), as the charge of the complexes would be unaffected by immobilization on EG-containing SAMs.

6.3.4.2 Cell adhesion on immobilized complexes

For complexes at the high N/P (Figure 6-4B), high transfection levels on SAMs with only EG alkanethiols suggest cell adhesion on these surfaces, which had resisted cell adhesion previously (Figure 6-1) and was expected to resist protein adsorption (166,167). However, adhesion studies on SAMs containing only EG alkanethiols (100% EG) with immobilized complexes or PEI alone demonstrate significant cell adhesion (Figure 6-5). PEI added alone at concentrations equivalent to N/P 10 (Figure 6-5A) or N/P 25 (Figure 6-5B) promoted cell adhesion, though cell monolayers were not as robust as those on surfaces with less EG alkanethiols and no PEI (Figure 6-1). DNA complexes were also able to enhance cell adhesion, at N/P 10 (Figure 6-5C) and N/P 25 (Figure 6-5D). For high N/P, protein levels determined on the surface were low, indicating low cell numbers. Correspondingly low luciferase levels (data not shown), normalized to these low protein levels, result in robust transfection levels, and could give the appearance of enhancement of transfection on 100% EG surfaces (Figure 6-4B).

As complexes bind to surfaces through mechanisms similar to proteins (82,117), their binding on surfaces containing PEG groups would also be expected to be reduced. However, binding studies reveal that increasing the percentage of EG groups on the surface did not affect the amount of DNA complex immobilization (Figure 6-2). The relatively high contact angles reported for EG-containing SAMs are consistent with an outer phase that exposes CH_2 groups to

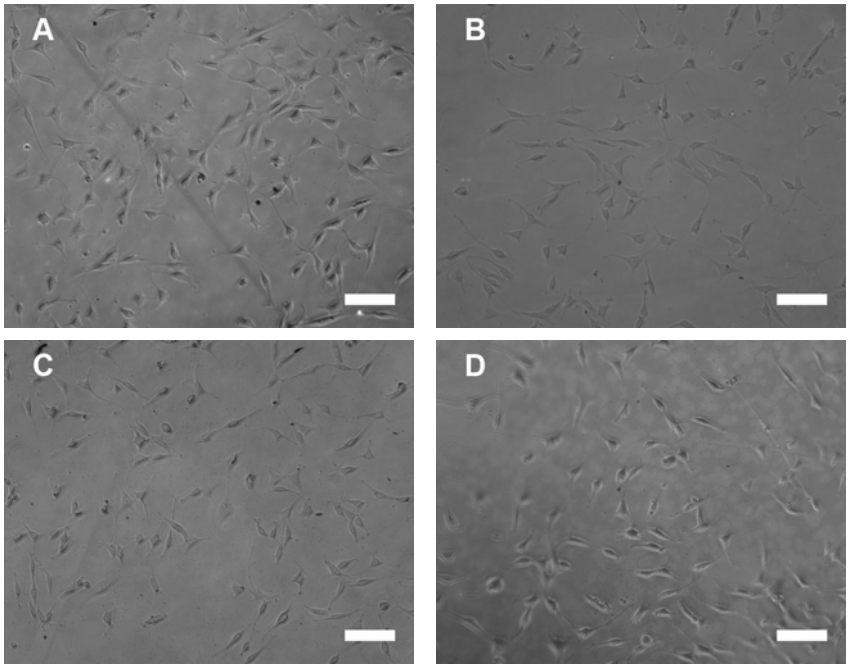

Figure 6-5 Cell adhesion on complexes immobilized on EG-containing SAMs. The morphology and adhesion of cells was observed 48 hours after seeding cells on SAMs of (A) 100% EG with PEI concentration equivalent to N/P 10, (B) 100% EG with PEI concentration equivalent to N/P 25, (C) 100% EG with PEI-DNA complexes formed at N/P 10 and (D) 100% EG with PEI-DNA complexes formed at N/P. Scale bars correspond to 100 μm.

solution (165). PEG, while known as a hydrophilic polymer, is truly amphiphilic, with both hydrophilic and hydrophobic components, and this combination of properties is a key to its biocompatibility (195). PEI molecules contain ethylene units along the backbone, and thus hydrophobic interactions could allow for immobilization of PEI-DNA complexes on EG-containing SAMs, similar to reports of DNA complex binding through hydrophobic interactions (115,117). By binding to the SAMs containing EG alkanethiols, PEI-DNA complexes or free PEI could coat the surface, producing substrates with net positive charge, which could allow for protein immobilization through electrostatic interactions (153), and subsequent cell adhesion.

This hypothesis agrees well with our transfection results, as complexes at high N/P (25) would have much more free PEI in solution than complexes at low N/P, which could further coat the surface and promote cell adhesion and thus transfection.

6.3.4.3. Transfection efficiency on SAMs

Transfection efficiency, reported as a percentage of transfected cells, was subsequently quantified for complexes immobilized on EG-containing SAMs (Figure 6-6). β-galactosidase expression was assayed at 48 hours using phase microscopy. For both N/P ratios, the transfection efficiency increased as the percentage of EG groups within the SAMs increased, similar to the trend observed with the transfection levels. However, for both complex formulations, SAMs containing only EG groups resulted in the highest percentage of transfected cells. At low N/P (Figure 6-6A), the transfection efficiency on 100% EG SAMs was statistically greater than surfaces containing 20% ($p < 0.05$) or no EG groups ($p < 0.01$). Additionally, 40% EG SAMs resulted in statistically greater transfection efficiency than 0% EG ($p < 0.05$). For N/P of 25 (Figure 6-6B), 100% EG SAMs supported the highest transfection efficiency, though the standard deviation was large and statistical tests did not indicate significant differences.

The transfection efficiency data indicate that more cells are transfected on surfaces containing more EG groups, but do not reflect that total cell numbers were reduced on the 100% EG SAMs. No trend could be determined between number of cells on surface (indirectly measured by BCA assay) and percentage of EG in monolayer with immobilized complexes (data not shown). For N/P 10, cell numbers were similar for all percentages of EG, but slightly higher for SAMs containing 20 and 100% PEG. For N/P of 25, cell numbers are nearly identical for all

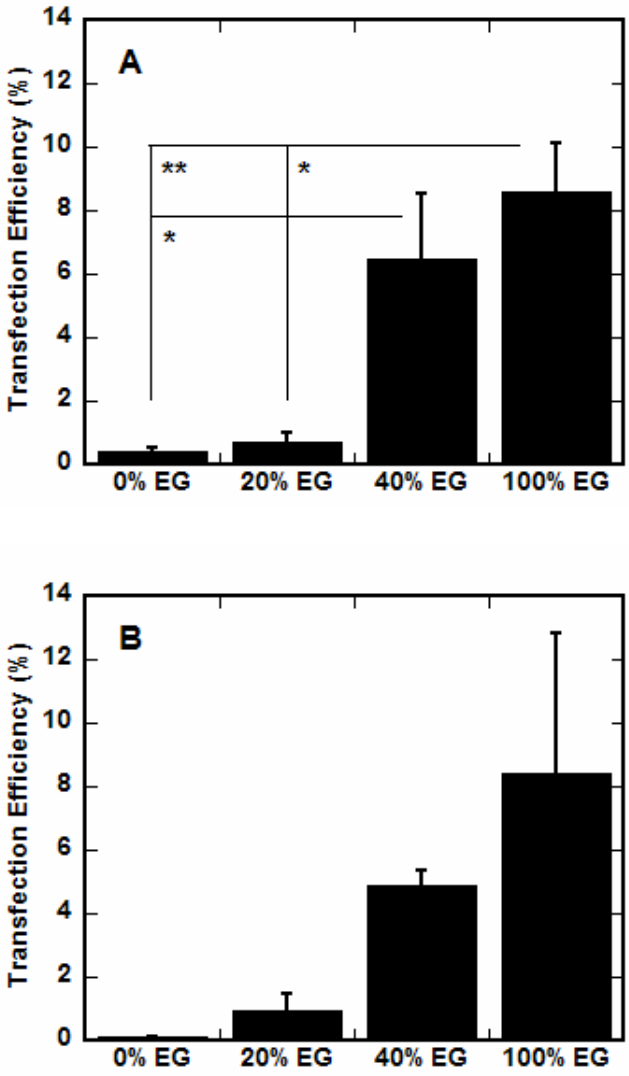

Figure 6-6 EG-containing SAMs and transfection efficiency. SAMs were formed with increasing percentages of EG groups in a background of MUA (COO^-) and transfection efficiency was assayed for complexes formed at N/P of 10 (A) and 25 (B) by counting the number of cell expressing β-galactosidase and dividing by the total number of cells. Values are reported as the mean ± s.d. *(*p < 0.05, **p < 0.01).*

SAMs, except much lower for 100% EG (data not shown), consistent with our transfection efficiency results, which demonstrate few cells adhered (data not shown). Those cells that did adhere to these surfaces (100% EG, N/P 25) were more likely to be transfected than in the corresponding N/P 10 condition, resulting in huge variability in transfection efficiency evidenced by the large standard deviation (Figure 6-6B).

6.3.4.4. Transfection enhancement specificity

SAMs containing combinations of alkanethiols with alternative functional groups were used to determine if the enhancement in transfection was specific to surfaces containing EG and COO^- groups (Figure 6-7). Alternative functional groups included OH and CH_3 in backgrounds of 40% EG (Figures 6-7A and 6-7B) and 60% COO^- (Figures 6-7C and 6-7D), as these compositions provide maximal expression levels and transfection efficiency with optimal cell adhesion and morphology. For complexes with N/P of 10 (Figures 6-7A and 6-7C), surfaces containing the combination of 40% EG and 60% COO^- groups resulted in statistically higher transfection than surfaces containing OH or CH_3 groups in background of EG ($p < 0.05$) or COO^- ($p < 0.01$). On SAMs with a background of 40% EG, complexes with the higher N/P of 25 (Figures 6-7B) resulted in statistically higher transfection ($p < 0.05$) on surfaces with either hydrophilic functional group (COO^- or OH). However, transfection by complexes with N/P 25 on SAMs with 60% COO^- background (Figure 6-7D) was statistically greater on surfaces with 40% EG, than SAMs with 40% OH ($p < 0.05$) or CH_3 ($p < 0.01$).

Therefore, for complexes with low N/P, highest transgene expression occurs on SAMs with combinations of EG groups and carboxylic acids, which could indicate that charged

functional groups contribute important properties within the monolayer, presumably providing reversible interactions between the substrate and complex that can also enhance transfection, similar to previous reports (Chapter 4, 117). For complexes with high N/P, expression levels were highest on SAMs containing EG groups in addition to hydrophilic functional groups (COO^- or OH). However, for a background of COO^-, the enhancement in transfection is more pronounced with EG groups, again indicating the importance of the secondary alkanethiols within the SAMs containing EG groups.

6.3.5 Atomic force microscopy imaging of immobilized complexes

The enhancement in transfection levels and efficiency on SAMs containing EG groups cannot be attributed to binding densities of complexes or release profiles, thus the morphology of the complexes was examined using atomic force microscopy (AFM). AFM has proven to be an excellent tool to image soft biological structures and can be performed after complex deposition on a surface, with high resolution. AFM images were obtained by scanning small areas of SAMs with immobilized complexes and representative images (Figure 6-8A,C,E,G) revealed the morphology of PEI-DNA complexes on SAMs containing 0% EG (100% COO^-) (Figures 6-8A and 6-8E) and 40% EG (60% COO^-) (Figures 6-8C and 6-8G). On surfaces with no EG groups, complexes formed at N/P of 10 (Figure 6-8A) exhibited large globular structures with varying heights (indicated by light intensity of image) and diameters, along with smaller structures throughout the background of the image. Further analysis of the height distribution of these complexes (Figure 6-8B) reveals a rather large distribution of particles, with average heights of

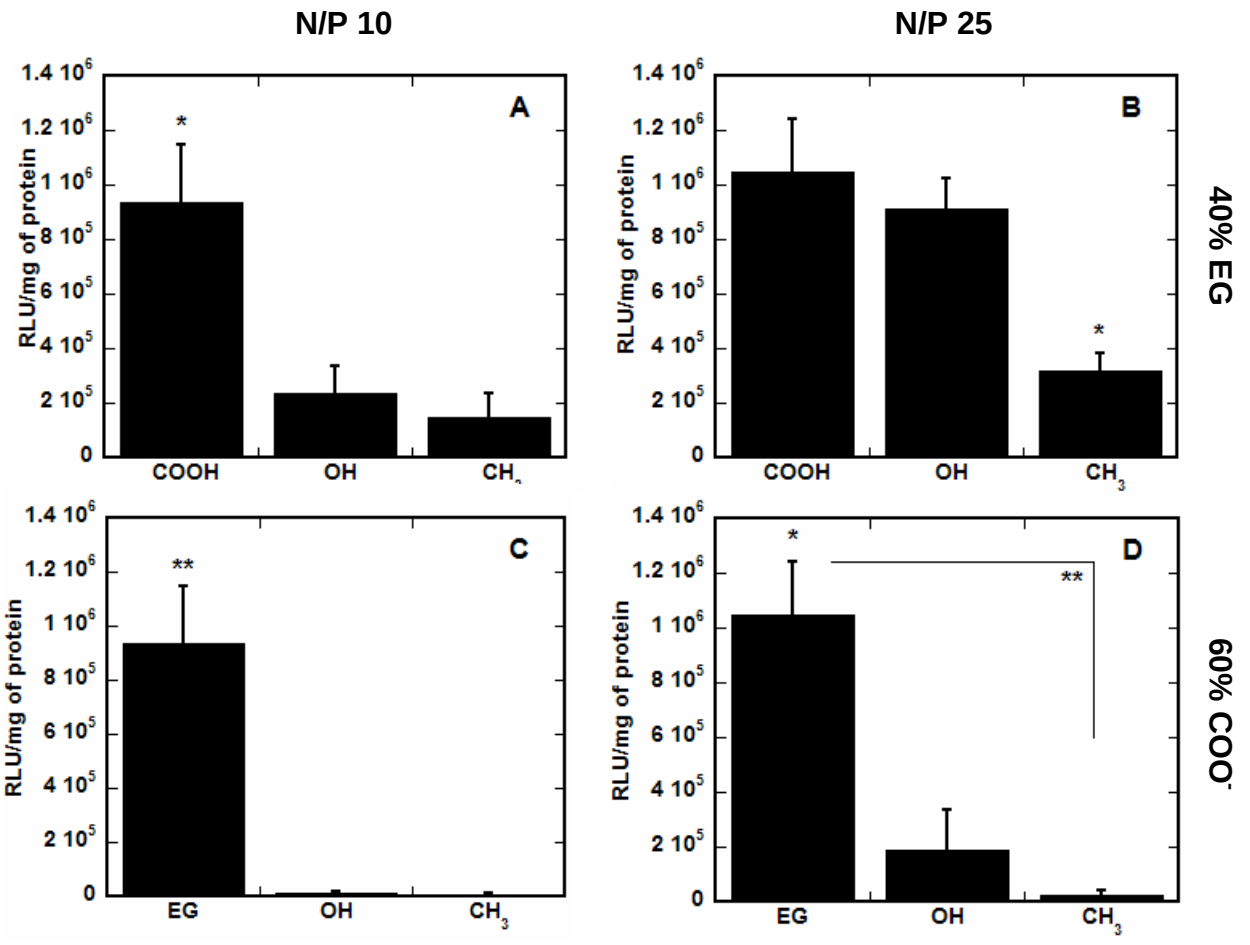

Figure 6-7 Substrate-mediated transfection on SAMs with backgrounds of EG and COO^-. SAMs were formed with alkanethiols containing various terminal functional groups, including OH, CH_3, EG and COO^-, in backgrounds of 40% EG (A and B) and 60% COO^- (C and D). Transfection was assayed for complexes formed at N/P of 10 (A and C) and 25 (B and D) by normalizing luciferase levels to total protein amounts. Values are reported as the mean ± s.d. *(*$p < 0.05$, **$p < 0.01$).*

20 nm (Table 6-1), with a mean roughness of 12 nm (Table 6-1) and area-perimeter ratios ranging from 337 to 1270 nm (Table 6-1), depending on the region of the image analyzed (regions of large globular structures versus regions with smaller, more uniform particles). All data analysis reported in Table 6-1 is for the images presented (Figure 6-8), but is representative of the entire surface. In contrast, complexes (N/P 10) on SAMs containing 40% EG (60% COO^-) (Figure 6-8C) had a very uniform morphology of small spherical particles evenly distributed across the surface. Analysis of the representative AFM image resulted in a narrow height distribution (Figure 6-8D), with average heights of 8 nm, mean roughness of 5 nm, and area-perimeter ratio of 100 nm (Table 6-1). These values are all much lower than for the 0% EG condition, indicating smaller, more uniform complexes on surfaces containing EG groups, which in turn resulted in higher transfection levels.

For complexes formed at N/P of 25, the correlation between complex morphology and surface chemistry was reversed. On SAMs containing no EG-terminated alkanethiols (Figure 6-8E), complexes exhibited a uniform morphology of small particles evenly distributed across the surface. Analysis of the representative AFM image resulted in a narrow height distribution (Figure 6-8F), with average heights of 8 nm, mean roughness of 2 nm, and area-perimeter ratio of 72 nm (Table 6-1), similar to complexes with N/P 10 on surfaces containing 40% EG (Figure 6-8C). In contrast, complexes (N/P 25) on surfaces with 40% EG (60% COO^-) (Figure 6-8G) exhibited large aggregates of globular structures with varying heights and diameters. Further analysis of the height distribution of these complexes (Figure 6-8H) reveals a rather large distribution of particles with two main populations of complexes, with average heights of 32 nm, with a mean roughness of 12 nm and area-perimeter ratios ranging from 196 to 355 nm (Table 6-

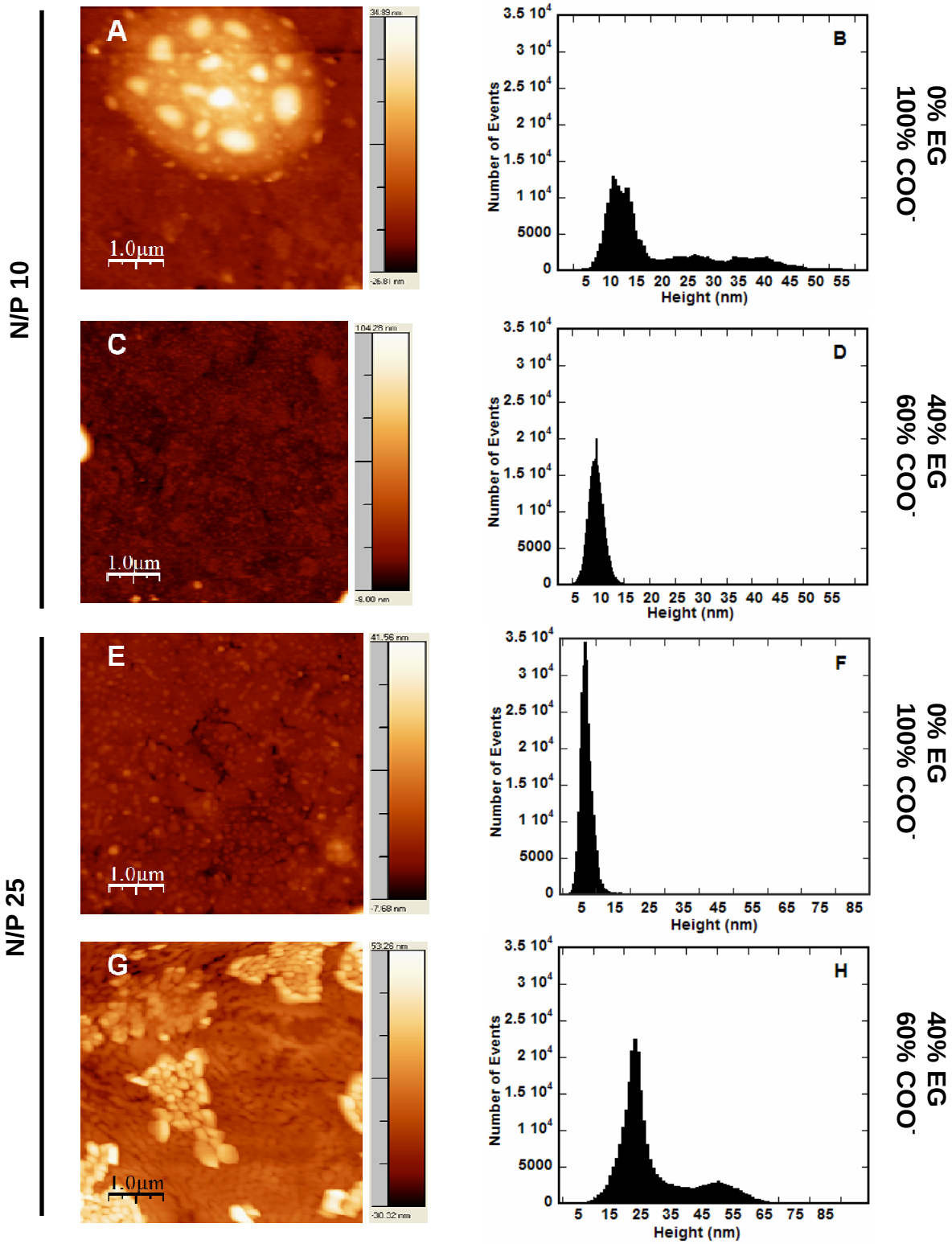

Figure 6-8 AFM images and analysis of complexes immobilized on SAMs. Complexes were formed at N/P of 10 (A-D) and N/P 25 (E-H) and immobilized on SAMs formed with 0%

EG/100% COO^- (A, B, E, F) or 40% EG/60% COO^- (C, D, G, H). Pixel brightness in images (A, C, E, G) corresponds to particle height. Scale bars correspond to 1.0 μm. Height analysis histogram (B, D, F, H) reports analysis of image to left.

1), depending on the region analyzed. These values are higher than for the corresponding 0% EG condition, indicating smaller, more uniform complexes on surfaces containing no EG groups, but which resulted in lower transfection levels.

Previous studies examining complexes using AFM, typically on mica substrates, reported complex morphologies similar to the results presented here. PEI-DNA complexes had a disperse distribution of condensates with rounded, globular forms (196,197). PEGylated PEI-DNA complexes analyzed by AFM had defined, spherical complexes (183-185) with less aggregation and smaller diameters than similar complexes without PEG, but were also demonstrated to be less uniform.

Table 6-1 AFM Analysis of PEI-DNA Complexes on SAMs

Surface	Complex N/P	Mean Height[a] (nm)	RMS Roughness[b] (nm)	Area-perimeter ratio[c] (nm)
0% EG	10	20	12	337 - 1270
40% EG	10	8	5	100
0% EG	25	8	2	72
40% EG	25	32	12	196 - 355

a. Mean height of Figure 8 histograms.
b. Root-mean-square roughness of Figure 8 images.
c. Area-perimeter ratio of Figure 8 images, ranges specify different regions of analysis.

In the AFM images and analysis of PEI-DNA complexes formed at a N/P of 10, the presence of EG groups on the SAM reduced the average height, area-perimeter ratio, and thus

size of complexes (Figure 6-8C vs. 6-8A), presumably by decreasing the aggregation of the complexes on the surfaces, similar to studies that have demonstrated that PEGylation of polymer-DNA complexes can prevent salt-induced aggregation (178,179,182,187), to produce discrete particles with similar appearance with AFM (183,184,186). Alternatively, treatment of microfluidic channels with Pluronic has also demonstrated lower aggregation of complexes, evidenced by a homogeneous layer of deposited lipoplexes (157). This change in complex morphology on SAMs containing EG terminal functional groups correlates with high transfection levels and transfection efficiencies and could indicate the ability of EG-containing SAMs to preserve complex morphology upon binding, by limiting electrostatic interactions with the surface and reducing aggregation of the complexes through steric stabilization, or alternatively by preventing complex unfolding, which could also contribute to the large height and area-perimeter ratios of the complexes immobilized on surfaces without EG.

However, in the AFM images and analysis of PEI-DNA complexes formed at N/P of 25 (Figure 6-8E and 6-8F), the presence of EG groups on the SAM appears to cause aggregation of complexes, in small clumps of particles, which also enhances transfection. The formation of these aggregates, which are morphologically different from the large, disperse globules observed for complexes of N/P of 10 on 0% EG SAMs, as well as the monodisperse smaller N/P 25 complexes on 0% EG SAMs, could be attributed to excess free PEI in the N/P 25 complexes, resulting in a layer of PEI on the surface prior to complex immobilization, which could alter the conformation of the complexes. Alternatively, these large aggregates could also be attributed, in part, to evaporation, which can cause artifactual aggregation induced by the receding meniscus during drying (198). Taken together, these AFM studies demonstrate how the design of both the

surface and vector contribute to the morphology of immobilized complexes and how that, in turn can affect substrate-mediated transfection.

6.4 Conclusions

Substrate-mediated delivery describes the immobilization of DNA, complexed with cationic lipids or polymers, to a biomaterial or substrate. Efficient delivery of DNA complexes from a surface is dependent on the interactions between the substrate and the complexes. SAMs presenting oligo(ethylene glycol) (EG) groups were used to investigate surfaces containing PEG-like moieties for complex binding, release, transfection and morphology. Nonspecific complex immobilization to SAMs containing combinations of EG- and COO^-- terminated alkanethiols resulted in substantially greater transfection, which increased with increasing amounts of EG in the monolayer. These significant differences in transfection levels and efficiency on SAMs containing EG groups could not be attributed to binding densities of complexes or release profiles, nor could they be replicated in SAMs composed of EG-terminated alkanethiols combined with alkanethiols presenting other functional groups. The enhancement of transfection by EG-containing SAMs could be attributed to the possible modulation of complex properties (surface charge, aggregation, complex-cell interaction) by mere association of the EG groups with the complexes on the surface. Atomic force microscopy imaging of immobilized complexes supports this hypothesis, revealing smaller complexes with reduced aggregation, for condensates formed at low N/P ratios on EG-containing SAMs. This complex morphology correlates with high transfection levels and transfection efficiencies and could indicate the ability of EG-containing SAMs to preserve complex morphology upon binding, by limiting electrostatic

interactions with the surface and reducing aggregation of the complexes through steric stabilization. Furthermore, the association of the cell membrane with the SAMs containing EG groups could also contribute to an enhancement of transfection. The ability to control the morphology of the immobilized complexes and thus influence transfection levels could be translated to scaffolds for gene delivery in tissue engineering applications (81,82) , as well as other applications of substrate-mediated gene delivery, including transfected cell arrays (Chapter 7, (199).

Chapter 7

Bioluminescence Imaging for Assessment and Normalization in Transfected Cell Arrays

7.1 Introduction

Analysis of multiple pathways or genes in a parallel format can be achieved using a transfected cell array, a high throughput technique to correlate gene expression with functional cell responses, based on gene delivery from a substrate that supports cell adhesion (2,5,6,117). While traditional microarrays can quantify the expression level of thousands of genes, they cannot accurately describe the functional activity of these genes in a cellular and physiological context (96). Transfected cell arrays present a powerful approach to study gene function in the context of a living cell, allowing proteins to be translated and folded correctly and to interact within the environment of the cell. Additionally, a large number of genes can be potentially screened in parallel for induction or repression of a given function (98). Transfected cell arrays offer compact, economical, and high-throughput analysis in living cells that provides greater consistency across assays and facilitates comparisons between conditions, while reducing the amount of reagents and cell numbers required, which is an important factor for difficult to prepare cell types (97,98).

Since the original report on transfected cell arrays (95), reverse transfection has been employed in several high-throughput cell based microarrays to screen for gene function or activity. Reverse transfection involves printing mixtures of different plasmids and gelatin into specific domains onto a substrate. A lipid-based transfection agent is then floated over the array,

and cells are subsequently seeded to form a living cell microarray of locally transfected cells in a lawn of nontransfected cells. The first transfected cell array was used to analyze genes for phosphotyrosine activity and identified six genes; five genes that encode known tyrosine kinase proteins and one that encodes a protein of unknown function (95). Transfected cell arrays have since been applied to study signaling pathways (100), screen antibody fragments (101), identify possible new lysophosphatidic acid receptors (102), perform protein localization studies (103,104), screen for proapoptotic genes (105,106), and annotate protein function (107). The transfected cell array has also been adapted to high-throughput RNAi studies (108), specifically for the analysis of spindle formation (109), secretory pathways (110), and chromosome segregation and nuclear structure in a time-lapse system (111).

Technological improvements have enhanced the capabilities of the arrays, yet further advancements are required for widespread application of this system. Most efforts have focused on increasing transfection efficiency within the array by using preformed complexes (101,107-110,112,114,115,117), incorporating fibronectin (112), atelocollagen (113), and recombinant proteins (114) with plasmid or DNA complexes, manipulating substrate hydrophobicity (115), or coating cationic polymer and collagen onto surfaces prior to transfection (116). Micropatterning strategies have also been used to fabricate arrays with improved transfection, using self-assembled monolayers to pattern DNA (Chapter 4, 117,118) or siRNA (119) complex immobilization on gold slides or electrodes (120,121). Arrays have been formed with dendrimers (123) and viral vectors (59,125,126) for enhanced gene delivery, magnetic beads (124) or hydrogels (122) to localize cells and vectors, and for alternative cell types, including Drosophila (127) and non-adherent cells (128). Further improvements are needed to

accommodate issues with transfection efficiency, spot-to-spot variability, normalization, post-transfection processing, sensitivity, image acquisition and quantification, cell types that are difficult to transfect, as well as to expand the biological endpoints.

In this chapter, we combine a two-plasmid system and dual-bioluminescence imaging (200-202) to quantify array output, normalize for variability in transfection efficiency, and address sensitivity concerns to overcome known shortcomings of the transfected cell arrays. Soft lithography principles (74) were used to create the transfected cell array, in which a rubber mold was used to confine deposition of preformed DNA complexes to designated regions of the substrate and pattern transfection upon cell seeding. Larger spot sizes were employed in the array to provide sufficient numbers of transfected cells and increase the reliability and statistical relevance of quantitative data obtained from each spot (107,119). To account for inherent variances in transfection between spots, transfection efficiency and protein production were normalized with the addition of a second plasmid within all spots of the array, encoding renilla luciferase driven by a constitutive promoter, in addition to a primary regulated plasmid reporting on the activation of a transcription factor through firefly luciferase expression. Bioluminescence imaging of the two luciferase reporters allows for quick image acquisition with no post-transfection processing.

We illustrate the utility of the array to quantitatively assay for the activity of a transcription factor in response to various activators or inhibitors. The estrogen receptor α (ERα) pathway in ER-positive, estrogen-responsive breast cancer cells was analyzed in an array format, using an ERE-regulated promoter reporter system. ERα expression is an important biomarker for determining treatment course for clinical breast cancer (138,139). Estrogens, via ERα, act as

potent mitogens of ER-positive breast cancer (140). In our plasmid system, the ER-regulated promoter directs firefly luciferase expression in response to transcriptional activation by 17β-estradiol (E_2)-bound ERα. Bioluminescence imaging was employed to quantify luciferase-based light emission resulting from the ER-regulated and normalization plasmids. The array can thus be employed to analyze the induction and inhibition of the transcription factors, which could be used in a high throughput format to elucidate gene function and cellular pathways responsible for diseases (96-98).

7.2 Material and methods

7.2.1 Cells

All studies used ER-positive MCF-7/WS8 mammary carcinoma cells, clonally derived from MCF-7 cells by selection for sensitivity to growth simulation by E_2 (203,204). Cells were cultured in fully estrogenized, phenol red-containing RPMI-1640 media supplemented with 10% fetal bovine serum (FBS), 100 μM non-essential amino acids, 100 units antibiotic/antimycotic, 2 mM L-glutamine, and 6 ng/ml insulin and maintained at 37°C in a humidified 5% CO_2 atmosphere. Prior to transfecting cells for an experiment, cells were cultured under estrogen-free conditions by substituting phenol red-free RPMI-1640 and dextran-coated charcoal-treated fetal bovine serum in the medium. For experiments in which transfected cells were assayed in 24-well plates using a luminometer, or imaged in arrays using a CCD camera, cells were cultured under estrogen-free condition for 4 days or 18 h, respectively, prior to seeding. All media and media components were purchased from GIBCO/Invitrogen (Carlsbad, CA).

7.2.2 Plasmids

Plasmids were purified from bacteria culture using Qiagen (Valencia, CA) reagents and stored in Tris–EDTA buffer solution (10 mM Tris, 1 mM EDTA, pH 7.4)) or water at −20 °C. Plasmid pEGFP-LUC encodes both the enhanced green fluorescent protein (EGFP) and firefly luciferase protein, under the direction of a CMV promoter (Clontech, Mountain View, CA). Plasmid pLUC encodes the firefly luciferase gene in the pNGVL1 (National Gene Vector Labs, University of Michigan) vector backbone with a CMV promoter. Estrogen-responsive plasmid pERE(3x)TK-ffLUC (205) contains three tandem copies of the palindromic estrogen response element (ERE) sequence, placed upstream of a minimal herpes simplex thymidine kinase (TK) promoter, directing expression of the firefly luciferase coding sequence in response to transcriptional activation by estradiol (E_2)-bound ERα, followed by recruitment of cofactor complexes and basal transcriptional machinery. Plasmid pTK-rLUC (phRL-TK, Promega, Madison, WI) contains the minimal TK promoter driving expression of a humanized renilla luciferase and was used for normalization of the firefly luciferase plasmids. Plasmid pβGAL encodes for nuclear-targeted β-galactosidase in the pNGVL1 (National Gene Vector Labs, University of Michigan) vector backbone with a CMV promoter and was used for control spots on the array.

7.2.3 DNA complex formation

DNA complexes were formed with Lipofectamine 2000 (Invitrogen, Carlsbad, CA), Lipofectamine LTX (Invitrogen, Carlsbad, CA) or Effectene (Qiagen, Valencia, CA), following manufacturer's instructions. Briefly, for both Lipofectamine 2000 and Lipofectamine LTX,

DNA complexes were formed at a DNA:lipid ratio of 1:2 in serum-free, Opti-MEM media (Invitrogen, Carlsbad, CA), by adding transfection reagent diluted in media dropwise to DNA in media, mixing by gentle pipeting, and then incubating for 20 minutes. Effectene complexes were formed by diluting DNA into EC buffer, to which the Enhancer buffer was added at a DNA to Enhancer ratio of 1:8. After 2-5 minutes of incubation at room temperature, the Effectene transfection reagent was then added to the DNA/Enhancer mixture at a DNA to Transfection reagent ratio of 1:4. After incubation at room temperature for 10 minutes, complexes were diluted with serum-free media before addition to surfaces or cells. DNA in complexes containing multiple plasmids was extensively mixed prior to complex formation. For induction studies in estrogen-free media, phenol red-free Opti-MEM media was used for complex formation.

7.2.4 Multiwell dish format reporter gene assays

Multiwell dish format reporter gene assays were performed to compare the ability of surface delivery of complexes to monitor ERα response in comparison to traditional bolus delivery. For surface delivery, the surface of wells of a 24-well plate (Becton Dickinson, Franklin Lakes, NJ) were serum-coated by incubation with dextran-coated charcoal-stripped FBS (10% in 1X PBS, pH 7.4, 380 μL) for 18 hours at 4°C, followed by two wash steps with PBS (2). Complexes were then immobilized following complex formation, as described above, by incubation of DNA complexes (475 μL) with the serum-coated wells for 2 hours. After complex incubation, the wells were washed twice with Opti-MEM (for Lipofectamine 2000 complexes) or EC buffer (for Effectene complexes) and 250,000 MCF-7 cells (which had been cultured in

estrogen-free media for 4 days) were seeded onto the immobilized DNA-lipid complexes in each well.

For bolus delivery, MCF-7 cells, which had been cultured in estrogen-free media for 4 days, were seeded in estrogen-free medium into 24-well plates at densities of 125,000 cells per well. Eighteen hours later, complexes, formed as described above, were diluted in antibiotic-free, estrogen-free media and then added to the cells.

For both surface and bolus delivery, complexes contained both the pERE(3x)TK-ffLUC plasmid and the normalization plasmid, pTK-rLUC, at a ratio of 4:1. Total DNA amounts added for surface delivery ranged from 0.13 – 1.32 μg/cm^2 (0.25 – 2.5 μg per well) and 0.05 – 0.26 μg/cm^2 (0.025 – 0.5 μg per well) for bolus delivery. Given binding profiles, these ranges result in approximately the same amount of DNA bound to the surface as delivered as a bolus (2).

Immediately after complex addition for bolus delivery and 4 hours after cell seeding for surface delivery, cells were treated with combinations of E_2 (Sigma-Aldrich, St. Louis, MO), the complete anti-estrogen (antagonist) fulvestrant [(FUL), also termed ICI 182,780, Tocris Bioscience, Ellisville, MO] or vehicle controls. E_2 and FUL were both dissolved in ethanol and diluted in estrogen-free media to obtain the indicated concentrations (10^{-12} to 10^{-9}M for E_2; 10^{-6}M for FUL) prior to addition to cells. Ethanol diluted in estrogen-free media served as the vehicle control. Cells were harvested and assayed for firefly and renilla luciferase reporter gene activities 48 hours after transfection using the Dual-Luciferase Reporter assay system (Promega, Madison, WI). In this dual-luciferase system, firefly and renilla luciferases are measured sequentially, in a single well. These measurements are accomplished by adding the firefly luciferase substrate first, measuring luminescence, and then adding reagents that quench the

firefly luciferase reaction and simultaneously provide the renilla luciferase substrate, followed by measuring renilla luciferase activity. The dual-luciferase assays were carried out using an automated microplate luminometer equipped with dual-injection ports (Mithras LB 940, Berthold Technologies, Oak Ridge, TN). Relative dual-luciferase activity was calculated by dividing the luminescent signal from the firefly reporter gene by the renilla luminescent signal.

7.2.5 Array fabrication

Soft lithography techniques were used to pattern DNA complex deposition. A polydimethylsiloxane (PDMS) mold was fabricated by curing PDMS into thin, flat disks. Briefly, PDMS was prepared in a 10:1 (v:v) ratio of Silicone Elastomer-184 and Silicone Elastomer Curing Agent-184 (Sylgard 184, Dow Corning, Midland, Michigan) by mixing the base and curing agent at least 50 times using a syringe mixing system. After allowing all air bubbles to escape, the PDMS was poured directly into a polystyrene tissue culture dish (100 mm, Corning, Corning, NY) and cured at 60°C for approximately 2 hours. The cured PDMS was removed from the dish and rods of precise diameters were then used to punch holes into the PDMS, with diameters of 2.4 mm. The PDMS mold was rinsed in 70% ethanol, oxidized using oxygen plasma and then reversibly sealed to polystyrene microscope slides (Nunc, Rochester, NY), which were fitted into custom-fabricated Teflon slide holders. The holes in the PDMS mold, termed microwells, served as reservoirs for deposition of DNA complexes onto the polystyrene slide. After 2 hours of complex deposition in humid conditions, the PDMS mold was peeled away from the polystyrene, and the slide was rinsed thoroughly with Opti-MEM. For

all array studies, DNA concentrations ranged from 0.007 μg/μL to 0.021 μg/μL, with 2.2 μL to 4 μL of complex volume added to the microwells of the PDMS mold.

To visualize DNA complex immobilization on the array and verify deposition replicated the pattern of the microwells in the PDMS mold, plasmid (pEGFP-LUC) was labeled with tetramethyl rhodamine (Label IT Nucleic Acid Labeling Kit, Mirus, Madison, WI), complexed as described above, and deposited in the microwells. After deposition, PDMS removal and rinsing, the resulting spots were visualized with fluorescence microscopy (see below).

Transfection of cells on the array was verified by depositing complexes formed with plasmid pEGFP-LUC in the microwells, as described above, and imaging with fluorescence microscopy. After complex deposition, PDMS removal and rinsing, MCF-7 cells were seeded onto the slide at a density of 10^6 cells per slide (18.75 cm^2). Transfection was analyzed after 24 and 48 hours and characterized through GFP expression. Transfected cells were visualized using an epifluorescence microscope (Leica; Bannockburn, IL) with a FITC filter and equipped with a digital camera. Transfection, as assayed through bioluminescence imaging, was verified by depositing complexes containing both pLUC and pTK-rLUC plasmids, at a 1:1 ratio. After deposition, PDMS removal and rinsing, cells were seeded as described above. Transfection was analyzed after 24 hours and characterized by dual-luciferase expression through light emission (see below).

For induction studies in the array, complexes formed with different plasmids were immobilized in different spots of the array, in triplicate. Briefly, complexes were formed with pLUC, pERE(3x)TK-ffLUC, pERE(3x)TK-ffLUC and pTK-rLUC (2:1 ratio), or pβGAL. After deposition, PDMS removal and rinsing, MCF-7 cells, which had been cultured in estrogen-free

media for 18 hours, were seeded in estrogen-free medium on arrays at a density of 10^6 cells per slide. Immediately after cell seeding, cells were treated with combinations of E2, FUL, or vehicle control, as described above. Dual-luciferase levels were analyzed 24 hours later by bioluminescence imaging.

7.2.6 Bioluminescence imaging

Expression of both luciferase reporter genes was assessed through imaging of light production upon sequential addition of the luciferase substrates to the bulk media. Bioluminescence imaging of the array was performed using an IVIS imaging system (Xenogen Corp., Alameda, CA), which utilizes a cooled CCD camera. For imaging, ViviRen (Promega, Madison, WI), a modified renilla luciferase substrate, was diluted to 0.66 mM in serum-containing media and then added to the arrays at a final concentration of 10 μM. After 2 minutes, the arrays were placed into a light-tight chamber and bioluminescence images were acquired for a total exposure time of 1 minute. Immediately following imaging with ViviRen, 1 mM D-luciferin (Molecular Therapeutics Inc., MI, 20 mg/mL in PBS), the firefly luciferase substrate, was added into the media above the cells cultured on the array, and bioluminescence images were acquired 3 minutes later, with 1 minute exposure. Gray scale and bioluminescence images were superimposed using the Living Image software (Xenogen Corp., Alameda, CA). A constant size region of interest (ROI) was drawn over the spots of the array to calculate light signals. The signal intensity was reported as an integrated light flux (photons/s), determined by IGOR software (WaveMetrics, Lake Oswego, OR). The signal due to firefly luciferase was determined by subtracting ViviRen signal from the luciferin signal. Normalization was

accomplished by dividing the firefly luciferase signal (luciferin signal minus ViviRen signal) by the renilla luciferase signal (ViviRen signal). A renilla signal threshold was set at 3.5E4 photon/s (2X background) to distinguish spots of unreliable signals indicating insufficient transfection.

7.2.7 Statistics

Statistical analysis was performed using JMP software (SAS Institute, Inc., Cary, NC). Comparative analyses were completed using one-way ANOVA with Tukey post-tests, at a 95% confidence level. Mean values with standard deviation are reported and all experiments were performed with a minimum sample size of three, performed in replicate.

7.3 Results

7.3.1 Multiwell dish format ERE- reporter gene induction studies

Multiwell dish format reporter gene assays were performed to compare ERα-regulated, ERE-dependent transcriptional activity in MCF-7 cells transfected via surface-mediated delivery of DNA complexes in comparison to traditional bolus delivery (Figure 7-1). DNA complexes, formed using an E_2-responsive firefly luciferase reporter plasmid pERE(3x)TK-ffLUC and a normalization plasmid pTK-rLUC encoding renilla luciferase, were delivered to cells via bolus or surface delivery. Transfected cells were treated with various combinations of the agonist E_2, the complete antiestrogen FUL, or ethanol. Surface delivery of the plasmids (Figure 7-1B) resulted in E_2-stimulated responses similar to bolus delivery (Figure 7-1A), with E_2 statistically inducing firefly luciferase expression 6-7 fold ($p < 0.001$) over vehicle control or the addition of

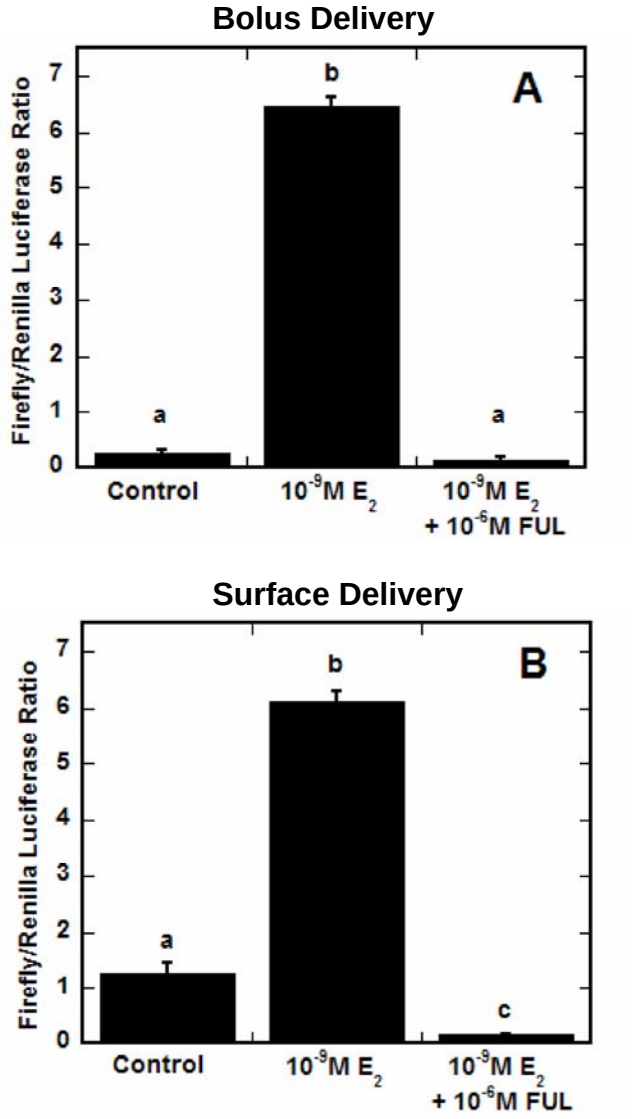

Figure 7-1 Multiwell dish format reporter gene assay to compare surface delivery to traditional bolus delivery. Surface delivery (B) of ERE reporter plasmid system (pERE(3x)TK-ffLUC and normalization plasmid pTK-rLUC) resulted in E_2-stimulated transcriptional responses in MCF-7 breast cancer cells similar to bolus delivery (A), reported as a ratio of firefly to renilla luciferase, with E_2 statistically inducing firefly luciferase expression 6-7 fold over vehicle control or the addition of FUL. *(Columns labeled with same letter designate conditions not statistically different; all other comparisons, $p < 0.001$).*

FUL. Hence, the physiologic state of the cells during surface-mediated delivery allowed the cells to transcriptionally respond to E_2. Further, the maximal induction of reporter gene activity was similar whether the DNA complexes were delivered via bolus or surface-mediated techniques.

The amount of transfected plasmid was subsequently investigated, which indicated a similar DNA mass-dependent effect in reporter gene activity for both surface and bolus-mediated transfection methods (Figure 7-2). For bolus delivery (Figure 7-2A), all DNA amounts resulted in significantly different responses ($p < 0.01$), except for 0.11 and 0.2 $\mu g/cm^2$, which were not statistically different from each other. Maximal induction was achieved at 0.13 $\mu g/cm^2$ (0.25 μg per well). For surface delivery (Figure 7-2B), all DNA amounts resulted in significantly different responses ($p < 0.05$), with 1.05 $\mu g/cm^2$ (2 μg per well) corresponding to the highest induction by E_2. These results indicate that sufficient amounts of DNA must be transfected for optimal reporter gene activity, and excess amounts of DNA lead to less efficient reporter gene activity, possibly due to toxicity, for both delivery methods.

Assuming that approximately 20% of DNA added to the cell culture dish surface is immobilized (2), the condition with the highest induction (1.05 $\mu g/cm^2$), would have presented approximately 0.21 $\mu g/cm^2$ of DNA to the cells, which is higher than the bolus condition with the highest induction (0.13 $\mu g/cm^2$), but still in the range of robust activity. Therefore, surface delivery required more DNA added to the surface than what would have been expected given binding profiles (2). The requirement for more DNA may be due to lower than anticipated binding efficiencies (~10%, but still within the range of profiles reported).

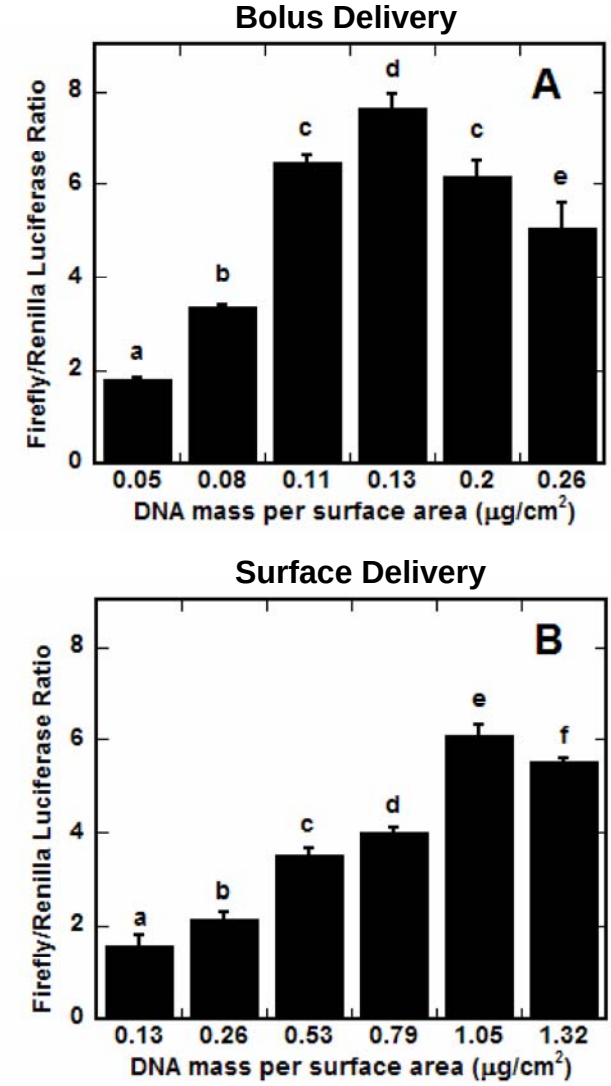

Figure 7-2 The effect of DNA amount on E_2 activation of ERE reporter plasmid system (pERE(3x)TK-ffLUC and normalization plasmid pTK-rLUC) delivered to MCF-7 breast cancer cells. Total amount of DNA added to the surface (B) or delivered as a bolus (A), in the presence of 10^{-9} M E_2, resulted in a similar dose-response effect. *(Columns labeled with same letter designate conditions not statistically different; all other comparisons, $p < 0.01$ for (A), $p < 0.05$ for (B)).*

The specific transfection reagent used to form DNA complexes, and E_2 concentration responses were subsequently investigated to determine the applicability and sensitivity of the reporter system (Figure 7-3). For Lipofectamine 2000-DNA complexes (Figure 3A), E_2-induction profiles were not significantly different using bolus versus surface delivery (Figure 7-3A), with E_2 eliciting a concentration response from 10^{-12} M to 10^{-10} M ($p < 0.05$), and maximal responsiveness observed from 10^{-10} M to 10^{-9} M E_2 ($p > 0.05$) for both delivery methods. For Effectene complexes (Figure 7-3B), bolus delivery resulted in statistically higher levels of ERE induction ($p < 0.05$) than surface delivery for all concentrations of E_2, except control. However, the level of ERE induction for surface-mediated delivery was similar whether complexing DNA with Effectene (Figure 7-3B) or with Lipofectamine 2000 (Figure 7-3A). Therefore, the particular transfection reagent used affected transcriptional activity via the conventional bolus delivery, but not via surface delivery. None the less, these results demonstrate that either Effectene or Lipofectamine 2000 can be used to deliver plasmids via surface-mediated transfection. Further, other transfection reagents can likely be adapted for use in surface-mediated delivery.

7.3.2 Array fabrication and verification

An array was created using soft lithography techniques to pattern DNA-lipid complex deposition and subsequent transfection upon cell seeding (Figure 7-4). Briefly, a PDMS mold with microwells (Figure 7-4A) was reversibly sealed to polystyrene microscope slides (Figure 7-4B), with the microwells serving as reservoirs for deposition of DNA complexes onto the polystyrene slide (Figure 7-4C). Rhodamine-labeled DNA complexes deposited within

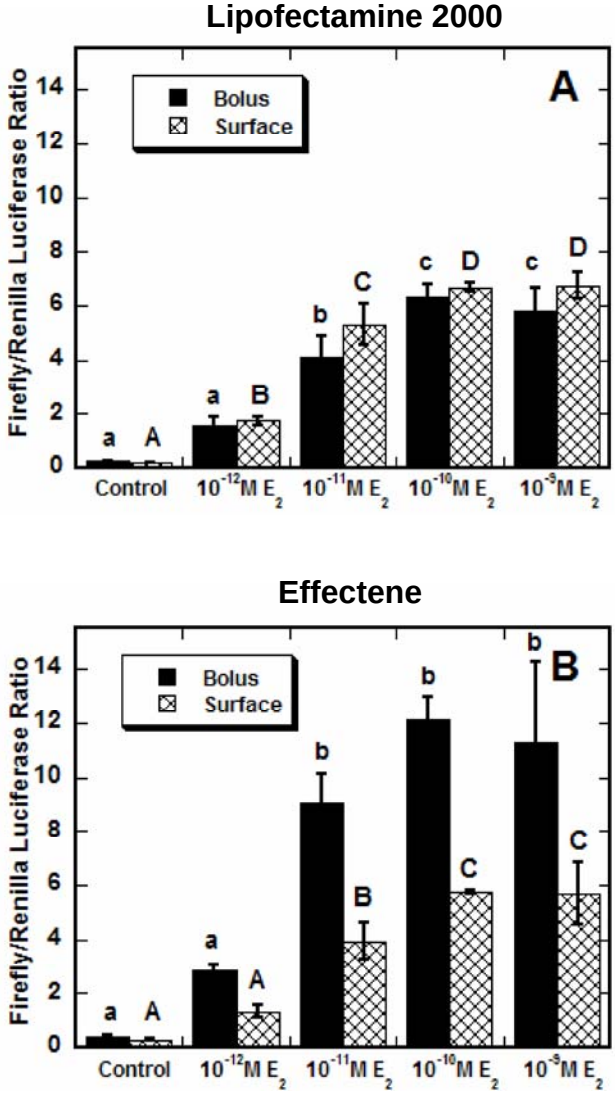

Figure 7-3 The effect of complexing agent and E_2 dose response on the ERE reporter plasmid system (pERE(3x)TK-ffLUC and normalization plasmid pTK-rLUC). Bolus and surface delivery of Lipofectamine 2000 complexes (A) resulted in induction profiles that were not statistically different from each other, for each concentration of E_2. Bolus delivery of Effectene complexes (B) resulted in statistically higher induction ($p < 0.05$) than surface delivery for all concentrations of E_2, except control, however surface delivery resulted in more statistically different induction responses. *(Columns labeled with same letter designate conditions not statistically different; all other comparisons, $p < 0.05$).*

microwells were immobilized to the slide in distinct regions, replicating the pattern of microwells in the PDMS mold (Figure 7-4,D-F). Transfection of MCF-7 cells seeded onto arrays of complexes was determined by GFP expression, and was also confined to the patterns (Figure 7-4,G-I).

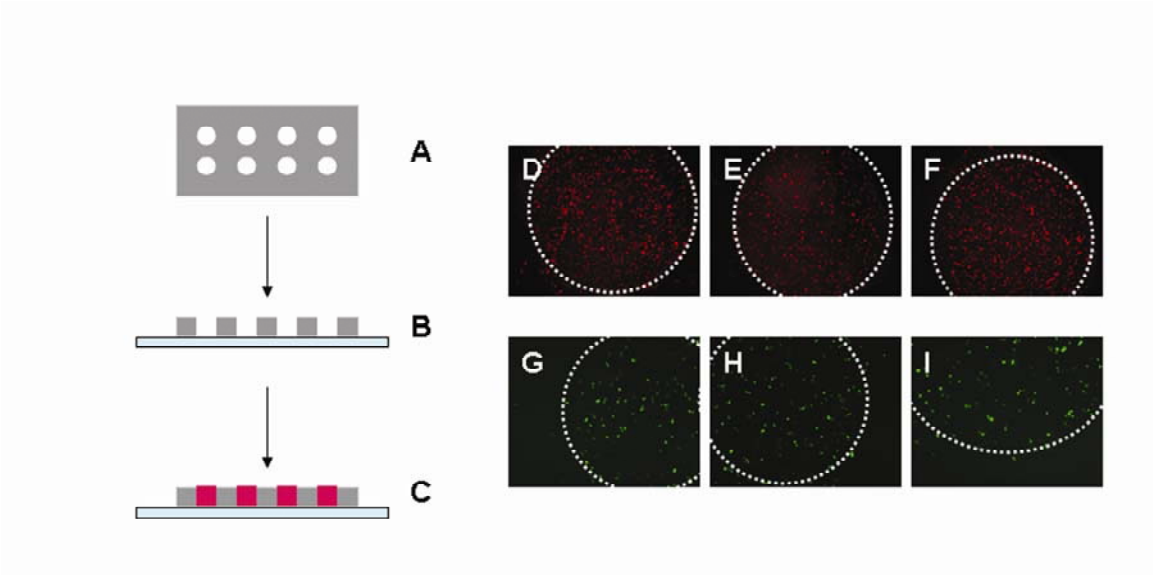

Figure 7-4 Array fabrication with soft lithography techniques to pattern DNA-lipid complex deposition and transfection. A polydimethylsiloxane (PDMS) mold (A) was reversibly sealed to polystyrene slides (B), so that the holes in the mold, termed microwells, served as reservoirs for deposition of DNA complexes onto the polystyrene (C). After complex deposition in the microwells, the PDMS mold was peeled away from the polystyrene slide, which was then rinsed thoroughly. Rhodamine-labeled DNA complexes were immobilized on the slide in distinct regions, replicating the pattern of microwells in the PDMS mold (D-F). Transfection of MCF-7 cells seeded onto these arrays of patterned complexes on polystyrene slides was also confined to the patterns, as determined by GFP expression (G-I).

7.3.3 Bioluminescence imaging of the array

Arrays formed with complexes containing plasmids encoding firefly and renilla luciferase reporter genes (pLUC and pTK-rLUC) were used to verify the ability of bioluminescence imaging to detect dual-luciferase expression (Figure 7-5). Transfection of MCF-7 cells seeded

onto these arrays was assayed after 24 hours by sequentially adding the renilla and firefly luciferase substrates. Following ViviRen addition, spot intensities averaged 1.10 x 10^5 ± 2.56 x 10^4 photon/s (Figure 7-5A), which are similar to signals obtained with arrays of only pTK-rLUC plasmid (data not shown). D-Luciferin was subsequently added to the same array, which was then imaged to acquire a dual signal (Figure 7-5B), with average spot intensities of 3.66 x 10^6 ± 4.34 x 10^5 photon/s. Firefly luciferase expression was determined by subtracting the initial ViviRen signal from the signal obtained through imaging with the D-luciferin. Firefly expression averaged 3.55 x 10^6 ± 4.30 x 10^5 photon/s, also similar to intensities obtained with arrays formed with only pLUC plasmid (data not shown). After normalization, the firefly luciferase signal was 34 ± 8 fold greater than the respective renilla expression. Timecourse studies revealed that the ViviRen signal remained constant for 10 minutes after substrate

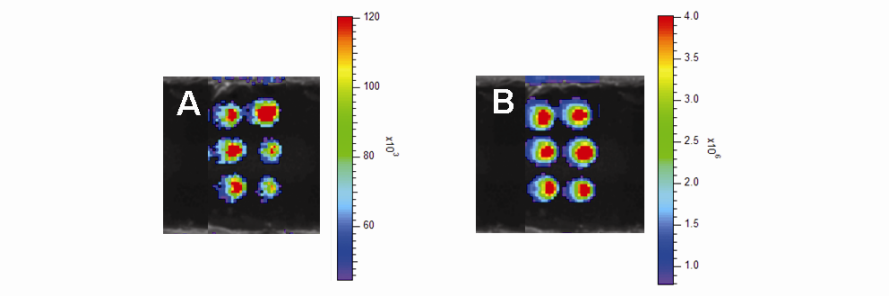

Figure 7-5 Bioluminescence imaging to detect dual-luciferase expression in an array format. Transfection of MCF-7 cells seeded onto arrays of complexes was assayed after 24 hours by sequentially adding the renilla and firefly luciferase substrates. The renilla substrate, ViviRen (10 μM), was first added into the media and the array was imaged to determine pTK-rLUC expression (A). D-Luciferin (1 mM) was subsequently added to the same array, which was then imaged to acquire a dual signal (B). Firefly luciferase expression (pLUC) was determined by subtracting the ViviRen signal from the signal obtained through imaging with the D-luciferin. When normalized, the firefly luciferase signal was 34 ± 8 fold greater than the respective renilla expression.

addition. Therefore the firefly luciferase signal could be obtained using this dual imaging strategy followed by subtraction techniques, given imaging was accomplished within 10 minutes of ViviRen addition (data not shown). Bioluminescence imaging was able to sensitively capture both luciferase signals, enabling the same cell population to be analyzed for the expression of multiple reporter genes.

7.3.4 Array format ERE-reporter gene induction studies

To assess the ability of the arrays to monitor induction of ERα transcriptional activity (Figure 7-6), complexes formed with different plasmids were immobilized as an array in triplicates as follows: 1. pLUC, 2. no DNA (mock), 3. pERE(3x)TK-ffLUC, 4. pERE(3x)TK-ffLUC and pTK-rLUC (2:1 ratio), and 5. pβGAL. Cells seeded on the arrays were treated with combinations of ethanol control (Figure 7-6, A-B), 10^{-9} M E_2 (Figure 7-6,C-D), or 10^{-9} M E_2 + 10^{-6} M FUL (Figure 7-6, E-F). Dual-luciferase levels were analyzed 24 hours later using bioluminescence imaging, by first imaging with ViviRen (Figure 7-6A, C, E), and then imaging each array with D-luciferin (Figure 7-6B, E, F). Renilla luciferase activity was only detected in cells transfected with pTK-rLUC plasmid (Figure 7-6A, C, E, column 4), and not in cells transfected with only firefly luciferase-encoding plasmids (Figure 7-6A, C, E, columns 1 and 3), a control βGAL-encoding plasmid (Figure 7-6A, C, E, column 5) or no DNA (Figure 7-6A, C, E, column 2). Accordingly, firefly luciferase activity was only detected in cells transfected with pLUC (Figure 7-6B, D, F, column 1) or pERE(3x)TK-ffLUC (Figure 7-6B, D, F, columns 3 and 4), but not in mock or βGAL control transfected cells (Figure 7-6B, D, F, columns 2 and 5) These results verify the specificity of renilla and firefly luciferase detection in this system.

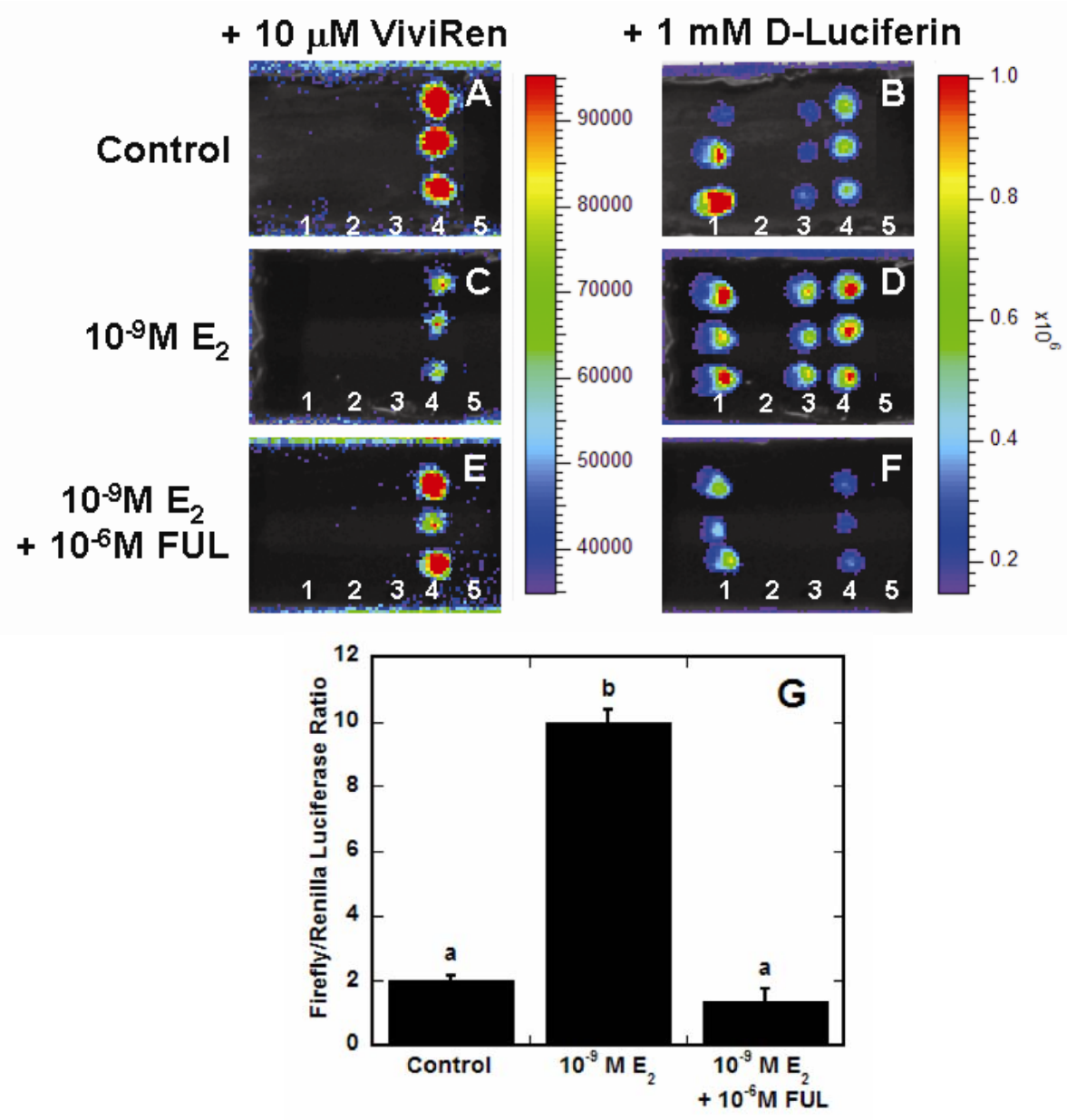

Figure 7-6 Arrays to monitor ERα induction of transcriptional activity. Complexes formed with different plasmids were immobilized in different spots of the array, in triplicate, as follows: 1. pLUC, 2. none, 3. pERE(3x)TK-ffLUC, 4. pERE(3x)TK-ffLUC and pTK-rLUC (2:1 ratio), and 5. pβGAL. Cells seeded on the arrays were treated with combinations of ethanol control (A-B), E_2 (C-D), or E_2 plus FUL (E-F). Dual-luciferase levels were analyzed 24 hours later with bioluminescence imaging, by first imaging with the renilla luciferase substrate, ViviRen (A, C, E) and then imaging each array with D-luciferin, the firefly luciferase substrate (B, E, F). Induction of the ERE-regulated plasmid system was calculated by normalizing firefly luciferase expression to renilla luciferase expression (G). Firefly luciferase expression was determined by subtracting the ViviRen signal from the signal obtained through imaging with the D-luciferin. For spots containing both the pERE(3x)TK-ffLUC and pTK-rLUC plasmids (column 4), E_2

statistically induced firefly luciferase expression 10-fold over control or FUL conditions, reported as a ratio of firefly to renilla luciferase (G). *(Columns labeled with same letter designate conditions not statistically different; all other comparisons, $p < 0.001$).*

As predicted, firefly luciferase activity was detected at substantially higher levels in cells transfected with pERE(3x)TK-ffLUC and treated with E_2 (Figure 7-6D, columns 3 and 4) compared to those treated with ethanol (Figure 7-6B, columns 3 and 4) or E_2 + FUL (Figure 7-6 F, columns 3 and 4). In control-treated arrays, spots of highest intensity were visualized for pLUC (Figure 7-6B, column 1), given its highly active CMV promoter. Cells transfected with both the pERE(3x)TK-ffLUC and pTK-rLUC plasmids (Figure 7-6B, column 4) resulted in higher signal intensities in the presence of luciferin than cells transfected with only the pERE(3x)TK-ffLUC (Figure 7-6B, column 3), as there was no carryover of ViviRen signal in the latter spots of transfected cells without pTK-rLUC. For E_2 addition to the array, signal intensities with luciferin increased as compared to the control condition for all cells transfected with pERE(3x)TK-ffLUC plasmids (Figure 7-6D, columns 3 and 4), indicating ERα–dependent transcriptional activation of the ERE-regulated plasmid. Expression of the pLUC plasmid was largely unaffected by E_2 (Figure 7-6D, column 1). Addition of the antiestrogen FUL to the arrays completely eliminated the signal in cells transfected with pERE(3x)TK-ffLUC alone (Figure 7-6F, column 3), or substantially reduced signal intensities in cells transfected with both pERE(3x)TK-ffLUC and pTK-rLUC (Figure 7-6F, column 4), in which the luminescence that was detected was again due to carryover of the ViviRen signal. Therefore, addition of 10^{-6} M FUL led to a complete blockade of ERα-stimulated activity by 10^{-9} M E_2. pLUC expression was also lowered in the presence of FUL (Figure 7-6F, column 1) indicating that some transcriptional

elements in the CMV may be indirectly regulated by ERα, possibly by ERα tethering to AP1 and SP1 proteins bound directly to DNA in this promoter.

Average renilla luminescence intensities in cells transfected with pERE(3x)TK-ffLUC and pTK-rLUC plasmids (Figure 7-6A, C, E, column 4) were similar in control and E_2 + FUL treated cells, but lower in E_2 alone treated cells. This lower renilla luciferase activity is likely due to competition for transcriptional cofactors between the ERE(3x)TK and TK-only regulated promoters. Under E_2 stimulation conditions, ERα transcriptional coregulators and basal transcriptional machinery may be preferentially recruited to ERE-containing promoters rather than promoters lacking EREs. Hence, in cells treated with E_2, squelching likely occurs at the TK-renilla luciferase promoter due to titrating out of limiting transcription factors.

Induction of the ERE-regulated plasmid system in the array mimicked results obtained through traditional assays methods. Firefly luciferase expression was determined by subtracting the ViviRen signal from the signal obtained through imaging with the D-luciferin, which was then normalized by the ViviRen signal (Figure 7-6G). For cells transfected with both the pERE(3x)TK-ffLUC and pTK-rLUC plasmids (Figure 7-6, column 4), E_2 statistically induced dual-luciferase activity 10-fold ($p < 0.001$) over control or FUL conditions (Figure 7-6G). This robust induction verifies that the array can accurately report on the activity of the ERα transcription factor. The concentration response of E_2 was examined to determine the sensitivity of the reporter system in an array format (Figure 7-7). For arrays with spots containing both the pERE(3x)TK-ffLUC and pTK-rLUC plasmids, increasing the concentration of E_2 statistically increased the induction of firefly luciferase expression ($p < 0.05$), capturing the concentration-response of E_2 in the induction of this plasmid system.

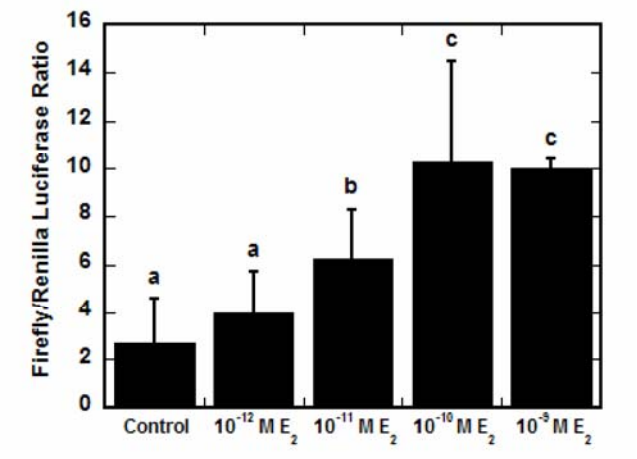

Figure 7-7 Concentration response of E_2 on the ERE reporter plasmid system in an array format. For spots containing both the pERE(3x)TK-ffLUC and pTK-rLUC plasmids, increasing the concentration of E_2 statistically increased the induction of firefly luciferase expression, verifying a true concentration-response of E_2 in the induction of this plasmid system in an array format. *(Columns labeled with same letter designate conditions not statistically different; all other comparisons, $p < 0.05$).*

7.4 Discussion

Methods to use mammalian cells as suitable screening systems need to be developed to elucidate gene function and cellular pathways responsible for diseases (99). Transfected cell arrays offer an advantage in their ability to analyze the expression of genes and the function of proteins in living cells, where the machinery is present to ensure correct function of the gene products. These live cell microarrays could provide a method to link gene expression to functional cell responses, with the potential to impact many aspects of science and medicine. Transfected cell arrays have been primarily used for identification of gene function (107) and discovery of novel genes and proteins (95), and have potential utility in emerging applications such as detection of biological warfare agents and environmental toxins through surface

receptors (101), detection of tumor-associated antigens (206), and determination of molecular markers or targets (98), prior to the costly development of novel diagnostic and therapeutic strategies. With many possible applications for transfected cell arrays, technological advances are needed to improve array accuracy and consistency and to facilitate endpoint analysis (97,98). We have combined dual plasmid delivery and bioluminescence imaging to create a transfected cell array that allows for normalization of transfection, and provides rapid and sensitive quantification of the cellular response with minimal post-transfection processing.

In our transfected cell array, we employed a dual plasmid system to provide normalization, sensitivity, and quantification, which are all intricately related, in part, through the transfection efficiency. Spot to spot variability in transfection can compromise the ability to quantify a response within an array, as sub-maximal responses may indicate either a limited effect or simply inefficient or unequal delivery. A variance in fluorescence intensity of transfected cells (GFP) has been noted between spots of the array, which likely correlates with the number of plasmids internalized (97). Therefore, to enable normalization of transfection efficiency, a two-plasmid system consisting of: i) a normalization plasmid that is present within each spot, and ii) a functional plasmid that varies between spots and is responsible for the functional endpoint of the array, was deposited in each spot. Both plasmids contain the same TK promoter, which is important for normalization, and should allow comparison between cell lines on the array. Delivery of two plasmids has been shown to result in a majority of cells expressing both reporter genes (unpublished observations). To normalize with a second plasmid, the efficiency of delivery must be sufficient to obtain a signal from each plasmid. This issue was addressed using larger spot sizes relative to many previous reports. Small spot size can

contribute to low transfection efficiencies (98), which are detrimental because each spot on the array may contain so few cells that an insufficient number of cells are transfected locally to be statistically informative (107). Small spots with low transfection efficiency make image acquisition and quantification difficult and lower sensitivity, which can lead to high false positive and false negative rates (106), further demonstrating a need to account for efficiency and normalization issues to increase the reliability of quantitative data obtained from each spot (119). To further address issues with transfection efficiency, and for cells difficult to transfect, our array fabrication and normalization approach could be compatible with viral delivery (59,125,126), however a plasmid system is more versatile due to the easier production and handling methods.

Bioluminescence imaging (202) was employed to quantify the response of the dual plasmids within the array, with minimal post-transfection processing and high sensitivity. Endpoint analysis for the arrays often requires tagging or staining (97) to report gene function, which can require extensive post-transfection processing, such as fixation and immunostaining (102,207). The normalization and functional plasmids contain renilla and firefly luciferase reporters respectively, which can both be rapidly quantified in each spot by sequential addition of the respective substrates to the culture media followed by imaging of the array. Luciferase reporters are known to be more sensitive than GFP, without the issues of autofluorescence and background signals (202). Luciferase is more quantitative and allows for small differences in expression to be determined, which enabled our system to determine a dose response to an external stimulus. An additional potential advantage, the short half-life of luciferase could allow for real-time imaging to follow the dynamics of gene activity (202). However, alternative imaging systems requiring automated microscopy and image processing (96,207) can allow for

detection of changes in cellular morphology and cellular level data, which is not possible with bioluminescence imaging.

The array was used to quantify the activity of the ERα in breast cancer cells with an ERE-regulated promoter reporter system, as an example of an inducible plasmid system in a cancer model. ERα, a member of the nuclear receptor superfamily of transcription factors, activates transcription through binding of its ligand, E_2. Expression of ERα is clinically used as a biomarker to determine treatment for breast cancer patients (138,139). However, simple expression of transcription factors like ERα does not necessarily reflect pathway activation, as transcription factor activity is regulated through diverse mechanisms (144), including heteromeric complexes, ubiquitination, methylation, acetylation, and other post-translational modifications such as phosphorylation. The transfected cell array allows for the determination of transcription factor activity. In the case of the ERα, we assayed for induction by E_2. Induction in the array mimicked results obtained through traditional luciferase assay methods, with E_2 inducing luciferase expression 10-fold over fulvestrant or vehicle controls. The array also captured the varying ER activity in response to a range of E_2 dosages, further demonstrating the sensitivity of the bioluminescence quantification system.

In summary, this chapter demonstrates the ability to quantitatively assess a transfected cell array using dual bioluminescence imaging to enable normalization of transfection efficiency, while reducing post-transfection processing and increasing sensitivity. Additionally, ER activity was quantified in a physiologically relevant model of breast cancer, indicating the effectiveness of the array system, as many of the published arrays have only used HEK293T cells, a cell line known to be easily transfected and not applicable to many relevant biological endpoints or

applications. The dual plasmid system and bioluminescence imaging are enabling technologies that, when combined with high throughput arrays involving large numbers of plasmids, have the potential to impact basic research in cancer and other disciplines through investigation of fundamental biological processes (206). With further advancements in the transfection of primary cells, transfected cell arrays have the potential for use in cancer medicine, to classify clinical cancer samples through prognostic profiles (208), to provide novel information regarding disease progression, and to identify molecular targets for patient-specific therapy (209).

Chapter 8

Conclusions and Future Directions

8.1 Substrate-mediated delivery of nonspecifically immobilized complexes

A fundamental goal of biotechnology is to develop systems capable of controlled and efficient gene transfer, which offer the potential to overcome extracellular barriers that limit gene delivery, including aggregation of DNA complexes, degradation of complexes, and in particular mass transport limitations that result in low concentration of DNA at the cell surface. DNA delivery can be enhanced by increasing the concentration of DNA in the cellular microenvironment through immobilization of DNA to a substrate that supports cell adhesion. Cells cultured on these substrates are exposed to elevated DNA concentrations, which enhances transfection (2-6). However, the parameters that govern substrate-mediated gene delivery need to be determined.

DNA, complexed with cationic polymers or lipids, can interact with substrates through non-specific mechanisms, including hydrophobic, electrostatic, and van der Waals interactions. Polyplexes and lipoplexes non-specifically immobilized to serum-coated substrates have been shown to enhance the extent of transgene expression (2), presumably by increasing the cellular association of immobilized DNA (3). Fibronectin coating of substrates prior to complex immobilization mediated high levels of transgene expression, potentially by targeting internalization through caveolae-mediated endocytosis (4). PEI-DNA complexes nonspecifically adsorbed to poly(lactide-co-glycolide) (PLGA) scaffolds (48) or collagen films (49) resulted in

robust substrate-mediated gene delivery. Substrate-mediated delivery of nonspecifically immobilized complexes has also been accomplished with complexes formed with dendrimers, adsorbed to PLGA and collagen membranes coated with phosphatidyl glycerol (1-5%) (46), and PEI-DNA complexes freeze-dried onto polystyrene wells (45). Furthermore, DNA has been co-precipitated with inorganic minerals (calcium phosphate) onto cell culture surfaces, (44) and PLGA matrices (47) for subsequent delivery to cells cultured on the substrates.

In each of these published studies, the parameters governing the delivery of the DNA complexes from the surface, in particular the mechanism by which the properties of the surfaces influenced complex binding and subsequent transfection, were not thoroughly examined. As surface properties are critical to the efficiency of the surface delivery approach (82), SAMs of alkanethiols on gold were used in this thesis as a well-defined tool to correlate the surface chemistry of the substrate to binding, release, and transfection of non-specifically immobilized complexes (Chapters 4 and 6). Surface hydrophilicity and ionization were found to mediate both DNA complex immobilization and transfection, with SAMs containing only carboxylic acids groups resulting in the greatest amounts of immobilization and transfection (Chapter 4). However, surface chemistry had no effect on complex release. Additionally, SAMs were used in conjunction with soft lithographic techniques to imprint substrates with specific patterns, resulting in patterned DNA complex deposition and transfection, with transfection efficiencies in the patterns nearing 40% (Chapter 4).

Subsequent studies used SAMs to provide a controlled surface to investigate the effect of surfaces presenting oligo(ethylene glycol) (EG) groups on substrate-mediated delivery (Chapter 6). We hypothesized that the presence of EG groups in a SAM could serve to convey the desired

properties of PEG on gene delivery (reduced aggregation, complex size stability), while potentially promoting complex-cell membrane interactions, but without attachment to complexes to inhibit binding to cells or subsequent transfection. Nonspecific complex immobilization to SAMs containing combinations of EG- and carboxylic acid- terminated alkanethiols resulted in substantially greater transfection than surfaces containing no EG groups or SAMs composed of EG groups combined with other functional groups. Enhancement in transfection levels could not be attributed to complex binding densities or release profiles. Atomic force microscopy imaging of immobilized complexes revealed that EG groups within SAMs affected complex size and appearance and could indicate the ability of these surfaces to preserve complex morphology upon binding, thereby enhancing the activity of substrate-mediated delivery of DNA complexes.

While the studies explored in this thesis examined substrate-mediated gene delivery by immobilization of entire complexes, an alterative strategy to nonspecifically immobilize DNA to substrates is to attach cationic groups to the material to promote naked DNA binding. Collagen was cationized through modification with amino groups or polylysine (50) for DNA binding. Alternatively, PEI or PLL was bound or blended with PLGA or collagen (51,52), resulting in DNA binding and cellular transfection in vitro. DNA has also been bound to substrates through polyelectrolyte films that promote localized delivery to cells (42). However, binding of plasmid DNA to a cationic material may prohibit cellular binding to these substrates (42) or exhibit limited cellular internalization due to the strong interactions between the DNA and the material and therefore immobilization of whole complexes to the surfaces, as presented in this thesis, appears to be a more effective strategy.

SAMs for substrate-mediated delivery of nonspecifically immobilized complexes could be used to further unravel the mechanisms of complex immobilization and subsequent transfection, as well as how complex-cell and cell-surface interactions contribute to delivery. Previous reports from our lab have shown that polyplexes and lipoplexes non-specifically immobilized to serum-coated substrates result in enhanced transgene expression in both cell lines and primary human-derived cells, along with an increased cellular viability. This enhancement was dependent on both the properties of the complex (e.g., complexation agent, N/P ratio), and substrate treatment (e.g. serum-coating vs. none) (2). The properties of the surfaces and vectors were further shown to be critical determinants of cellular association of immobilized DNA (3). These findings, combined with the results presented in this thesis, suggest that surface chemistry, either introduced through SAMs or by protein coatings, contribute to the type of complex binding to the surface. That is, on hydrophobic surfaces conformational changes may contribute to irreversible binding that limits cellular uptake, while hydrophilic substrates, which generally result in reversible interactions for proteins, may facilitate cellular internalization (82). Surface chemistries and, in particular, protein coatings can regulate the interaction of the complexes with the surface, but these surfaces may also alter the way in which cells attach to the surface. SAMs could be used to investigate how surface chemistry affects protein adsorption, which in turn affects complex conformation upon adsorption and potentially transfection efficiency, but also how surface chemistry and protein coatings affect the cells adhered to the surface.

SAMs have been used for numerous studies to investigate how underlying surface chemistry modulates protein adsorption in terms of adsorbed species density and biological activity. Surface chemistry modulates the structure (210) and activity of adsorbed fibronectin

(211,212) and fibrinogen (213), which can in turn modulate cellular activities, dramatically affecting focal adhesion assembly and signaling (214), which may regulate nonviral gene transfer (215). SAMs could be used to control the presentation of protein coatings, in particular fibronectin, which has been shown to enhance substrate-mediated gene delivery potentially by targeting internalization through caveolae-mediated endocytosis (4), to not only show how protein conformation can influence complex binding to the surface, but can further affect the cellular binding and activity on the surface, which could have dramatic effects on gene delivery. Further studies with EG-terminated thiols may also better elucidate the effect of complex conformation, and should include further AFM studies on a more diverse array of SAMs presenting a wider range of EG groups, as well as the ability of PEG to affect substrate-mediated gene delivery from alternative substrates.

Finally, the principles by which surface chemistry mediates surface delivery could be applied to biomaterials for tissue engineering applications. Specifically, the surfaces of hydrogels (22) or PLGA scaffolds (48) could be modified to present charged, carboxylic acid functional groups with combinations of EG groups to subsequently immobilize DNA complexes, for implantation in vivo. These DNA-loaded scaffolds could be used in wound healing applications, spinal cord regeneration bridges, or scaffolds for islet transplantation, in addition to cardiovascular applications (see Chapter 3).

8.2 Substrate-mediated delivery of tethered complexes

SAMs of alkanethiols on gold were also used to provide a controlled surface to investigate transfection resulting from DNA complexes immobilized to a substrate through

specific interactions. DNA complexes can be immobilized on the substrate through interactions introduced through complementary functional groups on the vector and surface. Previous studies on specific attachment of nonviral vectors investigated two cationic polymers, PLL and PEI, modified with biotin residues for subsequent complexation with DNA and binding to a neutravidin substrate (5,6,22). For complexes formed with PLL, the number of biotin groups and their distribution among the cationic polymer were critical determinants of both binding and transfection. Increasing the number of biotin groups per complex led to increased binding (5). However, *in vitro* transfection was maximal when complexes contained biotin residues attached to a small fraction of the cationic polymers (6) and transfection at this condition was increased 100 fold relative to bolus delivery of similar complexes (5). A specific interaction between cyclodextrin and adamantine has also been utilized to immobilize complexes of cyclodextrin-PEI with DNA on adamantine-functionalized surfaces by inclusion complex formation (38). However, in these previous studies, the specific tethering strategies have been plagued with nonspecific adsorption of complexes (6) or transfection was not investigated (38), making understanding or further use of these systems difficult.

In this thesis, DNA, complexed with PEI, was covalently linked to SAMs presenting appropriate functional groups through a fraction of the functional groups available on the PEI present in the complex (Chapter 5). Our goal was to directly attach unmodified complexes to substrates, rather than attaching moieties to PEI prior to complexation or after, to avoid complications with complexation and complex activity. SAMs were again used as model substrates, in that they present a uniform, defined surface chemistry and offer laterally well-defined sites at which biomolecules can be covalently attached to specific functional elements.

EG-terminated alkanethiols (165,166) were incorporated into the SAMs presenting the appropriate functional groups for the covalent tethering strategies to limit nonspecific complex adsorption. Covalent tethering by EDC/NHSS, glutaraldehyde, sulfo-SMCC, and AEDP resulted in lower complex binding than corresponding conditions without the addition of crosslinker. In each of these cases, the presumed covalent tethering of complexes resulted in no transfection, which could be evidence of successful tethering, or more probably, inactivation of the complexes, as the addition of a reducing agent to cleavable crosslinkers (AEDP, sulfo-LC-SMPT) did not affect complex binding densities or transfection.

In the covalent coupling studies presented in this thesis, the lowered binding densities and complete lack of transfection may be evidence for tethering, verifying our system could be the foundation for further studies. However, release profiles, toxicity issues, the inability to cleave cleavable crosslinkers and vast amounts of nonspecific binding suggest more work is needed to investigate complex tethering. Alternative studies that explore the presence of the tether, including XPS or FTIR, may be necessary to verify successful coupling. The extent of tethering, controlled through the amount of amines present within the complex (N/P ratio) and functional groups on surface, should be examined, as the extent of modification of complexes has been previously shown to be important to specific immobilization of complexes and subsequent transfection (6). The concentration of crosslinkers used, as well as conjugation times and ionic strength and pH of conjugation buffer (159), may also need to be investigated for optimal tethering. Additional strategies to reduce nonspecific binding may need to be investigated, including varying the length and percentage of EG groups within the monolayers, as well as utilizing alternative anti-fouling polymers. As PEI adsorption appears to promote cell adhesion

on EG-containing SAMs (Chapter 5), surfaces with greater percentages of EG groups could be used to potentially further reduce nonspecific binding, while still allowing for complex attachment, which in turn could allow for cell adhesion on these substrates. The addition of greater EG percentages could also serve to preserve complex morphology to further enhance transfection (Chapter 6).

Other specific tethering strategies may also need to be explored, including attachment of the amines within the PEI-DNA complexes to COOH-terminated SAMs through formation of an interchain carboxylic anhydride intermediate (162), coupling of amine-containing PEI-DNA complexes to NHS-terminated SAMs (158), tethering via photocleavable bonds (216), attachment using active-site directed ligands (217), tethering through ligand-receptor interactions (5,6,218), or coupling a His-tag to PEI for complex immobilization to nitrilotriacetic acid groups grafted onto SAMs (172,219). If attachment of whole complexes proves to be difficult, the above strategies could be modified to attach PEI alone, which could then be used to mediate binding of naked DNA (51) or complexes.

Once a tethering strategy is selected as a proof of principle that attachment of whole, unmodified complexes to SAMs is possible, the characteristics of the crosslinker bridge between the two known end moieties could be altered in terms of its length and degradation properties. Specific sites could be designed into the linker, to degrade under very specific conditions and to release complexes in desired spatial and temporal patterns, so that cell-associated enzymatic activity could cleave the linker to release the DNA for subsequent transfection, similar to studies exploring VEGF (220) or peptide-based gene delivery from fibrin matrices (39,86) released upon degradation of matrix metalloproteinase (MMP)-sensitive peptides within the matrix. These

covalent tethering strategies could be extended to biomaterial surfaces, to provide controlled and efficient delivery in tissue engineering applications.

8.3 Transfected cell arrays

Transfected cell arrays represent a high-throughput technique to correlate gene expression with functional cell responses (95,129,130), based on gene delivery from a substrate that supports cell adhesion. These arrays provide the ability to express, in parallel, thousands of exogenous genes in live cells, giving real-time information on cellular physiology and gene function. First developed by Sabatini's group in 2001 to analyze gene functions for phosphotyrosine activity (95), the transfected cell array has been adapted to a variety of applications, to study signaling pathways (100), screen antibody fragments (101), identify possible new lysophosphatidic acid receptors (102), perform protein localization studies (103,104), screen for proapoptotic genes (105,106), and annotate protein function (107). The transfected cell array has also been adapted to high-throughput RNAi studies (108-111). Efforts to improve transfected cell arrays have included incorporating fibronectin (112), atelocollagen (113), and recombinant proteins (114) with plasmid DNA or DNA complexes to mediate high transfection in the array. Studies have also investigated the effect of surface properties of the slide, including substrate hydrophobicity on transfection efficiency in array (115), as well as the effect of coating cationic polymer and collagen onto surfaces prior to transfection (116). Arrays have also been formed with dendrimers (123), magnetic beads (124) and viral vectors (59,125,126), for Drosophila cells (127) and nonadherent cells (128). Despite advances in transfected cell arrays, improvements are needed for the widespread application of this

technology, to accommodate issues with transfection efficiency, spot-to-spot variability, normalization, post-transfection processing, sensitivity, image acquisition and quantification, cell types that can be used, as well as to expand the biological endpoints.

We have developed a transfected cell array that combines a two-plasmid system and dual bioluminescence imaging to quantitatively normalize for variability in transfection and increase sensitivity (Chapter 7). The two plasmids consist of: i) normalization plasmid present within each spot, and ii) functional plasmid that varies between spots, responsible for the functional endpoint of the array. Bioluminescence imaging of dual luciferase reporters (renilla, firefly luciferase) provided sensitive and quantitative detection of the cellular response, with minimal post-transfection processing (202). The array was applied to quantify estrogen receptor α (ERα) activity in MCF-7 breast cancer cells. Estrogen receptor α (ERα) expression is an important biomarker for determining treatment course for clinical breast cancer. Estrogens, via ERα, act as potent mitogens of ER-positive breast cancer (138,139). A plasmid containing an ERα-regulated promoter directing firefly luciferase expression was mixed with a normalization plasmid, complexed with cationic lipids and spotted into an array using soft lithography techniques. ER-positive MCF-7 breast cancer cells were seeded onto the immobilized DNA-lipid complexes and treated with combinations of E_2, the complete antiestrogen (antagonist) fulvestrant (FUL) or vehicle controls. ER induction mimicked results obtained through traditional assay methods, with estrogen inducing luciferase expression 10-fold over FUL or vehicle. Furthermore, the array captured a dose response to estrogen, demonstrating the sensitivity of bioluminescence quantification.

Our transfected cell array system, which offers many improvements over existing technologies, provides a tool for basic science research but also offers the potential to impact cancer medicine. However, there are still further advancements to our system that need to be explored. The efficiency and reproducibility of array fabrication need to be improved, through robotic spotting techniques (95,112,115), which can be difficult to translate to spotting of whole complexes. The number of plasmids on each slide also needs to be increased, which will be facilitated by robotic spotting. By increasing the number of plasmids, single pathways can be examined in greater detail, for instance by including plasmids that express additional cofactors important in ERα transcriptional activity (221), or transcription factors involved in other signaling pathways in cancer can be explored. While our system was used with MCF-7 cells, other breast cancer cell lines need to be used in conjunction with these arrays, to probe for differences in signaling pathways employed by different breast cancer cell types, to demonstrate the ability of our system to support transfection in a multitude of cell types. Finally, the biggest test of our system will be to extend the array to primary cells isolated from patient biopsies, to correlate expression with grade and stage, which could lead to more appropriate, accurate and individualized treatments. Ultimately our system could impact cancer medicine, by increasing understanding of biological processes of cancer cells, and defining cancer subtypes and response to specific therapies, as well as classifying clinical cancer samples to identify patient-specific molecules and factors to assist in proper diagnosis and patient-specific therapy (206,208,209).

In summary, this thesis has presented basic studies on the mechanisms of substrate-mediated gene delivery, in particular the dramatic effect of surface chemistry on immobilization, transfection, and morphology of DNA complexes. When designing controlled release systems

for substrate-mediated gene delivery, whether for in vitro applications like transfected cell arrays, or for in vivo implantation in tissue engineering applications, the choice of surface chemistry should be carefully considered to optimize gene delivery. Furthermore, modulating the surface chemistry could allow for more tailored release profiles and subsequent gene expression. Finally, transfected cell arrays have the ability to be used in basic and diagnostic research applications, but have been limited primarily by shortcomings in quantification and normalization methods. Our system, employing two plasmids in each spot, combined with bioluminescence imaging, should serve as a standard for fabrication of transfected cell arrays to report on signaling pathways.

Chapter 9

References

1. Hagstrom, J.E. (2000) Self-assembling complexes for in vivo gene delivery. *Curr Opin Mol Ther*, **2**, 143-149.

2. Bengali, Z., Pannier, A.K., Segura, T., Anderson, B.C., Jang, J.H., Mustoe, T.A. and Shea, L.D. (2005) Gene delivery through cell culture substrate adsorbed DNA complexes. *Biotechnol Bioeng*, **90**, 290-302.

3. Bengali, Z. and Shea, L.D. (2007) Cellular association and distribution of DNA delivered by immobilization to a culture substrate. *J Control Release*, submitted.

4. Bengali, Z. and Shea, L.D. (2007) Gene expression and internalization following vector adsorption to immobilized proteins: dependence on protein identity and density. *J Gene Med*, submitted.

5. Segura, T. and Shea, L.D. (2002) Surface-tethered DNA complexes for enhanced gene delivery. *Bioconjug Chem*, **13**, 621-629.

6. Segura, T., Volk, M.J. and Shea, L.D. (2003) Substrate-mediated DNA delivery: role of the cationic polymer structure and extent of modification. *J Control Release*, **93**, 69-84.

7. Niidome, T. and Huang, L. (2002) Gene therapy progress and prospects: nonviral vectors. *Gene Ther*, **9**, 1647-1652.

8. Herweijer, H., and Wolff, J.A. (2003) Progress and prospects: naked DNA gene transfer and therapy. *Gene Ther*, **10**, 453-458.

9. Segura, T. and Shea, L.D. (2001) In Stupp, S. (ed.), *Ann. Rev. Mater. Sci.* Annual Reviews, Vol. 31, pp. 25-36.

10. Godbey, W.T., Wu, K.K. and Mikos, A.G. (1999) Poly(ethylenimine) and its role in gene delivery. *J Control Release*, **60**, 149-160.

11. Kircheis, R., Wightman, L. and Wagner, E. (2001) Design and gene delivery activity of modified polyethylenimines. *Adv Drug Deliv Rev*, **53**, 341-358.

12. Tranchant, I., Thompson, B., Nicolazzi, C., Mignet, N. and Scherman, D. (2004) Physicochemical optimisation of plasmid delivery by cationic lipids. *J Gene Med*, **6 Suppl 1**, S24-35.

13. Ledley, F.D. (1996) Pharmaceutical approach to somatic gene therapy. *Pharm Res*, **13**, 1595-1614.

14. Varga, C.M., Hong, K. and Lauffenburger, D.A. (2001) Quantitative analysis of synthetic gene delivery vector design properties. *Mol Ther*, **4**, 438-446.

15. Felgner, P.L., Gadek, T.R., Holm, M., Roman, R., Chan, H.W., Wenz, M., Northrop, J.P., Ringold, G.M. and Danielsen, M. (1987) Lipofection: a highly efficient, lipid-mediated DNA-transfection procedure. *Proc Natl Acad Sci U S A*, **84**, 7413-7417.

16. Nishikawa, M. and Huang, L. (2001) Nonviral vectors in the new millennium: delivery barriers in gene transfer. *Hum Gene Ther*, **12**, 861-870.

17. Elouahabi, A. and Ruysschaert, J.M. (2005) Formation and intracellular trafficking of lipoplexes and polyplexes. *Mol Ther*, **11**, 336-347.

18. Felgner, J.H., Kumar, R., Sridhar, C.N., Wheeler, C.J., Tsai, Y.J., Border, R., Ramsey, P., Martin, M. and Felgner, P.L. (1994) Enhanced gene delivery and mechanism studies with a novel series of cationic lipid formulations. *J Biol Chem*, **269**, 2550-2561.

19. Park, T.G., Jeong, J.H. and Kim, S.W. (2006) Current status of polymeric gene delivery systems. *Adv Drug Deliv Rev*, **58**, 467-486.

20. De Laporte, L., Cruz Rea, J. and Shea, L.D. (2006) Design of modular non-viral gene therapy vectors. *Biomaterials*, **27**, 947-954.

21. Akinc, A., Thomas, M., Klibanov, A.M. and Langer, R. (2005) Exploring polyethylenimine-mediated DNA transfection and the proton sponge hypothesis. *J Gene Med*, **7**, 657-663.

22. Segura, T., Chung, P.H. and Shea, L.D. (2005) DNA delivery from hyaluronic acid-collagen hydrogels via a substrate-mediated approach. *Biomaterials*, **26**, 1575-1584.

23. Wiethoff, C.M. and Middaugh, C.R. (2003) Barriers to nonviral gene delivery. *J Pharm Sci*, **92**, 203-217.

24. Medina-Kauwe, L.K., Xie, J. and Hamm-Alvarez, S. (2005) Intracellular trafficking of nonviral vectors. *Gene Ther*, **12**, 1734-1751.

25. Dean, D.A., Strong, D.D. and Zimmer, W.E. (2005) Nuclear entry of nonviral vectors. *Gene Ther*, **12**, 881-890.

26. Blessing, T., Kursa, M., Holzhauser, R., Kircheis, R. and Wagner, E. (2001) Different strategies for formation of pegylated EGF-conjugated PEI/DNA complexes for targeted gene delivery. *Bioconjug Chem*, **12**, 529-537.

27. Ogris, M., Steinlein, P., Carotta, S., Brunner, S. and Wagner, E. (2001) DNA/polyethylenimine transfection particles: influence of ligands, polymer size, and PEGylation on internalization and gene expression. *AAPS PharmSci*, **3**, E21.

28. Liang, E., Rosenblatt, M.N., Ajmani, P.S. and Hughes, J.A. (2000) Biodegradable pH-sensitive surfactants (BPS) in liposome-mediated nucleic acid cellular uptake and distribution. *Eur J Pharm Sci*, **11**, 199-205.

29. Duguid, J.G., Li, C., Shi, M., Logan, M.J., Alila, H., Rolland, A., Tomlinson, E., Sparrow, J.T. and Smith, L.C. (1998) A physicochemical approach for predicting the effectiveness of peptide-based gene delivery systems for use in plasmid-based gene therapy. *Biophys J*, **74**, 2802-2814.

30. Luo, D. and Saltzman, W.M. (2000) Enhancement of transfection by physical concentration of DNA at the cell surface. *Nat Biotechnol*, **18**, 893-895.

31. Luo, D., Han, E., Belcheva, N. and Saltzman, W.M. (2004) A self-assembled, modular DNA delivery system mediated by silica nanoparticles. *Journal of Controlled Release*, **95**, 333-341.

32. Kuhl, P.R. and Griffith-Cima, L.G. (1996) Tethered epidermal growth factor as a paradigm for growth factor-induced stimulation from the solid phase [published erratum appears in Nat Med 1997 Jan;3(1):93]. *Nat Med*, **2**, 1022-1027.

33. Sakiyama-Elbert, S.E., Panitch, A. and Hubbell, J.A. (2001) Development of growth factor fusion proteins for cell-triggered drug delivery. *Faseb J*, **15**, 1300-1302.

34. Zisch, A.H., Schenk, U., Schense, J.C., Sakiyama-Elbert, S.E. and Hubbell, J.A. (2001) Covalently conjugated VEGF--fibrin matrices for endothelialization. *J Control Release*, **72**, 101-113.

35. Proctor, R.A. (1987) Fibronectin: a brief overview of its structure, function, and physiology. *Rev Infect Dis*, **9 Suppl 4**, S317-321.

36. Bajaj, B., Lei, P. and Andreadis, S.T. (2001) High efficiencies of gene transfer with immobilized recombinant retrovirus: kinetics and optimization. *Biotechnol Prog*, **17**, 587-596.

37. Levy, R.J., Song, C., Tallapragada, S., DeFelice, S., Hinson, J.T., Vyavahare, N., Connolly, J., Ryan, K. and Li, Q. (2001) Localized adenovirus gene delivery using antiviral IgG complexation. *Gene Ther*, **8**, 659-667.

38. Park, I.K., von Recum, H.A., Jiang, S. and Pun, S.H. (2006) Supramolecular assembly of cyclodextrin-based nanoparticles on solid surfaces for gene delivery. *Langmuir*, **22**, 8478-8484.

39. Trentin, D., Hubbell, J. and Hall, H. (2005) Non-viral gene delivery for local and controlled DNA release. *J Control Release*, **102**, 263-275.

40. Putney, S.D. and Burke, P.A. (1998) Improving protein therapeutics with sustained-release formulations. *Nat Biotechnol*, **16**, 153-157.

41. Norde, W. and Lyklema, J. (1991) Why proteins prefer interfaces. *J Biomater Sci Polym Ed*, **2**, 183-202.

42. Jewell, C.M., Zhang, J., Fredin, N.J. and Lynn, D.M. (2005) Multilayered polyelectrolyte films promote the direct and localized delivery of DNA to cells. *J Control Release*, **106**, 214-223.

43. Yamauchi, F., Koyamatsu, Y., Kato, K. and Iwata, H. (2006) Layer-by-layer assembly of cationic lipid and plasmid DNA onto gold surface for stent-assisted gene transfer. *Biomaterials*, **27**, 3497-3504.

44. Shen, H., Tan, J. and Saltzman, W.M. (2004) Surface-mediated gene transfer from nanocomposites of controlled texture. *Nat Mater*, **3**, 569-574.

45. Reinisalo, M., Urtti, A. and Honkakoski, P. (2006) Freeze-drying of cationic polymer DNA complexes enables their long-term storage and reverse transfection of post-mitotic cells. *J Control Release*, **110**, 437-443.

46. Bielinska, A.U., Yen, A., Wu, H.L., Zahos, K.M., Sun, R., Weiner, N.D., Baker, J.R., Jr. and Roessler, B.J. (2000) Application of membrane-based dendrimer/DNA complexes for solid phase transfection in vitro and in vivo. *Biomaterials*, **21**, 877-887.

47. Kofron, M.D. and Laurencin, C.T. (2004) Development of a calcium phosphate co-precipitate/poly(lactide-co-glycolide) DNA delivery system: release kinetics and cellular transfection studies. *Biomaterials*, **25**, 2637-2643.

48. Jang, J.H., Bengali, Z., Houchin, T.L. and Shea, L.D. (2006) Surface adsorption of DNA to tissue engineering scaffolds for efficient gene delivery. *J Biomed Mater Res A*, **77**, 50-58.

49. Katz, J.M., Roth, C.M. and Dunn, M.G. (2005) Factors that influence transgene expression and cell viability on DNA-PEI-seeded collagen films. *Tissue Eng*, **11**, 1398-1406.

50. Aoyama, T., Yamamoto, S., Kanematsu, A., Ogawa, O. and Tabata, Y. (2003) Local delivery of matrix metalloproteinase gene prevents the onset of renal sclerosis in streptozotocin-induced diabetic mice. *Tissue Eng*, **9**, 1289-1299.

51. Zheng, J., Manuel, W.S. and Hornsby, P.J. (2000) Transfection of cells mediated by biodegradable polymer materials with surface-bound polyethyleneimine. *Biotechnol Prog*, **16**, 254-257.

52. Cohen-Sacks, H., Elazar, V., Gao, J., Golomb, A., Adwan, H., Korchov, N., Levy, R.J., Berger, M.R. and Golomb, G. (2004) Delivery and expression of pDNA embedded in collagen matrices. *J Control Release*, **95**, 309-320.

53. Denis-Mize, K.S., Dupuis, M., MacKichan, M.L., Singh, M., Doe, B., O'Hagan, D., Ulmer, J.B., Donnelly, J.J., McDonald, D.M. and Ott, G. (2000) Plasmid DNA adsorbed onto cationic microparticles mediates target gene expression and antigen presentation by dendritic cells. *Gene Ther*, **7**, 2105-2112.

54. Cavanagh, H.M., Dingwall, D., Steel, J., Benson, J. and Burton, M. (2001) Cell contact dependent extended release of adenovirus by microparticles in vitro. *J Virol Methods*, **95**, 57-64.

55. Mah, C., Fraites, T.J., Jr., Zolotukhin, I., Song, S., Flotte, T.R., Dobson, J., Batich, C. and Byrne, B.J. (2002) Improved method of recombinant AAV2 delivery for systemic targeted gene therapy. *Mol Ther*, **6**, 106-112.

56. Abrahams, J.M., Song, C., DeFelice, S., Grady, M.S., Diamond, S.L. and Levy, R.J. (2002) Endovascular microcoil gene delivery using immobilized anti-adenovirus antibody for vector tethering. *Stroke*, **33**, 1376-1382.

57. Klugherz, B.D., Song, C., DeFelice, S., Cui, X., Lu, Z., Connolly, J., Hinson, J.T., Wilensky, R.L. and Levy, R.J. (2002) Gene delivery to pig coronary arteries from stents carrying antibody-tethered adenovirus. *Hum Gene Ther*, **13**, 443-454.

58. Pandori, M., Hobson, D. and Sano, T. (2002) Adenovirus-microbead conjugates possess enhanced infectivity: a new strategy for localized gene delivery. *Virology*, **299**, 204-212.

59. Hobson, D.A., Pandori, M.W. and Sano, T. (2003) In situ transduction of target cells on solid surfaces by immobilized viral vectors. *BMC Biotechnol*, **3**, 4.

60. Parrott, M.B. and Barry, M.A. (2000) Metabolic biotinylation of recombinant proteins in mammalian cells and in mice. *Mol Ther*, **1**, 96-104.

61. Parrott, M.B. and Barry, M.A. (2001) Metabolic biotinylation of secreted and cell surface proteins from mammalian cells. *Biochem Biophys Res Commun*, **281**, 993-1000.

62. Lee, J.H., Baker, T.J., Mahal, L.K., Zabner, J., Bertozzi, C.R., Wiemer, D.F. and Welsh, M.J. (1999) Engineering novel cell surface receptors for virus-mediated gene transfer. *J Biol Chem*, **274**, 21878-21884.

63. Ulman, A. (1996) Formation and Structure of Self-Assembled Monolayers. *Chem Rev*, **96**, 1533-1554.

64. DiMilla, P.A., Folkers, J.P., Biebuyck, H.A., Harter, R., Lopez, G.P. and Whitesides, G.M. (1994) Wetting and protein adsorption on self-assembled monolayers of alkanethiolates supported on transparent films of gold. *J Am Chem Soc*, **116**, 2225-2237

.

65. Singhvi, R., Kumar, A., Lopez, G.P., Stephanopoulos, G.N., Wang, D.I., Whitesides, G.M. and Ingber, D.E. (1994) Engineering cell shape and function. *Science*, **264**, 696-698.

66. Nuzzo, R.G. and Allara, D.L. (1983) Adsorption of Bifunctional Organic Disulfides on Gold Surfaces. *Journal of the American Chemical Society*, **105**, 4481-4483.

67. Kane, R.S., Takayama, S., Ostuni, E., Ingber, D.E. and Whitesides, G.M. (1999) Patterning proteins and cells using soft lithography. *Biomaterials*, **20**, 2363-2376.

68. Bain, C.D. and Whitesides, G.M. (1989) Formation of Monolayers by the Coadsorption of Thiols on Gold - Variation in the Length of the Alkyl Chain. *Journal of the American Chemical Society*, **111**, 7164-7175.

69. Haddow, D.B., France, R.M., Short, R.D., MacNeil, S., Dawson, R.A., Leggett, G.J. and Cooper, E. (1999) Comparison of proliferation and growth of human keratinocytes on plasma copolymers of acrylic acid/1,7-octadiene and self-assembled monolayers. *J Biomed Mater Res*, **47**, 379-387.

70. Cooper, E., Wiggs, R., Hutt, D.A., Parker, L., Leggett, G.J. and Parker, T.L. (1997) Rates of attachment of fibroblasts to self-assembled monolayers formed by the adsorption of alkylthiols onto gold surfaces. *J Mater Chem*, **7**, 435-441.

71. McClary, K.B., Ugarova, T. and Grainger, D.W. (2000) Modulating fibroblast adhesion, spreading, and proliferation using self-assembled monolayer films of alkylthiolates on gold. *J Biomed Mater Res*, **50**, 428-439.

72. Kumar, A., Whitesides, G.M. (1993) Features of gold having micrometer to centimeter dimensions can be formed through a combination of stamping with an elastomeric stamp and an alkanethiol "ink" followed by chemical etching. *Appl. Phys. Lett.*, **63**, 2002-2004.

73. Kumar, A., Biebuyck, H.A. and Whitesides, G.M. (1994) Patterning self-assembled monolayers: applications in material science. *Langmuir*, **10**, 1498-1511.

74. Xia, Y. and Whitesides, G.M. (1998) Soft Lithography. *Angew Chem Int Ed*, **37**, 550-575.

75. Kumar, A. and Whitesides, G.M. (1994) Patterned condensation figures as optical diffraction gratings. *Science*, **263**, 60-62.

76. Lopez, G.P., Biebuyck, H.A., Frisbie, C.D. and Whitesides, G.M. (1993) Imaging of features on surfaces by condensation figures. *Science*, **260**, 647-649.

77. Xu, Y., Watson, J.T. and Bruening, M.L. (2003) Patterned monolayer/polymer films for analysis of dilute or salt-contaminated protein samples by MALDI-MS. *Anal Chem*, **75**, 185-190.

78. Brockman, J.M., Frutos, A.G. and Corn, R.M. (1999) A multistep chemical modification procedure to create DNA arrays on gold surfaces for the study of protein-DNA interactions with surface plasmon resonance imaging. *J Am Chem Soc*, **121**, 8044-8051.

79. Gillmore, S.D., Thiel, A.J., Strother, T.C., Smith, L.M. and Lagally, M.G. (2000) Hydrophilic/hydrophobic patterned surfaces as templates for DNA arrays. *Langmuir*, **16**, 7223-7228.

80. Zhang, G., Yan, X., Hou, X., Lu, G., Yang, B., Wu, L. and Shen, J. (2003) Binary DNA arrays on heterogeneous patterend surfaces. *Langmuir*, **19**, 9850-9854.

81. Pannier, A.K. and Shea, L.D. (2004) Controlled release systems for DNA delivery. *Mol Ther*, **10**, 19-26.

82. Bengali, Z. and Shea, L.D. (2005) Gene delivery by immobilization to cell-adhesive substrates. *MRS Bulletin*, **30**, 659-662.

83. Palsson, B. and Andreadis, S. (1997) The physico-chemical factors that govern retrovirus-mediated gene transfer. *Exp Hematol*, **25**, 94-102.

84. Tam, P., Monck, M., Lee, D., Ludkovski, O., Leng, E.C., Clow, K., Stark, H., Scherrer, P., Graham, R.W. and Cullis, P.R. (2000) Stabilized plasmid-lipid particles for systemic gene therapy. *Gene Ther*, **7**, 1867-1874.

85. Layne, S.P., Merges, M.J., Dembo, M., Spouge, J.L., Conley, S.R., Moore, J.P., Raina, J.L., Renz, H., Gelderblom, H.R. and Nara, P.L. (1992) Factors underlying spontaneous inactivation and susceptibility to neutralization of human immunodeficiency virus. *Virology*, **189**, 695-714.

86. Trentin, D., Hall, H., Wechsler, S. and Hubbell, J.A. (2006) Peptide-matrix-mediated gene transfer of an oxygen-insensitive hypoxia-inducible factor-1alpha variant for local induction of angiogenesis. *Proc Natl Acad Sci U S A*, **103**, 2506-2511.

87. Fishbein, I., Stachelek, S.J., Connolly, J.M., Wilensky, R.L., Alferiev, I. and Levy, R.J. (2005) Site specific gene delivery in the cardiovascular system. *J Control Release*, **109**, 37-48.

88. Stachelek, S.J., Song, C., Alferiev, I., Defelice, S., Cui, X., Connolly, J.M., Bianco, R.W. and Levy, R.J. (2004) Localized gene delivery using antibody tethered adenovirus from polyurethane heart valve cusps and intra-aortic implants. *Gene Ther*, **11**, 15-24.

89. Jewell, C.M., Zhang, J., Fredin, N.J., Wolff, M.R., Hacker, T.A. and Lynn, D.M. (2006) Release of plasmid DNA from intravascular stents coated with ultrathin multilayered polyelectrolyte films. *Biomacromolecules*, **7**, 2483-2491.

90. Klugherz, B.D., Jones, P.L., Cui, X., Chen, W., Meneveau, N.F., DeFelice, S., Connolly, J., Wilensky, R.L. and Levy, R.J. (2000) Gene delivery from a DNA controlled-release stent in porcine coronary arteries. *Nat Biotechnol*, **18**, 1181-1184.

91. Perlstein, I., Connolly, J.M., Cui, X., Song, C., Li, Q., Jones, P.L., Lu, Z., DeFelice, S., Klugherz, B., Wilensky, R. *et al.* (2003) DNA delivery from an intravascular stent with a denatured collagen-polylactic-polyglycolic acid-controlled release coating: mechanisms of enhanced transfection. *Gene Ther*, **10**, 1420-1428.

92. Fishbein, I., Alferiev, I.S., Nyanguile, O., Gaster, R., Vohs, J.M., Wong, G.S., Felderman, H., Chen, I.W., Choi, H., Wilensky, R.L. *et al.* (2006) Bisphosphonate-mediated gene vector delivery from the metal surfaces of stents. *Proc Natl Acad Sci U S A*, **103**, 159-164.

93. Saltzman, W.M. and Olbricht, W.L. (2002) Building drug delivery into tissue engineering. *Nat Rev Drug Discov*, **1**, 177-186.

94. Murphy, W.L. and Mooney, D.J. (1999) Controlled delivery of inductive proteins, plasmid DNA and cells from tissue engineering matrices. *J Periodontal Res*, **34**, 413-419.

95. Ziauddin, J. and Sabatini, D.M. (2001) Microarrays of cells expressing defined cDNAs. *Nature*, **411**, 107-110.

96. Pepperkok, R. and Ellenberg, J. (2006) High-throughput fluorescence microscopy for systems biology. *Nat Rev Mol Cell Biol*, **7**, 690-696.

97. Hook, A.L., Thissen, H. and Voelcker, N.H. (2006) Surface manipulation of biomolecules for cell microarray applications. *Trends Biotechnol*, **24**, 471-477.

98. Palmer, E. and Freeman, T. (2005) Cell-based microarrays: current progress, future prospects. *Pharmacogenomics*, **6**, 527-534.

99. Grimm, S. (2004) The art and design of genetic screens: mammalian culture cells. *Nat Rev Genet*, **5**, 179-189.

100. Webb, B.L., Diaz, B., Martin, G.S. and Lai, F. (2003) A reporter system for reverse transfection cell arrays. *J Biomol Screen*, **8**, 620-623.

101. Delehanty, J.B., Shaffer, K.M. and Lin, B. (2004) Transfected cell microarrays for the expression of membrane-displayed single-chain antibodies. *Anal Chem*, **76**, 7323-7328.

102. Lee, C.W., Rivera, R., Gardell, S., Dubin, A.E. and Chun, J. (2006) GPR92 as a new G12/13- and Gq-coupled lysophosphatidic acid receptor that increases cAMP, LPA5. *J Biol Chem*, **281**, 23589-23597.

103. Hu, Y.H., Vanhecke, D., Lehrach, H. and Janitz, M. (2005) High-throughput subcellular protein localization using cell arrays. *Biochem Soc Trans*, **33**, 1407-1408.

104. Hu, Y.H., Warnatz, H.J., Vanhecke, D., Wagner, F., Fiebitz, A., Thamm, S., Kahlem, P., Lehrach, H., Yaspo, M.L. and Janitz, M. (2006) Cell array-based intracellular localization screening reveals novel functional features of human chromosome 21 proteins. *BMC Genomics*, **7**, 155.

105. Mannherz, O., Mertens, D., Hahn, M. and Lichter, P. (2006) Functional screening for proapoptotic genes by reverse transfection cell array technology. *Genomics*, **87**, 665-672.

106. Palmer, E.L., Miller, A.D. and Freeman, T.C. (2006) Identification and characterisation of human apoptosis inducing proteins using cell-based transfection microarrays and expression analysis. *BMC Genomics*, **7**, 145.

107. Hodges, E., Redelius, J.S., Wu, W. and Hoog, C. (2005) Accelerated discovery of novel protein function in cultured human cells. *Mol Cell Proteomics*, **4**, 1319-1327.

108. Mousses, S., Caplen, N.J., Cornelison, R., Weaver, D., Basik, M., Hautaniemi, S., Elkahloun, A.G., Lotufo, R.A., Choudary, A., Dougherty, E.R. *et al.* (2003) RNAi microarray analysis in cultured mammalian cells. *Genome Res*, **13**, 2341-2347.

109. Silva, J.M., Mizuno, H., Brady, A., Lucito, R. and Hannon, G.J. (2004) RNA interference microarrays: high-throughput loss-of-function genetics in mammalian cells. *Proc Natl Acad Sci U S A*, **101**, 6548-6552.

110. Erfle, H., Simpson, J.C., Bastiaens, P.I. and Pepperkok, R. (2004) siRNA cell arrays for high-content screening microscopy. *Biotechniques*, **37**, 454-458, 460, 462.

111. Neumann, B., Held, M., Liebel, U., Erfle, H., Rogers, P., Pepperkok, R. and Ellenberg, J. (2006) High-throughput RNAi screening by time-lapse imaging of live human cells. *Nat Methods*, **3**, 385-390.

112. Yoshikawa, T., Uchimura, E., Kishi, M., Funeriu, D.P., Miyake, M. and Miyake, J. (2004) Transfection microarray of human mesenchymal stem cells and on-chip siRNA gene knockdown. *J Control Release*, **96**, 227-232.

113. Honma, K., Ochiya, T., Nagahara, S., Sano, A., Yamamoto, H., Hirai, K., Aso, Y. and Terada, M. (2001) Atelocollagen-based gene transfer in cells allows high-throughput screening of gene functions. *Biochem Biophys Res Commun*, **289**, 1075-1081.

114. Redmond, T.M., Ren, X., Kubish, G., Atkins, S., Low, S. and Uhler, M.D. (2004) Microarray transfection analysis of transcriptional regulation by cAMP-dependent protein kinase. *Mol Cell Proteomics*, **3**, 770-779.

115. Delehanty, J.B., Shaffer, K.M. and Lin, B. (2004) A comparison of microscope slide substrates for use in transfected cell microarrays. *Biosens Bioelectron*, **20**, 773-779.

116. Chang, F.H., Lee, C.H., Chen, M.T., Kuo, C.C., Chiang, Y.L., Hang, C.Y. and Roffler, S. (2004) Surfection: a new platform for transfected cell arrays. *Nucleic Acids Res*, **32**, e33.

117. Pannier, A.K., Anderson, B.C. and Shea, L.D. (2005) Substrate-mediated delivery from self-assembled monolayers: Effect of surface ionization, hydrophilicity, and patterning. *Acta Biomaterialia*, **1**, 511-522.

118. Yamauchi, F., Kato, K. and Iwata, H. (2004) Micropatterned, self-assembled monolayers for fabrication of transfected cell microarrays. *Biochim Biophys Acta*, **1672**, 138-147.

119. Fujimoto, H., Yoshizako, S., Kato, K. and Iwata, H. (2006) Fabrication of cell-based arrays using micropatterned alkanethiol monolayers for the parallel silencing of specific genes by small interfering RNA. *Bioconjug Chem*, **17**, 1404-1410.

120. Yamauchi, F., Kato, K. and Iwata, H. (2004) Spatially and temporally controlled gene transfer by electroporation into adherent cells on plasmid DNA-loaded electrodes. *Nucleic Acids Res*, **32**, e187.

121. Yamauchi, F., Kato, K. and Iwata, H. (2005) Layer-by-layer assembly of poly(ethyleneimine) and plasmid DNA onto transparent indium-tin oxide electrodes for temporally and spatially specific gene transfer. *Langmuir*, **21**, 8360-8367.

122. Peterbauer, T., Heitz, J., Olbrich, M. and Hering, S. (2006) Simple and versatile methods for the fabrication of arrays of live mammalian cells. *Lab Chip*, **6**, 857-863.

123. How, S.E., Yingyongnarongkul, B., Fara, M.A., Diaz-Mochon, J.J., Mittoo, S. and Bradley, M. (2004) Polyplexes and lipoplexes for mammalian gene delivery: from traditional to microarray screening. *Comb Chem High Throughput Screen*, **7**, 423-430.

124. Isalan, M., Santori, M.I., Gonzalez, C. and Serrano, L. (2005) Localized transfection on arrays of magnetic beads coated with PCR products. *Nat Methods*, **2**, 113-118.

125. Bailey, S.N., Ali, S.M., Carpenter, A.E., Higgins, C.O. and Sabatini, D.M. (2006) Microarrays of lentiviruses for gene function screens in immortalized and primary cells. *Nat Methods*, **3**, 117-122.

126. Michiels, F., van Es, H., van Rompaey, L., Merchiers, P., Francken, B., Pittois, K., van der Schueren, J., Brys, R., Vandersmissen, J., Beirinckx, F. *et al.* (2002) Arrayed adenoviral expression libraries for functional screening. *Nat Biotechnol*, **20**, 1154-1157.

127. Wheeler, D.B., Bailey, S.N., Guertin, D.A., Carpenter, A.E., Higgins, C.O. and Sabatini, D.M. (2004) RNAi living-cell microarrays for loss-of-function screens in Drosophila melanogaster cells. *Nat Methods*, **1**, 127-132.

128. Kato, K., Umezawa, K., Miyake, M., Miyake, J. and Nagamune, T. (2004) Transfection microarray of nonadherent cells on an oleyl poly(ethylene glycol) ether-modified glass slide. *Biotechniques*, **37**, 444-448, 450, 452.

129. Wu, R.Z., Bailey, S.N. and Sabatini, D.M. (2002) Cell-biological applications of transfected-cell microarrays. *Trends Cell Biol*, **12**, 485-488.

130. Bailey, S.N., Wu, R.Z. and Sabatini, D.M. (2002) Applications of transfected cell microarrays in high-throughput drug discovery. *Drug Discov Today*, **7**, S113-118.

131. Bild, A.H., Yao, G., Chang, J.T., Wang, Q., Potti, A., Chasse, D., Joshi, M.B., Harpole, D., Lancaster, J.M., Berchuck, A. *et al.* (2006) Oncogenic pathway signatures in human cancers as a guide to targeted therapies. *Nature*, **439**, 353-357.

132. Downward, J. (2006) Cancer biology: signatures guide drug choice. *Nature*, **439**, 274-275.

133. Jemal, A., Siegel, R., Ward, E., Murray, T., Xu, J., Smigal, C. and Thun, M.J. (2006) Cancer statistics, 2006. *CA Cancer J Clin*, **56**, 106-130.

134. Dorgan, J.F., Longcope, C., Stephenson, H.E., Jr., Falk, R.T., Miller, R., Franz, C., Kahle, L., Campbell, W.S., Tangrea, J.A. and Schatzkin, A. (1996) Relation of prediagnostic serum estrogen and androgen levels to breast cancer risk. *Cancer Epidemiol Biomarkers Prev*, **5**, 533-539.

135. Foster, J.S., Henley, D.C., Ahamed, S. and Wimalasena, J. (2001) Estrogens and cell-cycle regulation in breast cancer. *Trends Endocrinol Metab*, **12**, 320-327.

136. Russo, I.H. and Russo, J. (1998) Role of hormones in mammary cancer initiation and progression. *J Mammary Gland Biol Neoplasia*, **3**, 49-61.

137. Dees, C., Foster, J.S., Ahamed, S. and Wimalasena, J. (1997) Dietary estrogens stimulate human breast cells to enter the cell cycle. *Environ Health Perspect*, **105 Suppl 3**, 633-636.

138. Pearce, S.T. and Jordan, V.C. (2004) The biological role of estrogen receptors alpha and beta in cancer. *Crit Rev Oncol Hematol*, **50**, 3-22.

139. Ariazi, E.A., Ariazi, J.L., Cordera, F. and Jordan, V.C. (2006) Estrogen receptors as therapeutic targets in breast cancer. *Curr Top Med Chem*, **6**, 181-202.

140. Ikeda, K. and Inoue, S. (2004) Estrogen receptors and their downstream targets in cancer. *Arch Histol Cytol*, **67**, 435-442.

141. Jensen, E.V. and Jordan, V.C. (2003) The estrogen receptor: a model for molecular medicine. *Clin Cancer Res*, **9**, 1980-1989.

142. Paik, S., Shak, S., Tang, G., Kim, C., Baker, J., Cronin, M., Baehner, F.L., Walker, M.G., Watson, D., Park, T. *et al.* (2004) A multigene assay to predict recurrence of tamoxifen-treated, node-negative breast cancer. *N Engl J Med*, **351**, 2817-2826.

143. Oh, D.S., Troester, M.A., Usary, J., Hu, Z., He, X., Fan, C., Wu, J., Carey, L.A. and Perou, C.M. (2006) Estrogen-regulated genes predict survival in hormone receptor-positive breast cancers. *J Clin Oncol*, **24**, 1656-1664.

144. Levine, M. and Tjian, R. (2003) Transcription regulation and animal diversity. *Nature*, **424**, 147-151.

145. Kneuer, C., Sameti, M., Bakowsky, U., Schiestel, T., Schirra, H., Schmidt, H. and Lehr, C.M. (2000) A nonviral DNA delivery system based on surface modified silica-nanoparticles can efficiently transfect cells in vitro. *Bioconjug Chem*, **11**, 926-932.

146. Manuel, W.S., Zheng, J.I. and Hornsby, P.J. (2001) Transfection by polyethyleneimine-coated microspheres. *J Drug Target*, **9**, 15-22.

147. Zhang, J.T., Chua, L.S. and Lynn, D.M. (2004) Multilayered thin films that sustain the release of functional DNA under physiological conditions. *Langmuir*, **20**, 8015-8021.

148. Sigal, G.B., Mrksich, M. and Whitesides, G.M. (1998) Effect of surface wettability on the adsorption of proteins and detergents. *J Am Chem Soc*, **120**, 3464-3473.

149. van der Veen, M., Norde, W. and Stuart, M.C. (2004) Electrostatic interactions in protein adsorption probed by comparing lysozyme and succinylated lysozyme. *Colloid Surface B*, **35**, 33-40.

150. Troughton, E.B., Bain, C.D. and Whitesides, G.M. (1998) Monolayer films prepared by the spontaneous self-assembly of symmetrical and unsymmetrical dialkyl sulfides from solution onto gold substrates: structure, properties, and reactivity of constituent functional groups. *Langmuir*, **4**, 365-385.

151. Tsai, M.Y. and Lin, J.C. (2001) Surface characterization and platelet adhesion studies of self-assembled monolayer with phosphonate ester and phosphonic acid functionalities. *J Biomed Mater Res*, **55**, 554-565.

152. Barrias, C.C., Martins, M.A., Miranda, M.A. and Barbosa, M.A. (2005) Adsorption of a therapeutic enzyme to self-assembled monolayers: effect of surface chemistry and solution pH on the amount and activity of adsorbed enzyme. *Biomaterials*, **26**, 2695-2704.

153. Wadu-Mesthrige, K., Amro, N.A. and Liu, G.Y. (2000) Immobilization of proteins on self-assembled monolayers. *Scanning*, **22**, 380-388.

154. Stuart, M.A.C., Fleer, G.J., Lyklema, J., Norde, W. and Scheutjens, J.M.H.M. (1991) Adsorption of Ions, Polyelectrolytes and Proteins. *Adv Colloid Interfac*, **34**, 477-535.

155. Lopez, G.P., Albers, M.W., Schreiber, S.L., Carroll, R., Peralta, E. and Whitesides, G.M. (1993) Convenient methods for patterning the adhesion of mammalian cells to surfaces using self-assembled monolayers of alkanethiolates on gold. *J Am Chem Soc*, **115**, 5877-5878.

156. Korobko, A.V., Backendorf, C. and van der Maarel, J.R. (2006) Plasmid DNA encapsulation within cationic diblock copolymer vesicles for gene delivery. *J Phys Chem B Condens Matter Mater Surf Interfaces Biophys*, **110**, 14550-14556.

157. Houchin-Ray, T., Whittlesey, K.J. and Shea, L.D. (2007) Spatially patterned gene delivery for localized neuron survival and neurite extension. *Mol Ther*, **in press**.

158. Zaugg, F.G., Spencer, N.D., Wagner, P., Kernen, P., Vinckier, A., Groscurth, P. and Semenza, G. (1999) Microstructured bioreactive surfaces: covalent immobilization of proteins on Au(1 1 1)/silicon via aminoreactive alkanethiolate self-assembled monolayers. *J Mater Sci Mater Med*, **10**, 255-263.

159. Lahiri, J., Isaacs, L., Tien, J. and Whitesides, G.M. (1999) A strategy for the generation of surfaces presenting ligands for studies of binding based on an active ester as a common reactive intermediate: A surface plasmon resonance study. *Anal Chem*, **71**, 777-790.

160. Yadavalli, V.K., Forbes, J.G. and Wang, K. (2006) Functionalized self-assembled monolayers on ultraflat gold as platforms for single molecule force spectroscopy and imaging. *Langmuir*, **22**, 6969-6976.

161. Kato, K., Toda, M. and Iwata, H. (2007) Antibody arrays for quantitative immunophenotyping. *Biomaterials*, **28**, 1289-1297.

162. Yan, L., Huck, W.T.S., Zhao, X.M. and Whitesides, G.M. (1999) Patterning thin films of poly(ethylene imine) on a reactive SAM using microcontact printing. *Langmuir*, **15**, 1208-1214.

163. Biebricher, A., Paul, A., Tinnefeld, P., Golzhauser, A. and Sauer, M. (2004) Controlled three-dimensional immobilization of biomolecules on chemically patterned surfaces. *J Biotechnol*, **112**, 97-107.

164. Peelen, D. and Smith, L.M. (2005) Immobilization of amine-modified oligonucleotides on aldehyde-terminated alkanethiol monolayers on gold. *Langmuir*, **21**.

165. Pale-Grosdemange, C., SImon, E.S., Prime, K.L. and Whitesides, G.M. (1991) Formation of self-assembled monolayers by chemisorption of derivatives of oligo(ethylene glycol) of structure $HS(CH_2)_{11}(OCH_2CH_2)_mOH$ on gold. *J Am Chem Soc*, **113**, 12-20.

166. Prime, K.L. and Whitesides, G.M. (1993) Adsorption of proteins onto surfaces containing end-attached oligo(ethylene oxide): a model system using self-assembled monolayers. *J Am Chem Soc*, **115**, 10714-10721.

167. Ostuni, E., Chapman, R.G., Holmlin, R.E., Takayama, S. and Whitesides, G.M. (2001) A survey of structure-property relationships of surfaces that resist the adsorption of protein. *Langmuir*, **17**, 5605-5620.

168. Carot, M.L., Esplandiu, M.J., Cometto, F.P., Patrito, E.M. and Macagno, V.A. (2005) Reactivity of 1,8-octanedithiol monolayers on Au(1 1 1): Experimental and theoretical investigations. *J Electro Chem*, **579**, 13-23.

169. Rieley, H., Kendall, G.K., Zemicael, F.W., Smith, T.L. and Yang, S. (1998) X-ray studies of self-assembled monolayers on coinage metals. 1. Alignment and photooxidation in 1,8-octanedithiol and 1-octanethiol on Au. *Langmuir*, **14**, 5147-5153.

170. Kohli, P., Taylor, K.K., Harris, J.J. and Blanchard, G.J. (1998) Assembly of covalently-coupled disulfide multilayers on gold. *J Am Chem Soc*, **120**.

171. Kingshott, P., Wei, J., Bagge-Ravn, D., Gadegaard, N. and Gram, L. (2003) Covalent attachment of poly(ethylene glycol) to surfaces, critical for reducing bacterial adhesion. *Langmuir*, **19**, 6912-6921.

172. Lee, J.K., Kim, Y.G., Chi, Y.S., Yun, W.S. and Choi, I.S. (2004) Grafting nitrilotriacetic groups onto carboxylic acid-terminated self-assembled monolayers on gold surfaces for immobilization of histidine-tagged proteins. *Journal of Physical Chemistry B*, **108**, 7665-7673.

173. Sullivan, T.P. and Huck, W.T.S. (2003) Reactions on monolayers: organic synthesis in two dimensions. *Eur J Org Chem*, 17-29.

174. Horton, R.C., Herne, T.M. and Myles, D.C. (1997) Aldehyde-terminated self-assembled monolayers on gold: immobilization of amines on gold surfaces. *J Am Chem Soc*, **119**, 12980-12981.

175. Hermanson, G.T. (1996) *Bioconjugate Techniques*. 1st ed. Academic Press, Burlington, MA.

176. Cavallini, M., Bracali, M., Aloisi, G. and Guidelli, R. (1999) Electrochemical STM investigation of 1,8-octanedithiol self-assembled monolayers on Ag(111) in aqueous solution. *Langmuir*, **15**, 3003-3006.

177. Volcke, C., Pirotton, S., Grandfils, C., Humbert, C., Thiry, P.A., Ydens, I., Dubois, P. and Raes, M. (2006) Influence of DNA condensation state on transfection efficiency in DNA/polymer complexes: an AFM and DLS comparative study. *J Biotechnol*, **125**, 11-21.

178. Ogris, M., Brunner, S., Schuller, S., Kircheis, R. and Wagner, E. (1999) PEGylated DNA/transferrin-PEI complexes: reduced interaction with blood components, extended circulation in blood and potential for systemic gene delivery. *Gene Ther*, **6**, 595-605.

179. Sung, S.J., Min, S.H., Cho, K.Y., Lee, S., Min, Y.J., Yeom, Y.I. and Park, J.K. (2003) Effect of polyethylene glycol on gene delivery of polyethylenimine. *Biol Pharm Bull*, **26**, 492-500.

180. Banerjee, P., Weissleder, R. and Bogdanov, A., Jr. (2006) Linear polyethyleneimine grafted to a hyperbranched poly(ethylene glycol)-like core: a copolymer for gene delivery. *Bioconjug Chem*, **17**, 125-131.

181. Erbacher, P., Bettinger, T., Belguise-Valladier, P., Zou, S., Coll, J.L., Behr, J.P. and Remy, J.S. (1999) Transfection and physical properties of various saccharide, poly(ethylene glycol), and antibody-derivatized polyethylenimines (PEI). *J Gene Med*, **1**, 210-222.

182. Mishra, S., Webster, P. and Davis, M.E. (2004) PEGylation significantly affects cellular uptake and intracellular trafficking of non-viral gene delivery particles. *Eur J Cell Biol*, **83**, 97-111.

183. Mao, S., Neu, M., Germershaus, O., Merkel, O., Sitterberg, J., Bakowsky, U. and Kissel, T. (2006) Influence of polyethylene glycol chain length on the physicochemical and biological properties of poly(ethylene imine)-graft-poly(ethylene glycol) block copolymer/SiRNA polyplexes. *Bioconjug Chem*, **17**, 1209-1218.

184. Petersen, H., Fechner, P.M., Martin, A.L., Kunath, K., Stolnik, S., Roberts, C.J., Fischer, D., Davies, M.C. and Kissel, T. (2002) Polyethylenimine-graft-poly(ethylene glycol) copolymers: influence of copolymer block structure on DNA complexation and biological activities as gene delivery system. *Bioconjug Chem*, **13**, 845-854.

185. Merdan, T., Kunath, K., Petersen, H., Bakowsky, U., Voigt, K.H., Kopecek, J. and Kissel, T. (2005) PEGylation of poly(ethylene imine) affects stability of complexes with plasmid DNA under in vivo conditions in a dose-dependent manner after intravenous injection into mice. *Bioconjug Chem*, **16**, 785-792.

186. Toncheva, V., Wolfert, M.A., Dash, P.R., Oupicky, D., Ulbrich, K., Seymour, L.W. and Schacht, E.H. (1998) Novel vectors for gene delivery formed by self-assembly of DNA with poly(L-lysine) grafted with hydrophilic polymers. *Biochim Biophys Acta*, **1380**, 354-368.

187. Mannisto, M., Vanderkerken, S., Toncheva, V., Elomaa, M., Ruponen, M., Schacht, E. and Urtti, A. (2002) Structure-activity relationships of poly(L-lysines): effects of pegylation and molecular shape on physicochemical and biological properties in gene delivery. *J Control Release*, **83**, 169-182.

188. Guo, Y., Sun, Y., Li, G. and Xu, Y. (2004) The molecular structures of poly(ethylene glycol)-modified nonviral gene delivery polyplexes. *Mol Pharm*, **1**, 477-482.

189. Rackstraw, B.J., Martin, A.L., Stolnik, S., Roberts, C.J., Garnett, M.C., Davies, M.C. and Tendler, S.J. (2001) Microscopic investigations into PEG-cationic polymer-induced DNA condensation. *Langmuir*, **17**, 3185-3193.

190. Lee, M. and Kim, S.W. (2005) Polyethylene glycol-conjugated copolymers for plasmid DNA delivery. *Pharm Res*, **22**, 1-10.

191. Falconnet, D., Csucs, G., Grandin, H.M. and Textor, M. (2006) Surface engineering approaches to micropattern surfaces for cell-based assays. *Biomaterials*, **27**, 3044-3063.

192. Ademovic, Z., Holst, B., Kahn, R.A., Jorring, I., Brevig, T., Wei, J., Hou, X., Winter-Jensen, B. and Kingshott, P. (2006) The method of surface PEGylation influences leukocyte adhesion and activation. *J Mater Sci Mater Med*, **17**, 203-211.

193. Ross, P.C. and Hui, S.W. (1999) Polyethylene glycol enhances lipoplex-cell association and lipofection. *Biochim Biophys Acta*, **1421**, 273-283.

194. Yamazaki, M. and Ito, T. (1990) Deformation and instability in membrane structure of phospholipid vesicles caused by osmophobic association: mechanical stress model for the mechanism of poly(ethylene glycol)-induced membrane fusion. *Biochemistry*, **29**, 1309-1314.

195. Zhang, F., Kang, E.T., Neoh, K.G. and Huang, W. (2001) Modification of gold surface by grafting of poly(ethylene glycol) for reduction in protein adsorption and platelet adhesion. *J Biomater Sci Polym Ed*, **12**, 515-531.

196. Dunlap, D.D., Maggi, A., Soria, M.R. and Monaco, L. (1997) Nanoscopic structure of DNA condensed for gene delivery. *Nucleic Acids Res*, **25**, 3095-3101.

197. Neu, M., Sitterberg, J., Bakowsky, U. and Kissel, T. (2006) Stabilized nanocarriers for plasmids based upon cross-linked poly(ethylene imine). *Biomacromolecules*, **7**, 3428-3438.

198. Hansma, H.G., Golan, R., Hsieh, W., Lollo, C.P., Mullen-Ley, P. and Kwoh, D. (1998) DNA condensation for gene therapy as monitored by atomic force microscopy. *Nucleic Acids Res*, **26**, 2481-2487.

199. Pannier, A.K., Ariazi, E.A., Bellis, A.D., Bengali, Z., Jordan, V.C. and Shea, L.D. (2007) Bioluminescence imaging for assessment and normalization in transfected cell arrays. *submitted*.

200. Pichler, A., Zelcer, N., Prior, J.L., Kuil, A.J. and Piwnica-Worms, D. (2005) In vivo RNA interference-mediated ablation of MDR1 P-glycoprotein. *Clin Cancer Res*, **11**, 4487-4494.

201. Rafiq, I., Kennedy, H.J. and Rutter, G.A. (1998) Glucose-dependent translocation of insulin promoter factor-1 (IPF-1) between the nuclear periphery and the nucleoplasm of single MIN6 beta-cells. *J Biol Chem*, **273**, 23241-23247.

202. Rutter, G.A., Kennedy, H.J., Wood, C.D., White, M.R. and Tavare, J.M. (1998) Real-time imaging of gene expression in single living cells. *Chem Biol*, **5**, R285-290.

203. Jiang, S.Y., Wolf, D.M., Yingling, J.M., Chang, C. and Jordan, V.C. (1992) An estrogen receptor positive MCF-7 clone that is resistant to antiestrogens and estradiol. *Mol Cell Endocrinol*, **90**, 77-86.

204. Levenson, A.S. and Jordan, V.C. (1997) MCF-7: the first hormone-responsive breast cancer cell line. *Cancer Res*, **57**, 3071-3078.

205. Catherino, W.H. and Jordan, V.C. (1995) Increasing the number of tandem estrogen response elements increases the estrogenic activity of a tamoxifen analogue. *Cancer Lett*, **92**, 39-47.

206. Hoeben, A., Landuyt, B., Botrus, G., De Boeck, G., Guetens, G., Highly, M., van Oosterom, A.T. and de Bruijn, E.A. (2006) Proteomics in cancer research: Methods and application of array-based protein profiling technologies. *Analytica Chimica Acta*, **564**, 19-33.

207. Wheeler, D.B., Carpenter, A.E. and Sabatini, D.M. (2005) Cell microarrays and RNA interference chip away at gene function. *Nat Genet*, **37 Suppl**, S25-30.

208. Chen, D.S. and Davis, M.M. (2006) Molecular and functional analysis using live cell microarrays. *Curr Opin Chem Biol*, **10**, 28-34.

209. Kozarova, A., Petrinac, S., Ali, A. and Hudson, J.W. (2006) Array of informatics: Applications in modern research. *J Proteome Res*, **5**, 1051-1059.

210. Keselowsky, B.G., Collard, D.M. and Garcia, A.J. (2003) Surface chemistry modulates fibronectin conformation and directs integrin binding and specificity to control cell adhesion. *J Biomed Mater Res A*, **66**, 247-259.

211. Lan, M.A., Gersbach, C.A., Michael, K.E., Keselowsky, B.G. and Garcia, A.J. (2005) Myoblast proliferation and differentiation on fibronectin-coated self assembled monolayers presenting different surface chemistries. *Biomaterials*, **26**, 4523-4531.

212. Lee, M.H., Ducheyne, P., Lynch, L., Boettiger, D. and Composto, R.J. (2006) Effect of biomaterial surface properties on fibronectin-alpha5beta1 integrin interaction and cellular attachment. *Biomaterials*, **27**, 1907-1916.

213. Rodrigues, S.N., Goncalves, I.C., Martins, M.C., Barbosa, M.A. and Ratner, B.D. (2006) Fibrinogen adsorption, platelet adhesion and activation on mixed hydroxyl-/methyl-terminated self-assembled monolayers. *Biomaterials*, **27**, 5357-5367.

214. Keselowsky, B.G., Collard, D.M. and Garcia, A.J. (2004) Surface chemistry modulates focal adhesion composition and signaling through changes in integrin binding. *Biomaterials*, **25**, 5947-5954.

215. Kong, H.J., Hsiong, S. and Mooney, D.J. (2007) Nanoscale cell adhesion ligand presentation regulates nonviral gene delivery and expression. *Nano Lett*, **7**, 161-166.

216. Milanesi, L., Reid, G.D., Beddard, G.S., Hunter, C.A. and Waltho, J.P. (2004) Synthesis and photochemistry of a new class of photocleavable protein cross-linking reagents. *Chemistry-a European Journal*, **10**, 1705-1710.

217. Hodneland, C.D., Lee, Y.S., Min, D.H. and Mrksich, M. (2002) Selective immobilization of proteins to self-assembled monolayers presenting active site-directed capture ligands. *P Natl Acad Sci USA*, **99**, 5048-5052.

218. de Wolf, F.A. and Brett, G.M. (2000) Ligand-binding proteins: their potential for application in systems for controlled delivery and uptake of ligands. *Pharmacol Rev*, **52**, 207-236.

219. Sigal, G.B., Bamdad, C., Barberis, A., Strominger, J. and Whitesides, G.M. (1996) A self-assembled monolayer for the binding and study of histidine tagged proteins by surface plasmon resonance. *Analytical Chemistry*, **68**, 490-497.

220. Zisch, A.H., Lutolf, M.P., Ehrbar, M., Raeber, G.P., Rizzi, S.C., Davies, N., Schmokel, H., Bezuidenhout, D., Djonov, V., Zilla, P. *et al.* (2003) Cell-demanded release of VEGF from synthetic, biointeractive cell ingrowth matrices for vascularized tissue growth. *Faseb J*, **17**, 2260-2262.

221. Su, L.F., Wang, Z. and Garabedian, M.J. (2002) Regulation of GRIP1 and CBP Coactivator activity by Rho GDI modulates estrogen receptor transcriptional enhancement. *J Biol Chem*, **277**, 37037-37044.